Quality Of Service and MObility driven cognitive radio Systems

FP7-ICT-2009-4/248454

QoSMOS

D3.6

QoSMOS Radio environment measurement, modeling and emulation

Contractual Date of Delivery to the CEC:	30-Nov-2012
Actual Date of Delivery to the CEC:	02-Dec-2012
Editor(s):	Jonathan Duplicy (Agilent Technologies)
Author(s):	J. Duplicy (AGI), M. Zelenak (AGI), D. Depierre (TCF), K. Briggs (BT), B. Ye (BT), L. Gonçalves (IT), J. Matos (IT), N. Borges (IT), A. Silva (IT), J. Lehtomäki (OULU), J. Vartiainen (OULU), O. Durowoju (UNIS), T. Brown (UNIS).
Workpackage:	WP3
Est. person months:	63PM
Security:	PU
Nature:	Report
Version:	1.0
Total number of pages:	80

Abstract:

This deliverable D3.6 first reports the results from the different measurement campaigns under taken in the framework of the project to assess the potential of cognitive radio. Activity / Opportunity models are then derived from the measurements. At last, we report the development of a radio scene emulator, third pillar of the proposed MME (Measurement, Modeling & Emulation) framework to assess the performance of cognitive radio systems.

Keyword list:

Cognitive Radio, Measurement, Modeling Emulation, TV White Space, GSM, UMTS, polarization, Scene Emulator.

The research leading to these results was derived from the European Community's Seventh Framework Programme (FP7) under Grant Agreement number 248454 (QoSMOS)

Acronyms

AWGN	Arbitrary White Gaussian Noise
BCH	Broadcast Channel
BTS	Base Station
CDMA	Code Division Multiple Access
CDF	Cumulative distribution function
COR	Channel Occupancy Rate
CR	Cognitive Radio
CRS	Cognitive Radio Systems
DC	Duty Cycle
DPCH	Dedicated Physical Channel
DVB	Digital Video Broadcasting
E-GSM	Extended GSM
FCC	Federal Communications Commission
GSM	Global System for Mobile communications
GPS	Global Positioning System
HSDPA	High Speed Downlink Packet Access
HW	Hardware
IEEE	Institute of Electrical and Electronics Engineers
ISM	Industrial, Scientific and Medical (band)
ITM	Irregular Terrain propagation Model
ITS	US Institute for Telecommunications Science
ITU	International Telecommunication Union
LAD	Least Absolute Deviation (algorithm)
LNA	Low Noise Amplifier
MAE	Maximum Absolute Error

MED-FCME	Median filtered Forward Consecutive Mean Excision
MME	Measurement Modeling Emulation
NLOS	Non-Line-Of-Sight
OFDM	Orthogonal Frequency Division Multiplexing
OVSF	Orthogonal Variable Spreading Factor
PMF	Probability Mass Function
PoC	Proof-of-Concept
RAT	Radio Access Technology
RF	Radio Frequency
SA	Spectrum Analyzer
SMA	SubMiniature version A
TCH	Traffic Channel
TDMA	Time Division Multiple Access
TVWS	TV WhiteSpace
TVWSDB	TV WhiteSpace Database
UE	User Equipment
UMTS	Universal Mobile Telecommunications System
WLAN	Wireless Local Area Network

Table of contents

List of figures

List of tables

1 Executive Summary

Deliverable D3.6 reports a big portion of the work under Task 3.1. The main goals consist in evaluating the spectral potential for cognitive radio systems in various bands and the derivation of models and systems to evaluate their performance.

The first part consists in the presentation of the different measurement campaigns that were conducted in the course of the project. These were conducted at different locations (France, Portugal, Finland, UK) at different timings and targeting different radio access technologies (GSM, UMTS, WiFi, TV). To perform the measurements, some innovative methods were derived to fix the appropriate decision thresholds. Furthermore, a new two-node measurement setup was developed to measure spatial correlation.

The results clearly show some unused spectrum capacity that could be exploited with the QoSMOS cognitive radio technology. We have also shown that the typical spectrum occupancy metric can be significantly different from the actual traffic occupancy. Statistics were derived from the measurements and from there activity / opportunity models built. As for the TVWS case, we have taken a different approach by deriving white space levels from the position of the transmitters and a model of the propagation channel. Furthermore, the importance of the polarization of TV signals was emphasized through a series of measurements.

In additional, we have developed a 'radio scene emulator' which aims at emulating a given radio scene. This tool (for which a patent application was filed) gives full freedom to the user along the time/frequency/waveform/power axis/domains.

The three pillars discussed above (**M**easurement, **M**odeling & **E**mulation) are the basis of the MME methodology we propose to assess the performance of cognitive radio systems. In its simple form, this integrated approach consists in emulating models derived from measurements in order to stimulate the cognitive radio system under test with a realistic radio scene, similar to what it would experience in the field.

2 Motivation

Rather than being scarce as pointed out by operators, according to the cognitive radio community, the spectrum is rather inefficiently used. Exclusive ownership of spectrum bands leads to some overcrowded bands with consequent drop calls while others are only a used at a small percentage.

It is then fundamental to identify *where* the cognitive radio technology could leverage its usage potential. *Where* has to be seen as slots in the tri-dimensional set of coordinates: time / frequency / location. Hence, the QoSMOS project has performed a series of measurement campaigns at different times, frequencies and locations. These are reported in the present deliverable.

Besides the above goal of evaluating the potential of cognitive radio systems, the work performed in this work-package has led to the development of the so-called 'MME approach' (standing for Measurement, Modeling & Emulation) to assess the performance of such systems. Generally, the testing aspects have been overlooked by the CR (Cognitive Radio) community. This is however crucial for the regulators to choose the more liberal approach that is cognitive radio. This QoSMOS branded methodology is described hereafter. This was also published in the following magazine article, where more details can be found:

[1] D. Tandur, J. Duplicy, K. Arshad, K. Moessner, D. Depierre, J. Lehtomäki, K. Briggs, L. Goncalves, A. Gameiro, ``Cognitive Radio Systems Evaluation: Measurement, Modeling, and Emulation Approach,'' *IEEE Vehicular Technology* Magazine, June 2012.

The MME approach aims at bringing realism into the technology assessment. It is illustrated by Figure 2-1. In general, the Radio Frequency (RF) scene is first measured over a range of frequencies, time instants, and locations. The data collected can then be converted to a mathematical model, which can further be emulated in a controlled environment either in software or hardware. It should be noted that, besides this sequence (Flow 1), it is possible that models are built from the scratch and then confirmed or fine-tuned through measurements, before being finally emulated (Flow 2). Finally, it is also possible that the modeling block is completely bypassed (Flow 3). The last sequence is called the deterministic case, where the measurement is immediately followed by emulation of the measured signals.

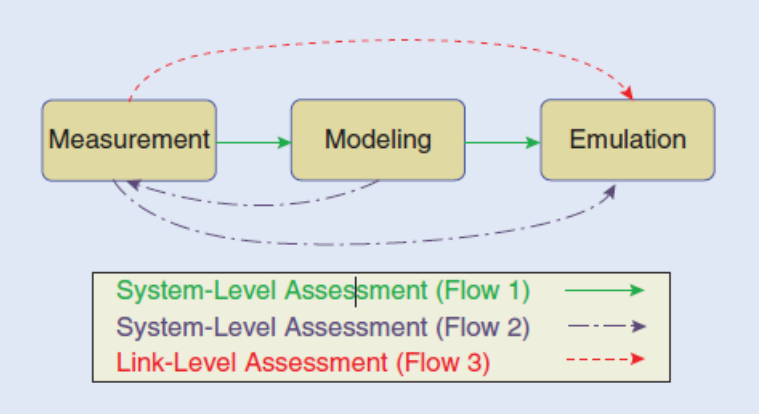

Figure 2-1: MME-integrated approach.

The timescale and target of Flows 1 and 2 are different from the one from Flow 3. In the first two cases, a system level evaluation is targeted, and its aim is to evaluate the capacity of CR systems or the macrospectrum occupancy pattern. In particular, this methodology should assist design engineers in evaluating the potential of CR system in various bands and locations. This activity will require measurements over multiple periods and may involve days or weeks. In the last case (Flow 3), a link-level evaluation is targeted. Typically, short radio scenes are captured and then directly replayed in the laboratory to evaluate CR-sensing algorithms. The timescale in this case can be considered to be in the order of a fraction of seconds. The MME-integrated approach brings the real-world environment to the laboratory and aims to offer fully trustable results to the various CR stakeholders.

3 Measurement campaigns and models

3.1 Introduction

Our goal in the section is first to report the results from the measurement campaigns conducted in the course of the project. The GSM, UMTS, ISM and TV bands are addressed. Second, it presents the different techniques developed to perform the measurements. Furthermore, some occupancy / opportunity models are given. Then, the importance of the (often overlooked) polarization is emphasized thanks to some measurement analysis. At last, we illustrate the above defined 'flow2' of the MME approach where a modelling of the TV channels activity is first performed and then confronted with measurements.

3.2 Paris GSM measurements

3.2.1 Introduction

In the literature on cognitive radio sensing, the issue is mainly "is the spectrum band used (and sometimes by who)?" But this approach highly reduces the scope of how spectrum can be reused. Indeed for certain RATs (Radio Access Technologies), the spectral resource can be used even if no user is actually transmitting data. It is the case for all downlink CDMA (Code Division Multiple Access) systems where the common channels (pilot, synchronization and broadcast) are always emitted even if no data is transmitted to a user. Even with a TDMA (Time Division Multiple Access) standard such as GSM a huge difference exists between spectrum occupancy and the real amount of traffic. Indeed two factors, depending on the operator network planning, can increase the GSM (Global System for Mobile communications) spectrum occupancy for a fixed amount of traffic:

- The number of frequency channels used as Broadcast Channels (BCH).
- The frequency hopping; the spectrum occupancy is increased by a factor equal to the number of frequency channels on which a user can hop.

Moreover the spectrum occupancy does not reflect the actual usage of the spectral resource by the users. Indeed, it does not give any information about the number of time slots used and the temporal occupancy of each time slot.

That is why it might be useful to develop more precise metrics than the classical spectrum occupancy. The "traffic occupancy" gives a much better image of how the spectral resource is actually used to transmit data. In the GSM case, it can be defined as the average occupancy over the TDMA time slots on each of the Traffic Channels (TCH) that can be potentially used by a UE (User Equipment) at the sensing location (as stated in the "frequency used" messages of the best servers BCH).

The idea behind this measurement campaign is to observe the real usage of the GSM bands along one day and verify the difference that may exist between spectrum occupancy and traffic occupancy. It is going to be shown that classical spectrum occupancy sensing does not necessarily reflect the actual usage of the GSM band.

3.2.2 Measurement Set-up and Equipment

One can refer to D3.1 to have a precise documentation about Thales equipment (ESMERALDA XE) used for wide-band (I, Q) signal acquisition as well as the planning of the measurements on GSM bands.

In the framework of the QoSMOS project, the ESMERALDA XE equipment is used to digitize and store onto a hard disk a baseband (I, Q) signal with a bandwidth of 40 MHz at a sampling frequency of 51.2 MHz. The advantage of storing the baseband (I, Q) signal is that any sensing algorithm can be performed off-line. No new measurement campaigns need to be realized each time a new metric is proposed. Moreover, each metric can be computed on the same signal (i.e. recorded at the same time, at the same location) in order to efficiently compare them.

The ESMERALDA XE is used to quickly digitize downlink GSM bands, meaning:

- The E-GSM band, from 925 MHz to 935 MHz
- The GSM 900 band, from 935 MHz to 960 MHz

Therefore, with only one single 40MHz-acquisition, all the E-GSM and GSM 900 bands can be digitized for off-line processing. The GSM 1800 bands are not analyzed with this set-up.

Once the signal is digitized, the CASTLE software is used. CASTLE allows filtering the 40 MHz signal file into separate files for each GSM frequency channel (with a bandwidth equal to 200 kHz). The downlink GSM frequencies depending on the frequency channels are described in Table 3-1.

Table 3-1 : Downlink channel frequency for GSM bands

Band	Channel number	Downlink frequency formula	Downlink frequency band
GSM 900	$1 \leq n \leq 124$	$935\ \text{MHz} + 0.2 \times n$	935 MHz to 960 MHz
E-GSM	$975 \leq n \leq 1023$	$935 + 0.2 \times (n-1024)$	925 MHz to 935 MHz

Once the filtered signal files are generated, **downlink interference analysis** is processed. This processing allows detecting all the BTS (Base Station) emitting on a given frequency channel, determining if it is a broadcast channel or a traffic channel and extracting metrics on these channels as described hereafter. For each detected base station, the characteristics recorded and displayed by the CASTLE tool are the following:

- Identification of the type of channel (broadcast or traffic)
- Base station power
- Base station C/I
- The channel impulse response (amplitude and phase)
- On traffic channels
    - Training Sequence Code (TSC)
    - Demodulation of the pilot bits and estimation of the RxQual
    - Time slot occupation rate
- On broadcast channels
    - Cell Identity (CI)

- Mobile Country Code (MCC)
- Mobile Network Code (MNC)
- Frame number
- DTX
- Used frequencies
- Adjacent frequencies

3.2.3 Measurement Campaign

This campaign is fully passive, i.e., no signal is emitted.

The measurement campaign took place in Colombes in Thales Communications premises (146, Bd de Valmy) the 7th and the 8th of March 2011. The equipment (including the antenna) was installed in a laboratory, on the third floor of Magellan building (8-floor building) of Thales premises.

288 successive acquisitions were performed, one every 5 minutes (i.e. during 24 hours). Each acquired file is 500 ms long. This is sufficient to be able to detect in 100% of the cases (in good reception condition) the presence of a TCH or a BCH. Nevertheless, it is not sufficient to be able to demodulate the broadcast message in 100% of the cases but it does not matter as in our measurement campaign, on the 288 files, the BCH message need to be decoded only from time to time.

The measurement files characteristics are summarized in Table 3-2.

Table 3-2 : Downlink GSM measurement characteristics

Center frequency	940 MHz
Bandwidth before filtering	40 MHz
Bandwidth after filtering	200 kHz
Time	From Monday the 7th of March at 15h30 to Tuesday the 8th of March at 15h25

3.2.4 Measurement analysis

The main two metrics to be computed are the **spectrum occupancy** and the **traffic occupancy**. Each of them is computed for a given operator. The results shown hereafter are for the main French operator, Orange.

For **spectrum occupancy**, on all the 200kHz GSM frequency channels belonging to Orange (channels 1 to 62), the downlink interference analysis is run in order to detect the channels used for BCH, the ones used for TCH and the free ones. Figure 3-1, on the left side, represents the presence or not of a BCH or a TCH on each frequency channel along the day. On the right side, the percentage of used channels, that is the spectrum occupancy, is computed. The values are averaged on a 60 minutes sliding window in order to obtain smoother curves. One can notice that the spectrum occupancy is always high, over 45%. That is due to the important amount of frequency channels used as BCH. This point also explains the low difference of occupancy between daytime and night-time. The frequency hopping of the TCH also increases the spectrum occupancy.

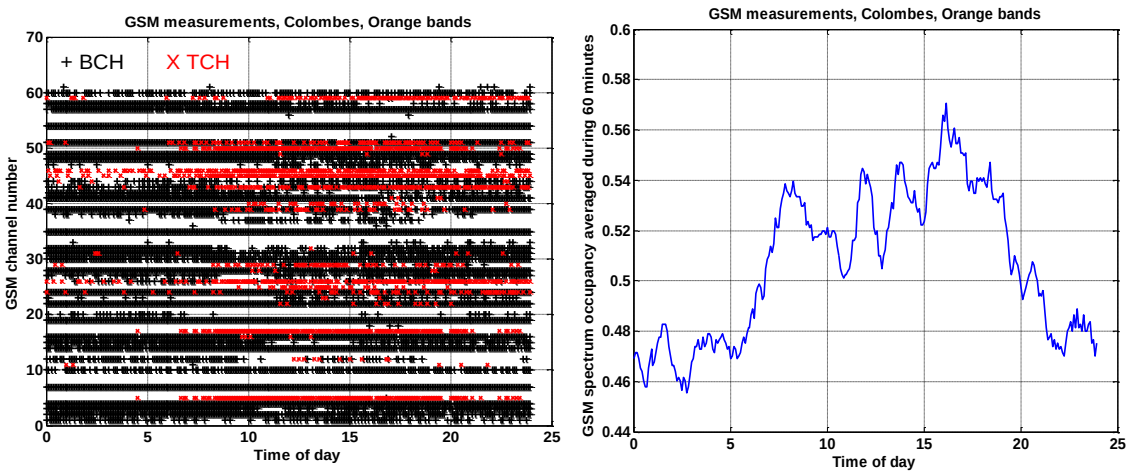

Figure 3-1 : Spectrum occupancy along the day on Orange bands

The **traffic occupancy** is computed as described in Figure 3-2. The idea is to compute the load of traffic at a given measurement point as it would be seen by a UE. It can be split into three steps:

- The frequency channels used as BCH at the measurement point are detected. The presence of a BCH is confirmed if it is detected on 100% of the 288 measurements. The idea is to keep only the best servers, as a UE would do, and reject weak BTSs.
- The BCH message is decoded in order to extract the field "frequency used" which indicates to a UE the frequency channels it can use for traffic.
- On the frequency bands from the "frequency used" pool, the mean traffic occupancy is computed the following way:

$$Occ_{GSM} = \frac{1}{8N_{TCH}} \sum_{k=1}^{N_{TCH}} \sum_{p=1}^{8} occ(k,p)$$

where N_{TCH} is the number of TCH in the "frequency used" pool, and $occ(k,p)$ is the occupation rate on the k^{th} frequency channel and on the p^{th} time slot (among the 8 available time slot in a GSM frame).

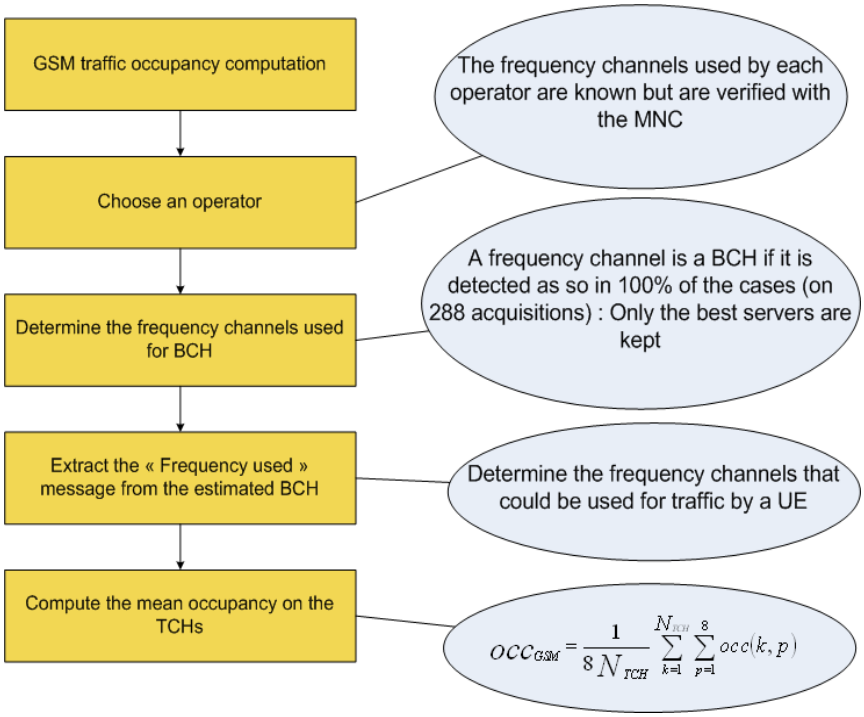

Figure 3-2 : Traffic occupancy computation diagram

When run on Orange frequency bands, at the measurement point, the number of detected BCH, as seen by a UE, is equal to 4. The number of TCH a UE can use is equal to 6. Figure 3-3 represents the traffic occupancy along the day. As for the spectrum occupancy, the values are averaged on a 60 minutes sliding window in order to obtain smoother curves. This figure emphasises the existing difference between the spectrum occupancy and its actual usage on GSM bands. One can observe that the traffic occupancy is much lower than the spectrum occupancy with important fluctuation during the day. The average is 10% during business hour (from 9am to 6pm) and 2.5% outside business hour while it was around 50% for spectrum occupancy. Instantaneous peaks can reach 35% and traffic increases are observed around 10am, 12:30pm and 5pm.

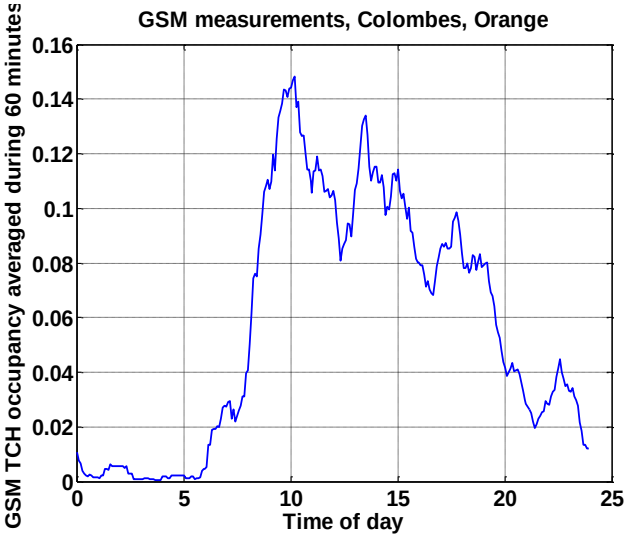

Figure 3-3 : Traffic occupancy along the day on Orange bands

3.2.5 Conclusions

The presented measurement campaign showed that the commonly used metric in cognitive radio that is spectrum occupancy does not reflect the actual usage of the GSM frequency bands. The difference between spectrum occupancy and traffic occupancy can be quite large (46% versus 0% during nighttimes). This is mainly due to the broadcast channels that are always used. Frequency hopping also increases this difference. It means that the network planning used by an operator can drastically change spectrum occupancy for a fixed amount of traffic. This does not directly impact the way a cognitive radio will sense spectrum to improve its usage. Nevertheless, in order to optimize the way the whole spectrum band is used by all its users (incumbent and opportunistic) it might be important that even incumbent systems think about reducing their spectrum usage (without reducing their QoS), if possible.

3.3 Paris UMTS measurements

3.3.1 Introduction

The concept of sensing in code is described in details in D3.5. The idea is to transmit on CDMA bands using codes that are orthogonal to the one in use. In order to do so, the opportunistic system must be able to detect the codes that are used. Classical sensing techniques are not relevant for CDMA RATs, as the spectrum channel is always used by common logical channels. CDMA channels detection algorithms and their performance are presented in D3.5. In this section, one algorithm is tested and validated on real UMTS (Universal Mobile Telecommunications System) signals. Moreover, the way UMTS bands are used along the day and for various types of services (voice, data) is described.

3.3.2 Measurement Set-up and Equipment

The equipment used for UMTS measurement campaign is the one described in Figure 3-4. It allows to acquire UMTS (I, Q) data at twice the chip frequency (7.68 MHz) and to process them using advanced antenna processing algorithms. It is made of a set of 4 antennas, a 4-channel receiver, a 4-channel acquisition board, and a laptop for data storage and off-line multi-antenna signal processing.

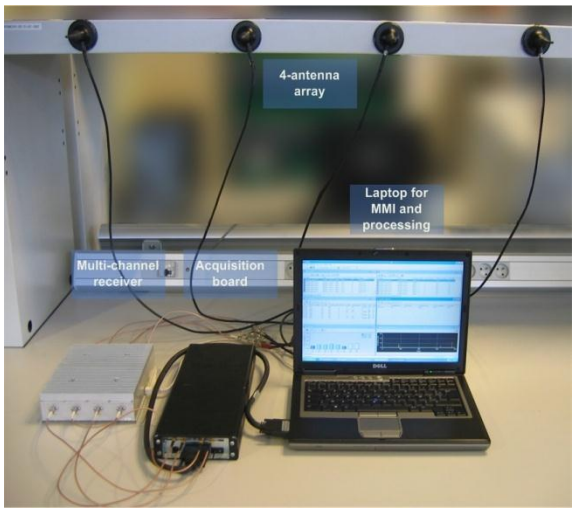

Figure 3-4 : UMTS sensing device.

The whole measurement and analysis process is described in Figure 3-5. The downlink interference analysis block is described in details in D3.5. It allows detecting all the UMTS BTS transmitting on the analysed frequency channel and for each of them detecting the traffic channels used with their characteristics (spreading factor, spreading code, slot format, offset).

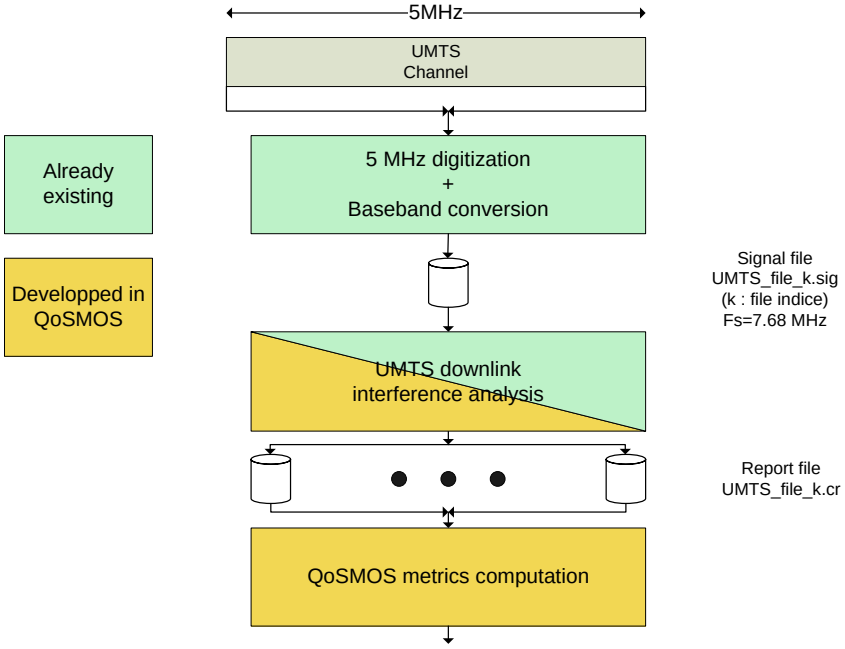

Figure 3-5 : UMTS measurement process.

3.3.3 Measurement campaign

This campaign is fully passive i.e. that no signal is emitted. The measurement campaign took place in Colombes in Thales Communications premises (146, Bd de Valmy) the 6th/7th of September 2012. The equipment (including the antenna) was installed in a laboratory, on the third floor of Magellan building (8-floor building) of Thales premises.

288 successive acquisitions were performed, one every 5 minutes (i.e. during 24 hours). Each acquired file is 100 ms long.

The measurement files characteristics are summarized in Table 3-3.

Table 3-3 : Downlink UMTS measurement characteristics.

Center frequency	2157.2 MHz (Orange band)
Acquisition bandwidth	5 MHz
Time	From Thursday the 6th of September at 9h53 to Friday the 7th of September at 9h48

3.3.4 Measurement analysis

In this section, we are presenting results concerning the DPCH (Dedicated Physical Channel, i.e. the traffic channels) emitted by the base stations of the active set. The active set is defined as the BTS being within 5 dB below the most powerful detected BTS. Once the signal files are processed and the metrics computed, they are sorted in order to give an overall picture. A set of two curves is plotted:

- The number of DPCH emitted by the BTS of the active set versus time, depending on the spreading factor. The number of DPCH is averaged over 60 minutes in order to have a steadier plot.
- The mean OVSF (Orthogonal Variable Spreading Factor) code occupancy on the BTS of the active set versus time. The OVSF code occupancy for each BTS is defined as follows:

$$Occ_{UMTS,SF} = \sum_{n=1}^{N_{DPCH}} \frac{1}{SF(n)}$$

where $SF(n)$ is the spreading factor of the nth traffic channel. The code occupancy corresponds to the percentage of possible OVSF codes used by the DPCH of the BTS. The OVSF code occupancy is averaged over 60 minutes in order to have a steadier plot.

On the acquired signal files, the active set comprises one single BTS. The results presented are therefore for this BTS only. Figure 3-6 represents the number of DPCH along the day for all the spreading factors and for each spreading factor (256, 128 and 32). The values are averaged on a 60 minutes sliding window in order to obtain smoother curves. It is important to recall that each spreading factor corresponds to a data rate and therefore to a type of service. A spreading factor of 256 corresponds to dedicated control messages, 128 to voice and 32 to high data rate service (64 kbps).

First one can see that the number of traffic channels highly fluctuates during the day. The average if 15 channels used during the business hour (from 9am to 6pm) and 2 outside business hour. It can reach 26 at the most. The most surprising result is that this UMTS channel is mainly used for voice traffic and not at all for high data rate services. The explanation may come from the fact that the operator Orange separates its UMTS bands from its HSDPA (High Speed Downlink Packet Access) bands. Therefore, high rate smart phone services use HSDPA bands as long as they are not fully loaded and not UMTS ones. UMTS bands are then used for lower rate services.

A very interesting result is that if we compare the green curve of Figure 3-6 (that is voice traffic on UMTS band) to the curve of Figure 3-3 (that is traffic occupancy on GSM bands), they look very similar. The correlation between both has been calculated and is equal to 0.92. It means that on two different days, at the same location, the voice traffic in GSM and UMTS bands are highly correlated. It validates approaches which model the traffic along the day.

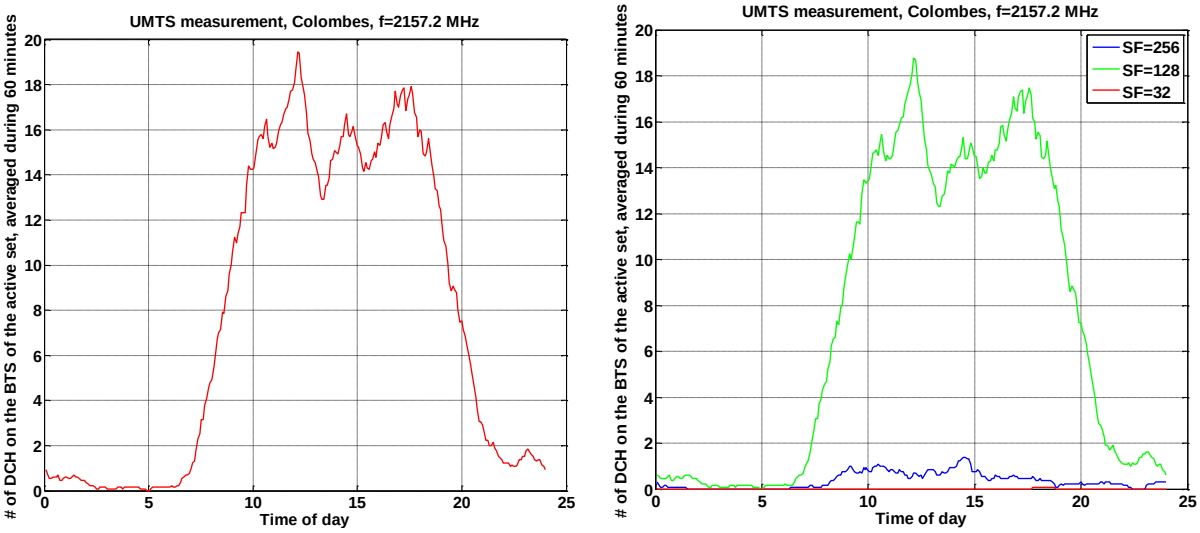

Figure 3-6 : Number of DPCHs along the day on one UMTS band, for all SF (left) and for each SF (right)

Figure 3-7 presents the code occupancy during the day. First, it can seem quite low compared to the maximum occupancy that orthogonal codes can provide in theory. Nevertheless, it has been shown in 0 that the maximum number of users, using voice service, per cell which is equal to 88 for an AWGN (Additive White Gaussian Noise) propagation channel drops down to 43 for a propagation channels with 4 paths at a speed of 120 km/h. It corresponds to a code occupancy of 0.33. It means that at peak hour, the code occupancy is not that low.

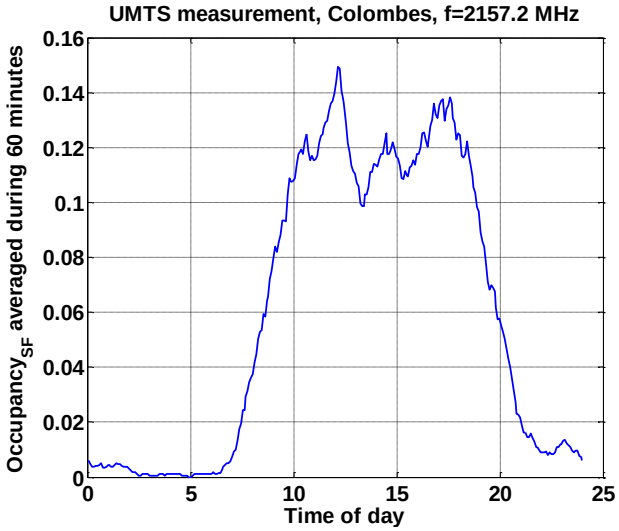

Figure 3-7 : Code occupancy during the day

Nevertheless, the code tree is not a limitation. UMTS downlink capacity is limited by DPCH power, which in turns depends on interference [Chevallier06]. An analytical definition of downlink capacity estimates the required power per user, because high-power amplifier is the most limiting downlink resource. DPCH power is mainly affected by system loading (DPCH E_c/I_{or}), interference, the required E_b/N_t, the channel conditions that influence the achieved E_b/N_t, and handover state.

As far as sensing in code is concerned, this limiting factor is interesting. Indeed it means that even if the frequency channel is fully loaded (in term of network capacity), the code resource should never be completely used. Therefore, there will always be some available orthogonal codes that a CR device can use.

3.3.5 Conclusion

The presented measurement campaign showed that the UMTS bands are mainly used for voice traffic, as long as the HSDPA channels are not fully loaded. Moreover, knowing that the number of codes is not the limiting factor for downlink UMTS traffic, there should always be available code resource for an opportunistic CR device using sensing in code approach. This measurement campaign tends to validate the sensing in code concept, at least in term of available code resource.

3.4 Aveiro wideband and GSM measurements and models

In this section we report on the measurements carried out in Aveiro. The setups are described, the measurements are reported and the resulting models analysed and proposed. The first section describes the single setup, respective measurements and statistics derived, and the final one describes the double location setup that was developed to assess space correlation and results obtained up to now.

3.4.1 Measurement Single Set-up and Equipment

A measurement setup was assembled for a static spectrum occupancy evaluation. In order to make it suitable for these types of measurements a number of requirements were taken into account. First requirement included the need to evaluate sensing in different frequency bands that are used for different wireless technologies. This narrows the selection of sensing techniques down to energy detection since it is the only method that does not rely on any a priori knowledge of the primary user technology. The second requirement, according to [3], is the need for a very sensitive detection setup. Third requirement included a full analysis on the measurement setup in terms of attenuation/gain to every single component and according to these requirements a setup was assembled in terms of measurement quality and measurement management.

This chapter presents the main aspects in terms of hardware and software used in/with the measurement setup, and it is organized as follows: section 3.4.1.1 gives a brief description of the measurements setup location; section 3.4.1.2 presents the measurements setup itself and a description of it; section 3.4.1.3 gives a characterization on every single component of the measurement setup.

3.4.1.1 Measurement set-up location

All the measurements were performed in a scenario that showed characteristics of having some spectrum occupancy. The measurement equipment was placed on the rooftop of the Electronics, Telecommunications and Informatics Department (DETI) at the University of Aveiro marked with a yellow circle (latitude: 40º 38’ 00” north; longitude: 8º 39’ 35” west) and its location is presented in Figure 3-8. All the measurements were performed outdoors and during the classes’ period, in order to guarantee the most realistic scenario in an urban environment.

Figure 3-8: Location of the measurement set-up.

3.4.1.2 Measurement set-up Components

The schematic of the measurement setup is shown in Figure 3-9, identifying all the elements used in the assembled setup for this work. In Figure 3-10, we show the components located indoor as the antenna was left outside the building.

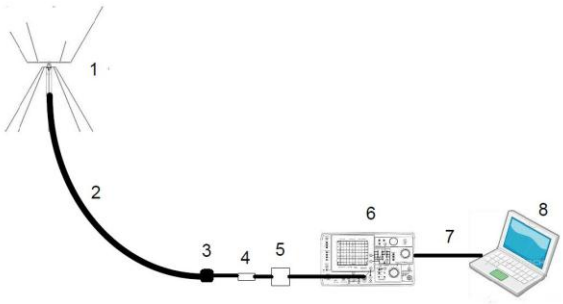

Figure 3-9: Schematic of the measurement setup.

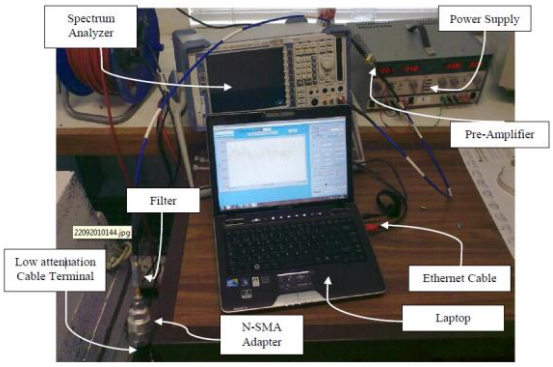

Figure 3-10: Indoor components of the measurement setup.

The measurement setup is composed of a high bandwidth omnidirectional (Multi-Polarized) antenna (25MHz − 6GHz) from MP Antenna company, with typical 3dBi gain. A semi-rigid low attenuation cable (typical < 0.12 dB/metre at 5GHz) with about 8 meters, a very steep passband filter (500MHz − 1GHz for GSM900, 1GHz − 2GHz for DCS1800), a high bandwidth preamplifier (15dB gain at 950MHz), a Spectrum Analyzer (SA) and a portable computer with an acquisition program. From the low attenuation cable, to the SA, the components are connected with thin cable with SMA (SubMiniature version A) connectors. The preamplifier gain is such that a GSM signal (−102dBm in 200 KHz, sensitivity level) is brought above the noise level of the SA, but not enough to generate visible intermodulation products due to non linearity of the input mixer of the SA. The SA is set to the highest sensitivity *i.e.*, with 0dB attenuation of the input attenuator. The total signal in 500MHz − 1GHz band (pass band of the filter) at the input of the SA was about −17dBm. The secure signal level in terms of intermodulation is below −10dBm. Another criterion in choosing the filter is that the higher passband frequency is not more than one octave from the lower passband frequency. This avoids the second order intermodulation products to be inside the passband. The characteristics above mentioned represent the main ones we worked with. As a whole the measurement setup covers the bandwidth from 25MHz up to 6GHz.

The antenna (Figure 3-11) was deployed on top of the DETI at the University of Aveiro in line of sight with the Telecommunications antenna's operators. This Super-M Ultra Base Station antenna covers the frequency range from 25 MHz to 6 GHz and provides wireless communication in "Real World" obstructed Non-Line-Of-Sight (NLOS) environments. In NLOS obstructed environments the M-POL Super-M Ultra Base Station can outperform non-multipolarized 8dBi gain antennas.

Figure 3-11: Antenna deployment.

The total power in the spectrum bandwidth considered was one of the main concerns for the measurement setup. The use of a filter was needed to prevent an overload in the SA. The overload in the SA would not allow the acquisition properly. For this reason, customized filters were acquired to prevent this situation. One with a range from 500MHz to 1GHz and another one with a range from 1GHz to 2GHz. The combination of the filters with the antenna allows covering the range of 500MHz-2GHz without saturating the amplifiers. The other bands can still be covered but its strong signals may overload the sensitivity of the receiver. The use of the filters allows making precise measurements in the GSM900 and the GSM1800 bands.

The characterization of the whole set-up has shown than the antenna gain is 3dBi and the noise figure 3.5dB. Therefore the lowest GSM signal detectable with this setup is -117dBm (/200 kHz) which is about 20dB below the sensitivity specified for GSM receivers,

3.4.1.3 Data Acquisition and Processing Software

To be able to record the measurements, appropriate software was tested/used on the measurements setup. The software is compatible with the spectrum analyser and provided by the manufacturer. This raw data acquisition software was then integrated with MATLAB that imports the data and makes it available for any desired data processing.

The software was tested and calibrated using known signals allowing concluding about the accuracy of the power measurements. In the following chapter, all the measurements/statistics are presented.

3.4.2 Measurements and Statistics

This section presents all the analysis done on the data recorded and obtained through the measurement setup as described in the previous chapter. The analysis of the collected data enabled the modelling of spectrum's behaviour. Before taking specific measurements in the GSM band an overview of the spectrum occupancy was measured to see which bands would be propitious to take measures from, and to better understand a simple occupation of the spectrum from 25MHz to 4 GHz. With this, specifications are presented for the selected frequencies. Following, the results of the statistical measurements and occupancy results are presented to provide with sufficient information that will be applied in creating models of spectrum behaviour.

3.4.2.1 Spectrum Occupancy

To be aware of the spectrum occupancy some measurements were taken covering the full 25MHz-4GHz bandwidth covered by the setup. The results are shown (Figure 3-12) where some of the most important services / systems used can be easily identified.

.

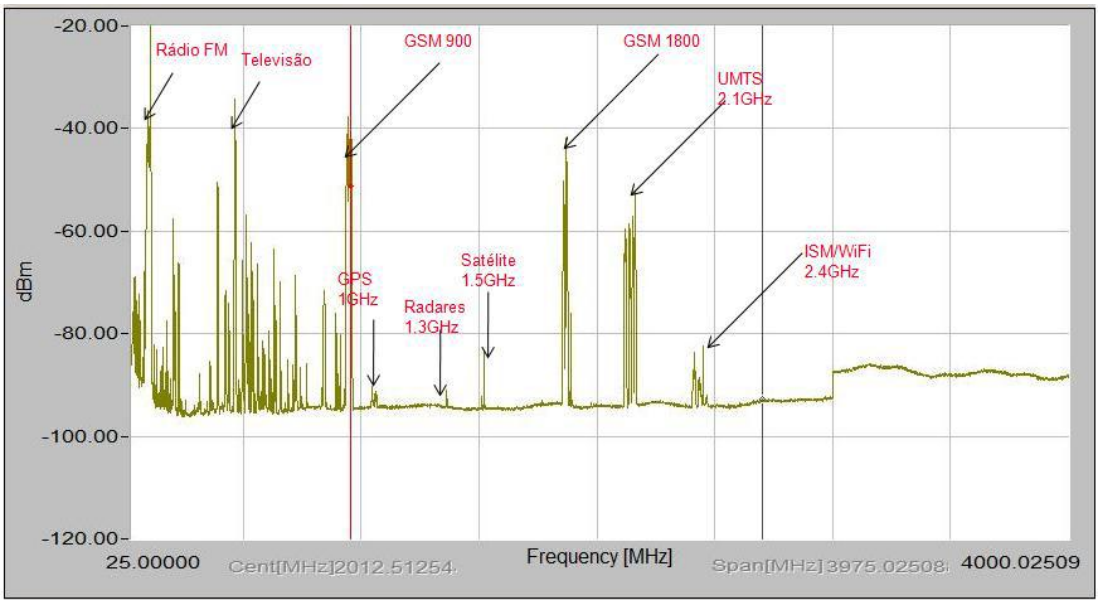

Figure 3-12: Spectrum Occupancy from 25MHz to 4GHz.

In order to evaluate the spectrum occupancy more specifically, the first algorithm according to the specifications issued in Deliverable D3.1 defines the band as occupied if the recorded power is above a given threshold. The bandwidth step was programmed to be 1MHz and we considered three values of thresholds: -80dBm, -90dBm and -95dBm. At each step of 1MHz the band is considered available or occupied if the measured power is below or above the threshold.

Figure 3-13 represents the spectrum occupancy in % with different values of power reference. By integrating over the whole bandwidth (25MHz-6GHz), a global occupation percentage is obtained and given in Table 3-4.

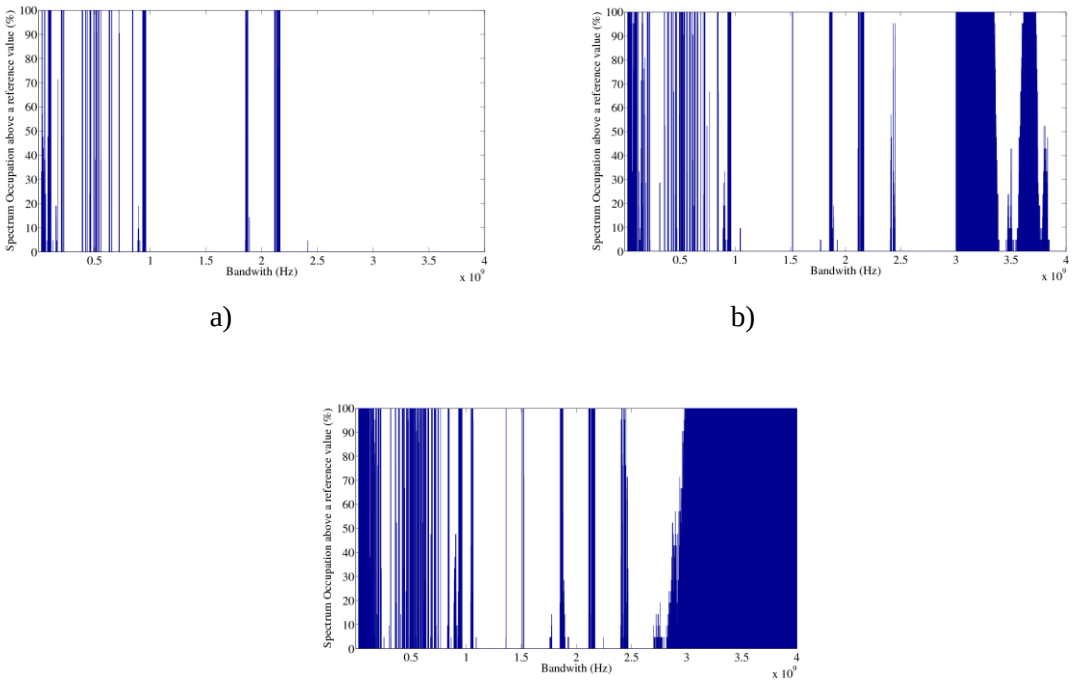

Figure 3-13 Illustration of the spectrum occupancy for different threshold values: a) -80dBm b) -90dBm c) -95dBm.

Table 3-4: Global occupancy percentage.

Threshold (dBm)	Average occupancy (%)
-80	5,2
-90	34
-95	64,9

What resorts from the averaging measurements performed, is that as long as the services under consideration do not require high sensitivity, there are significant opportunities. However if it requires high sensitivity then the opportunities significantly decrease. Furthermore the most favourable range is within the 1-2GHz where the occupancy is more sparse, with some band highly used (the cellular ones), in the middle of bands sparsely used. It is worth to point out that the measurements were conducted outdoors, and therefore for indoor service we can logically expect a better situation.

3.4.2.2 GSM bands measurements

The measurements were taken at a distance of 250 meters (measured with GPS (Global Positioning System)) from the nearest GSM base station during school period. This base station covers the University Campus with a population of approximately 15000 students, using GSM900 and DCS1800 bands. Two GSM operators are co-located at this base station belonging to the studied GSM900 band to one operator and the studied DCS1800 band to the other. The measurements were done with a resolution bandwidth of 100 KHz at 501 points covering in excess all GSM900 downlink band. A typical measurement carried out at two different times for GSM900 is shown in Figure 3-14 , and for GSM1800 in Figure 3-15.

The power measurements done for this sectorised base station shows that the power received from the other sectors, is always at least 20dB below (measured in the Broadcast Control Channels (BCCH) which has no frequency hopping).

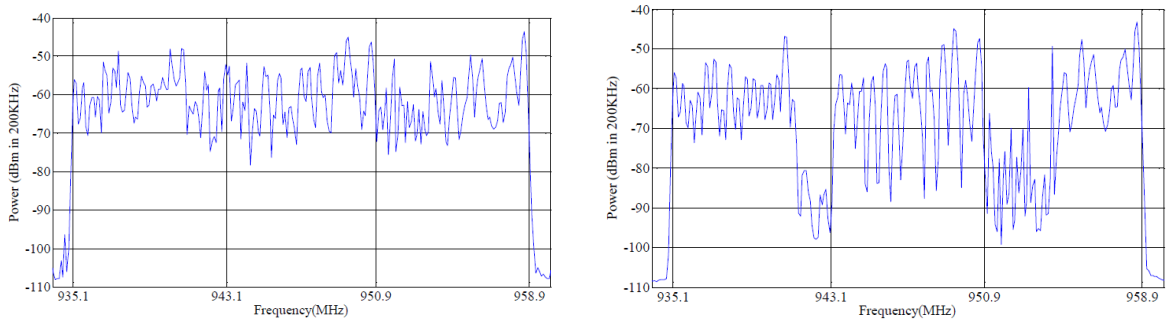

Figure 3-14: Typical measurements for GSM900 (Carried out at two different times of the day).

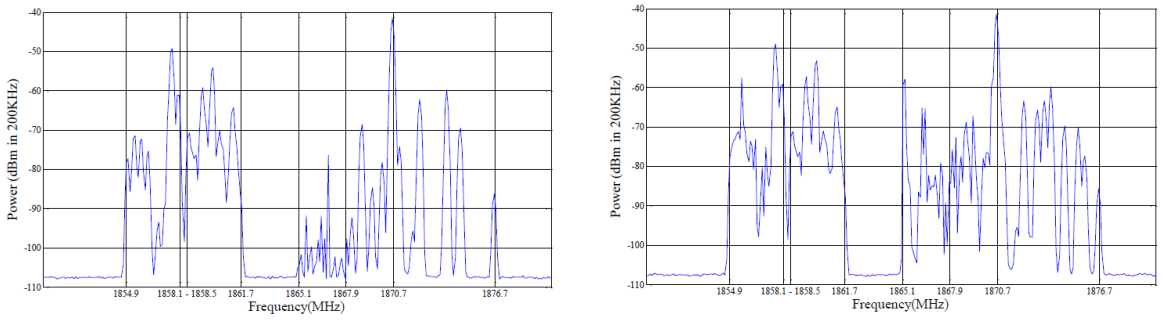

Figure 3-15: Typical measurements for GSM1800 (Carried out at two different times of the day).

To obtain reliable statistics, measurements were made during four consecutive working days and it was observed that the power pattern was similar for the different days. Figure 3-16 shows the power variation for the specific GSM channel 953.9 − 954.1MHz for a full 24h duration.

The processing of the collected raw data, led to the histogram of correspondent power occurrence is presented in Figure 3-17.

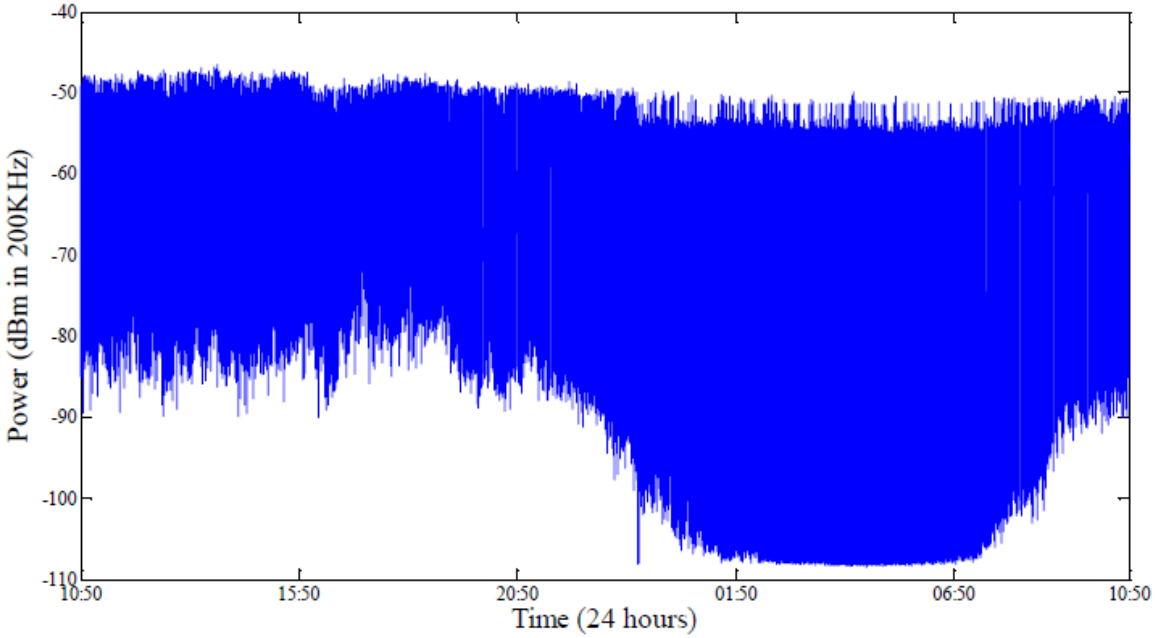

Figure 3-16: Power Evolution for a 24h period within the GSM channel 953.9 − 954.1MHz.

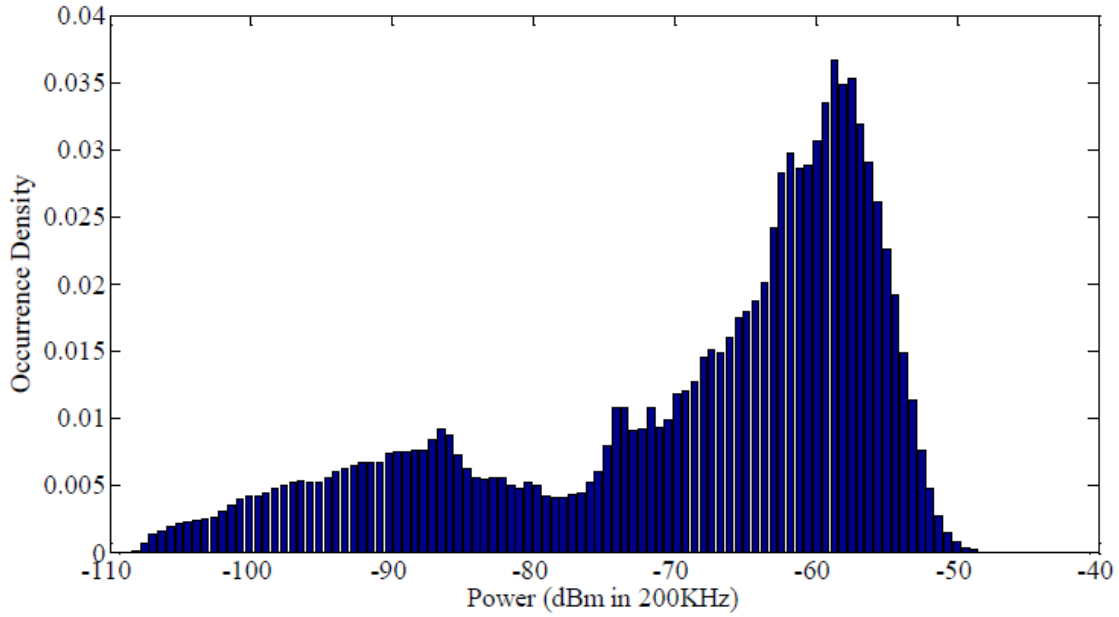

Figure 3-17: Histogram for the observed power levels during a 24h period for the GSM channel 953.9 − 954.1MHz.

The same type of curves is shown in Figure 3-18 and Figure 3-19 for the GSM1800. The channel considered is the 1856.9 − 1857.1 MHz one. For the time statistics a threshold must be defined. The threshold was set approximately 10dB above the noise level, just a few dBs below the minimum level needed to detect the signal with an adequate error probability. The decision level for GSM900 was −98dBm/200KHz and −90dBm/200KHz for DCS1800.

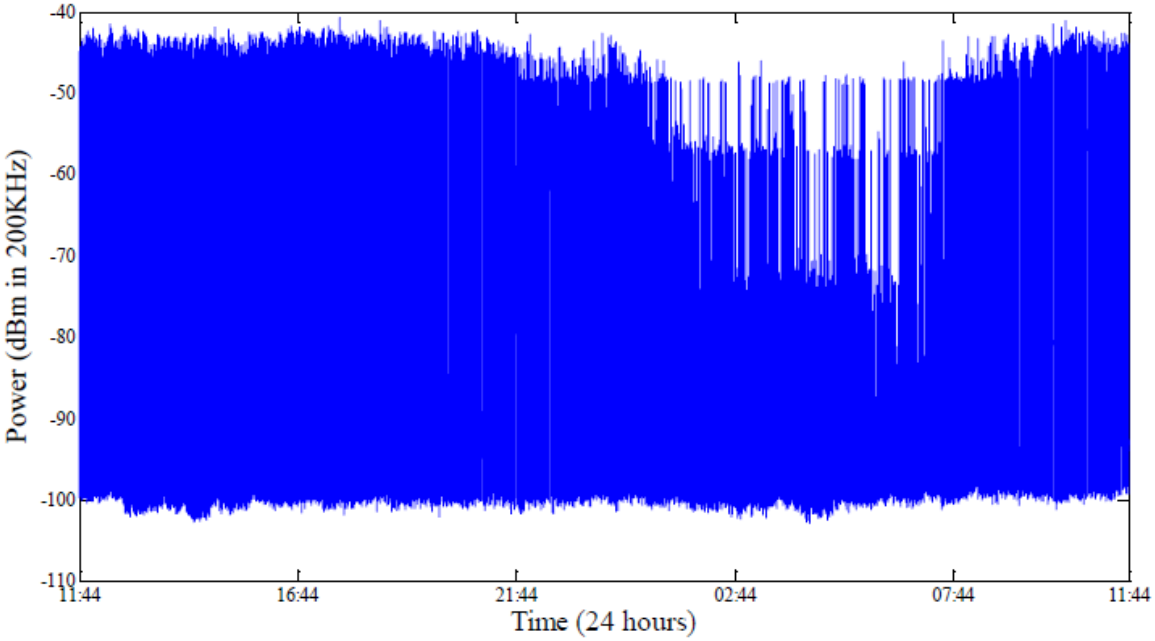

Figure 3-18: Power Evolution for a 24h period within the GSM1800 channel 1856.9 − 1857.1MHz.

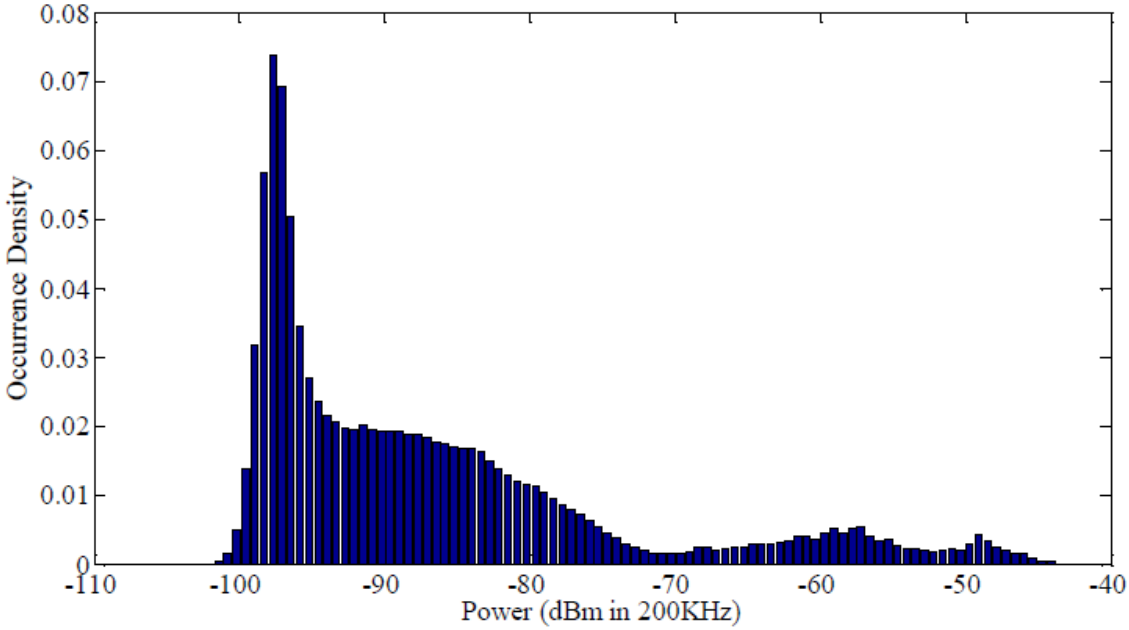

Figure 3-19: Histogram for the observed power levels during a 24h period for the GSM1800 channel 1856.9 − 1857.1MHz.

With the measurements completed, a characterization of the spectrum in terms of occupancy was done. The metrics considered were the duration of the opportunities and the time between them according to what was defined in Deliverable D3.1. An opportunity is considered to be available if the received power is below a given threshold. The thresholds considered were set approximately 10dB above the noise level, just a few dBs below the minimum level needed to detect the signal with an adequate error probability. The decision level for GSM900 was −98dBm/200KHz and −90dBm/200KHz for GSM1800. As the thresholds are below the sensitivity of the GSM receivers, any opportunistic user is ensured that in the region it is operating no user will for sure be detecting GSM signals. An opportunity is considered if the power is below the threshold for the whole duration of one frame.

Figure 3-20 a) shows the time period of opportunities distribution for the measured GSM900 band. It can be concluded that this distribution has an exponential behaviour with the first bin ill-conditioned. The total time of the opportunities is about 50 minutes in 24 hours which indicates high occupancy. About 39 minutes (of 50) is one frame opportunities. Figure 3-20 Figure 3-20 b) represents the correspondent time between opportunities distribution. This distribution has also an exponential behaviour with the first bin ill-conditioned. The exponential behaviour suggests that apart from the ill conditioned low bin, the opportunities appear according to a Poisson process.

The same type of results is shown in Figure 3-21. This distribution presents a deviation from an exponential behaviour and could not be fit to one of the elementary distributions we know. The total time of the opportunities is about 10 hours in 24 hours, which indicates relative low occupancy. About 2.4 hours (of 10) is one frame opportunities. Opportunities longer than 28 GSM frames (outside the horizontal axes represented in Figure 3-21 a)) were identified. Figure 3-21b) represents the distribution of time interval between opportunities. This distribution has an exponential behaviour with the first bin ill-conditioned.

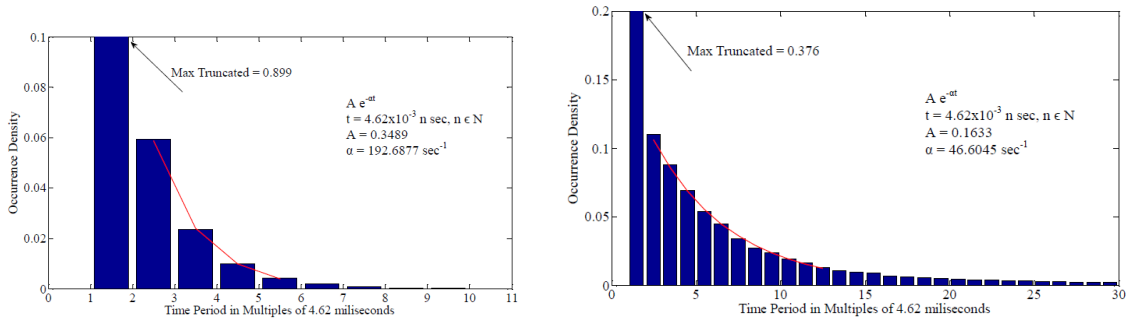

a) b)

Figure 3-20: Statistics about the opportunities in GSM900. Duration of the opportunities a). Time difference between the opportunities b).

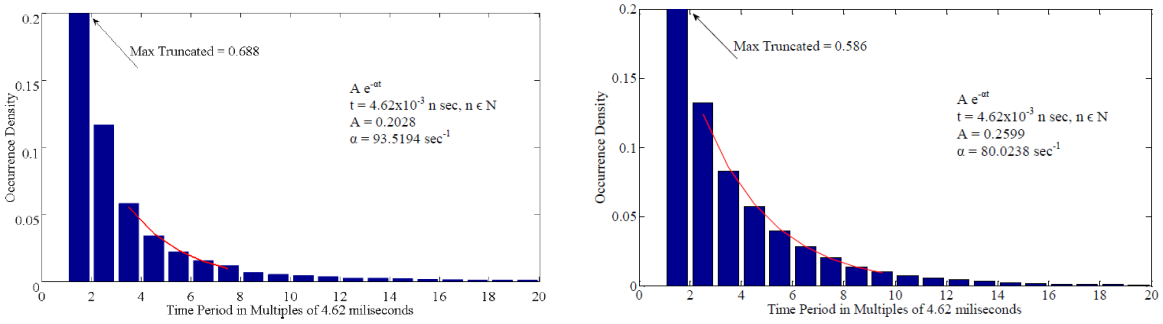

a) b)

Figure 3-21: Statistics about the opportunities in GSM1800. Duration of the opportunities a). Time difference between the opportunities b).

3.4.2.3 Conclusions about opportunities in the GSM bands

The measurements taken and the subsequent processing undertaken, has shown for GSM900 that apart from an ill conditioned lower bin, the distribution of the length of the opportunities as well as their temporal separation follows an exponential distribution. It is well known that an exponential distribution in the number of occurrences is synonymous of a Poisson arrival process. The duration of the opportunities is however very close to one frame (78% of the opportunities detected have the duration of a single frame), and since the occurrence follows approximately a Poisson process, which is known to be memoryless. This means that no predictions can be done by an opportunistic radio about how long the opportunity will last. As an opportunity is defined as the frame duration of GSM (4.62ms), this means that the opportunistic usage of the GSM band would require very frequent sensing (with a time period less than 4.62ms), and therefore it may be very difficult for systems whose basic radio resource has a length in the order of ms. The potential systems that could opportunistically use the opportunities in the GSM band are short packet radio systems. If the length of the packets is below the ms order then an opportunistic radio has time to detect the opportunity, send a packet with length up to the hundreds of ms and detect the occupancy of the band after packet was transmitted. Even if the GSM starts using such a band during the packet transmission it will not be significantly harmed, as at most one time slot of the GSM frame will be disturbed.

In the GSM1800 case, the situation is slightly different. The average duration of the opportunities is much larger (about 7 GSM frames), and cannot be exactly fitted to an exponential distribution. The differences in the average duration are due probably because in the specific site where the measurements were taken, the GSM traffic is mainly carried out through the GSM900. In other places / countries they may be similar to the GSM 900.

As a final conclusion it seems that the opportunistic usage of the GSM band is only viable for short packet radio systems. The reason is that the length of opportunities is so low in the GSM system is due to that fact that it employs slow frequency-hopping and therefore, even if the traffic is low there won't be a frequency that will be free for a long time.

3.4.3 Double setup measurements

The work dome with the single setup of Figure 3-9 was extended to a double setup with the objective of determining the spatial correlation in the measurements. Note that some work related to the same topic was reported in the literature [4][5][6]. The setup is shown in Figure 3-22 and the scenario envisioned is shown in Figure 3-23.

The key difficulty of this spatial extension has been in the synchronization between the different sensors (measuring instruments), since it is crucial to ensure that the differences are due to the spacing and not to the time differences.

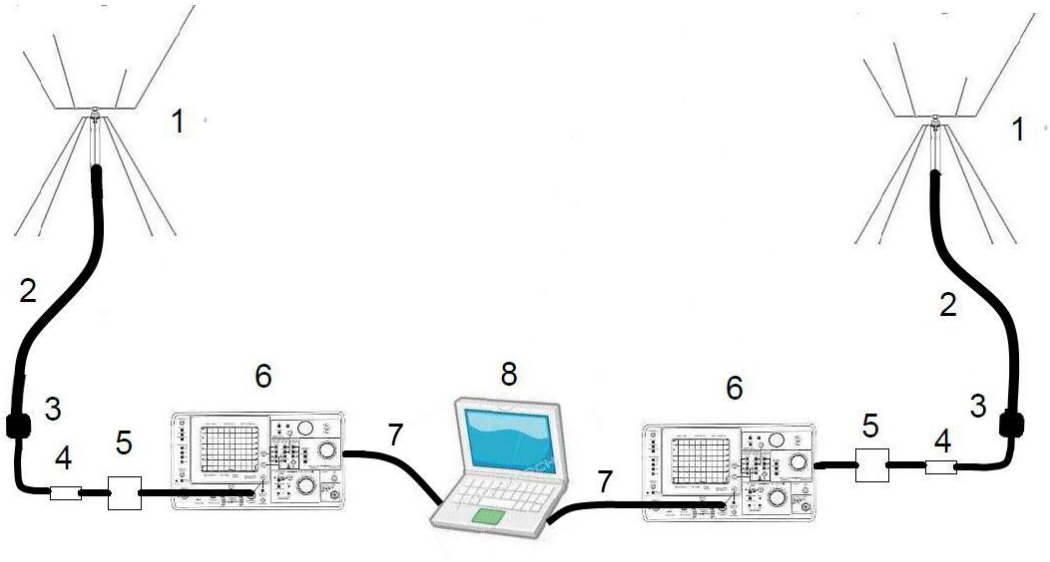

Figure 3-22: Measurements double Setup (1 – M-POL Antenna; 2 – Low Attenuation Cable; 3 – N-SMA Adapter; 4 – Filter; 5 – Pre-Amplifier; 6 – Spectrum Analyzer; 7 – Ethernet LAN Cable; 8 – Portable Computer).

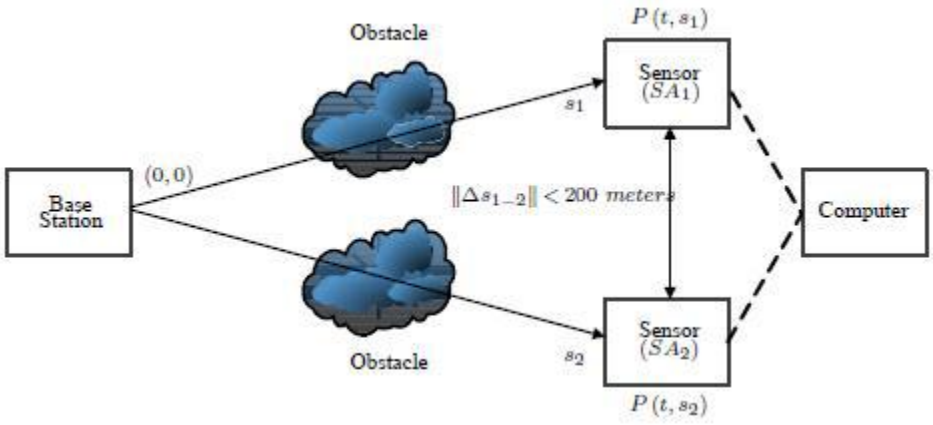

Figure 3-23: Envisaged scenario (SA1 and SA2 are respectively Spectrum Analyzer 1 and 2).

3.4.3.1 The synchronization challenge

Synchronization between the two SAs is mandatory to get the appropriate measurements. A method was developed to measure the relative measurement delays between the two SAs, consisting in sending a square wave to the two pieces of equipment. The used devices were the FSQ8 and FSP40 from R&S. The tests revealed that because of the sweeping differences between the two SAs there is no guarantee of a fixed delay and they can be quite high as shown in Figure 3-24, and therefore unacceptable for the length of GSM frames.

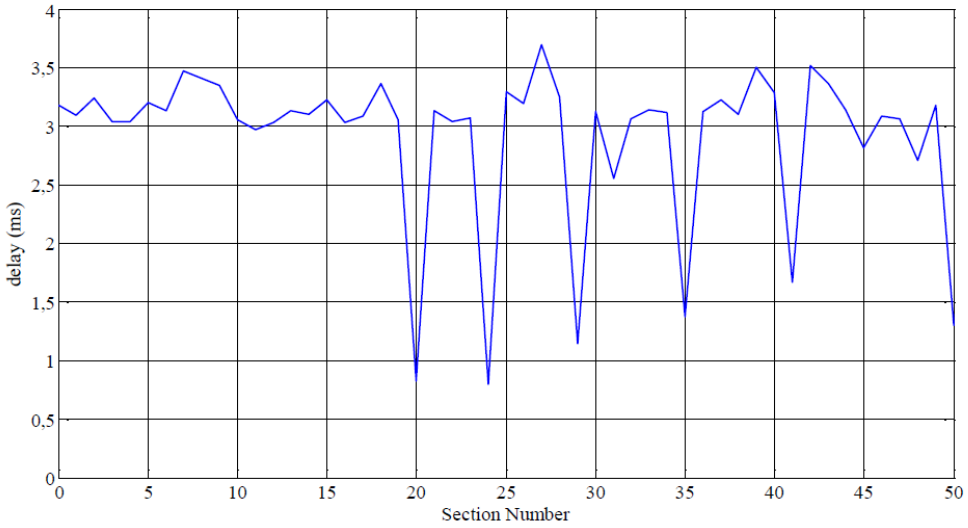

Figure 3-24: Delay behaviour of 50 measurement sets.

To overcome the delay issues, a synchronization method based on the use of an external hardware (HW) trigger was developed as shown in Figure 3-25, where an IO card sends a trigger signal to initiate the measurements. The use of the setup considerably reduces and stabilizes the delay as shown in Figure 3-26.

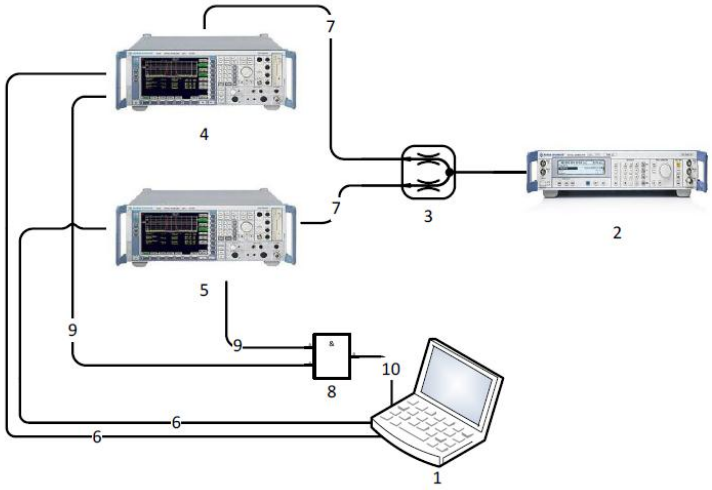

Figure 3-25: Measurement Setup_2 with hardware trigger, 1 - Portable Computer, 2 - Signal Generator, 3 -Signal Splitter, 4,5.

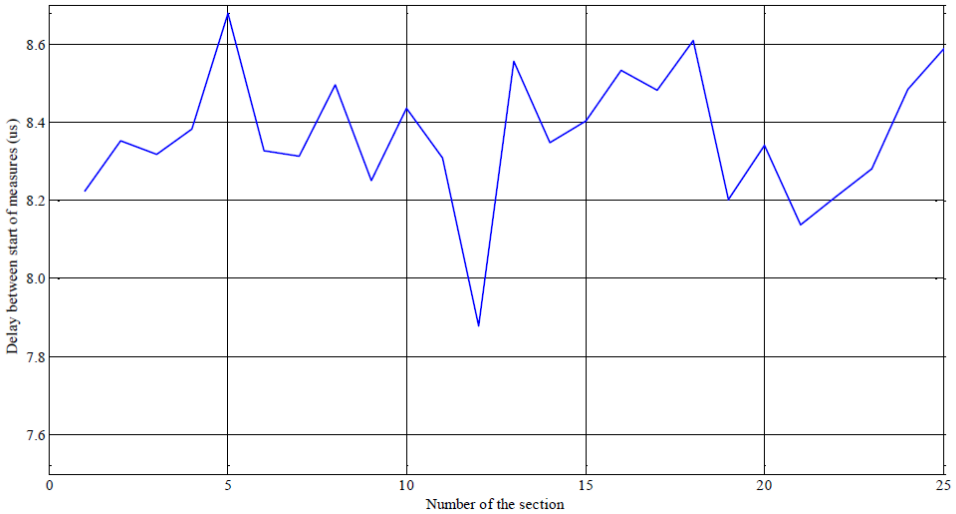

Figure 3-26: Delay behaviour of 25 measurement sections with HW trigger.

3.4.3.2 Measurement results

The double setup was used to perform measurements of the space correlation. The two antennas were placed outdoor separated by 30m. In the campus area no significant obstacles were in view. Power measurements were taken on the 953.9 − 954.1MHz band for several hours and the correlation between the data collected by the two spectrum analysers performed. As in the case of the single setup measurements, they were done with a resolution bandwidth of 100 kHz at 501 points covering in excess all GSM900 downlink band. The correlation presented in Figure 3-27, is a running correlation where each point is taken over 100 measurements. The results show that for the setup selected an outdoor environment with the antennas separated by 30m, the correlation is always very close to 1, and the differences are so small that they can be attributable both to the residual delays between the measurements or the space. In any case it is clear that to really notice spatial differences one has to go either for indoor environments or with the antennas moving.

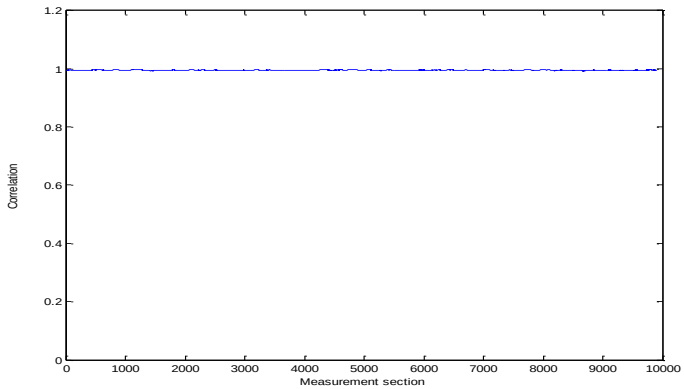

Figure 3-27: Power correlation for an outdoor spacing of 30m.

3.5 Oulu ISM measurements

3.5.1 Introduction

The purpose of the UOULU measurements was to study the 2.4 GHz Industrial, Scientific and Medical (ISM) band occupancy in the city of Oulu, Finland. The city of Oulu locates in the Northern Scandinavia. Most of the existing measurements have been done in big cities. It is important to perform measurements in as diverse set of environments as possible so that results are useful for future cognitive radios (which should be able to operate under diverse operating environments). An additional aspect for the UOULU measurement campaign was to develop new measurement algorithms capable of characterising the Channel Occupancy Rate (COR) more accurately than before.

3.5.2 Measurement Set-up and Equipment

The receiver used in the measurements was the Agilent N6841A RF sensor. The antenna signal was filtered with an ISM band filter and amplified with a Low Noise Amplifier (LNA). During the laboratory testing of the proposed new algorithms, the Agilent E4438C ESG signal generator and the EB Propsim F8 channel emulator were used. The developed programme (called "Spectrum Analyzer") was used for fetching the measurement data from the Agilent RF Sensor, processing it, displaying it, and recording it (all in real-time).

Figure 3-28 toFigure 3-30 present the used antenna, ISM-band filter, RF sensor and low noise amplifier.

Figure 3-28: Linksys 7 dBi antenna.

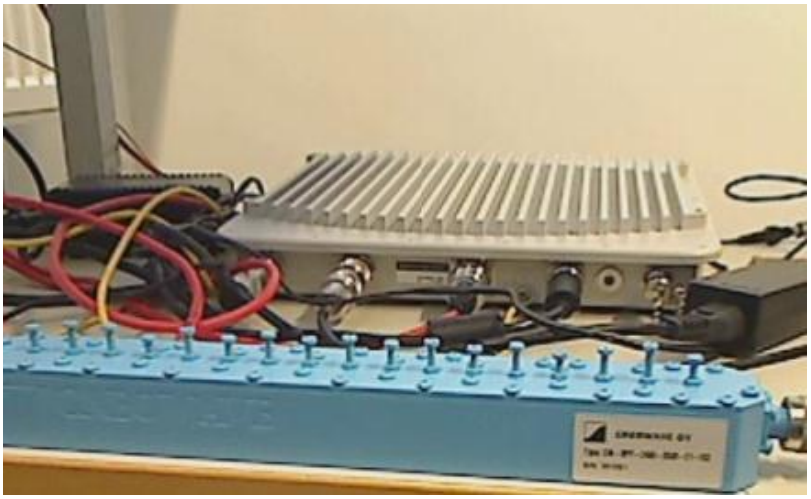

Figure 3-29: Creowave ISM-band filter (front) and Agilent N6841A RF sensor (back).

Figure 3-30: Mini-Circuits ZRL-3500 low noise amplifier (LNA).

Table 3-5: Measurement configuration.

Instrument	Agilent N6841A RF sensor
Centre frequency	2450 MHz
Frequency span	100 MHz
Resolution bandwidth	242.27 kHz
Frequency bin separation	109.3750 kHz
Window type	Gausstop window
Number of frequency points	916
Sweep time	~ 10 ms
Average type	Off
Antenna	Linksys ISM band dipole antenna
Filter	Creowave ISM band filter
Low noise amplifier	Mini-Circuits ZRL-3500
Signal generation	Agilent E4438C ESG + Agilent Signal Studio software
Radio channel emulator	Elektrobit (EB) Propsim F8

3.5.3 Proposed algorithms

3.5.3.1 MED-FCME (Adaptive noise floor estimation)

In [10] an adaptive noise floor estimation method called MED-FCME (median filtered forward consecutive mean excision) was proposed. It is based on the previously known FCME (forward consecutive mean excision) algorithm. Due to the use of median filtering, the noise floor estimates by the MED-FCME have much less variance and are more robust to outliers. The standard FCME can catastrophically fail when there is heavy utilisation of the frequency band. This will reduce the estimation performance and will also severely harm the calculation of channel idle and busy time distributions. It is important in occupancy measurements that the noise floor estimates are robust. The proposed MED-FCME was found suitable for noise floor estimation during several long real-life measurements.

3.5.3.2 Maximum combining (Accurate COR estimation)

Most of the previous spectrum use measurement campaigns have measured Duty Cycles (DCs) for each studied frequency bin. In empirical measurements, it is relatively easy to measure the DC. The average of the DC values is then calculated for the studied frequency band. However, real Cognitive Radio Systems (CRSs) need channels. Due to the throughput requirements of the CRS a channel corresponds to several frequency bins. The average combining of the DC estimates is in many cases not sufficiently accurate for characterising the actual (channel) COR. For example, even if only a part of the channel is occupied, the channel is considered occupied for the CRS since a CRS shall protect the other users. The average combining could lead to significantly too small COR estimate, depending on how narrowband the signal is. Also, since the channels used by the CRS should be flexible and not limited any particular channels used by other users, a CRS channel could have signals from several users. In order to remedy this problem we have proposed maximum combining of the DC values

within the studied CRS channel [10]. This means that the highest individual DC value and not the average value must be used. The accuracy of the maximum based combining was verified in [8] [9] [10] with both laboratory measurements and real measurements.

3.5.3.3 MED-LAD ACC (Enhanced double threshold detection)

In [9][10], MED-LAD ACC (enhanced LAD (Least Absolute Deviation) ACC based on m-dB method and MED-FCME) was proposed. It is based on the localisation algorithm based on double thresholding (LAD) with adjacent cluster combining (ACC). The LAD ACC method is described in Deliverable D3.3. The modifications in MED-LAD ACC include using the robust MED-FCME for noise floor estimation, more flexible threshold setting based on the m-dB principle, and more accurate control of the false alarm probability. The MED-LAD ACC is utilised for COR measurements with the maximum combining.

3.5.3.4 MED-FCME CORε (Hard decision fusion for accurate COR estimation)

In [9][10], the MED-FCME CORε was proposed as a practical alternative to channel energy detection. The MED-FCME CORε is based on recording the full binary matrix of occupancy decisions for each frequency and for each sweep. Due to bit packing and compression the full binary matrix can be recorded even during long measurements. Then COR for any arbitrary CRS channel is obtained by using hard decision fusion of the frequency domain decisions from the same sensor. This is different than cooperative sensing, where hard decisions from several sensors are combined in the fusion centre. Doing the same for standard energy detection would require storing the soft energy values for each frequency bin. In many cases, this is not possible (for example due to storage speed limitations). The results in [9][10] show that the MED-FCME CORε performance loss compared to channel energy detection is not significant. Since it has more practical requirements, the MED-FCME CORε is enabler for accurate COR measurements even in long measurements.

3.5.3.5 Summary of results

Figure 3-31 shows results from testing of the proposed algorithms.

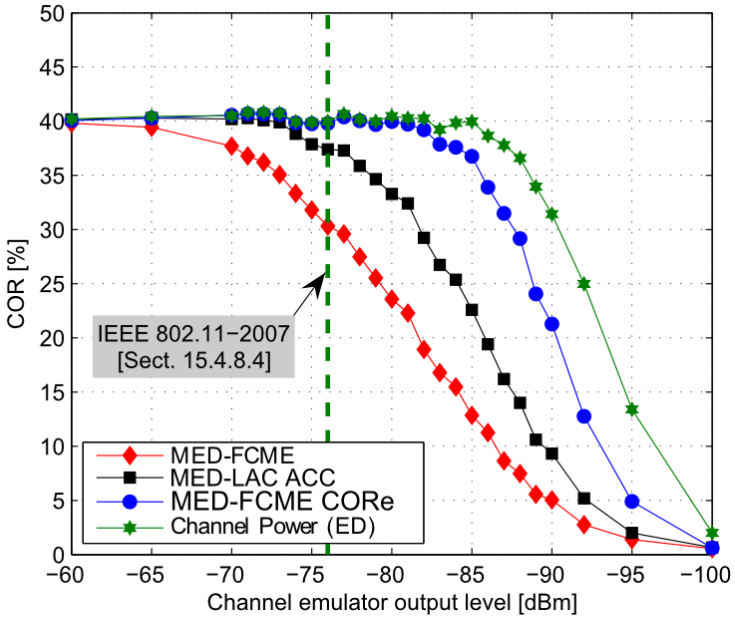

Figure 3-31: Comparison of the performance of the various measurement algorithms.

The IEEE 802.11b signal was generated with a signal generator and the signal was passed through a channel emulator before being fed to the input of the measurement system. The channel utilised herein was the ETSI BRAN WLAN (Wireless Local Area Network) Channel Model A [7] and the considered CRS channel was 15 MHz wide. The results show that the proposed hard decision fusion method (MED-FCME CORε) gives almost as good performance as the channel power based detection method while being significantly more practical. It can also be seen that the MED-LAD ACC method based on two thresholds (upper and lower) gives much improved performance as compared to the method using standard single threshold detection (MED-FCME). Figure 3-31 shows with the dotted line an energy detection threshold specified in the IEEE 802.11-2007 standard for clear channel assessment. It can be seen that apart from the single threshold detection approach the considered methods give performance equal to or exceeding the standard requirements. Thus, the performance of the measurement setup can be considered as sufficient for accurate COR field measurements.

3.5.4 Measurement campaigns

Several one-week long measurements were carried in diverse locations. The studied locations included the Oulu Airport (second biggest airport in Finland), the University of Oulu campus (including a library), and the city centre of Oulu. The results from these measurements have been used, for example, in 0 where the Measurement, Modeling, and Emulation (MME) Approach has been proposed for evaluating CRSs. Therein, WLAN channels at ISM band were studied. Figure 3-32 toFigure 3-34 present some example snapshots about the occupancy measurements at WLAN channels.

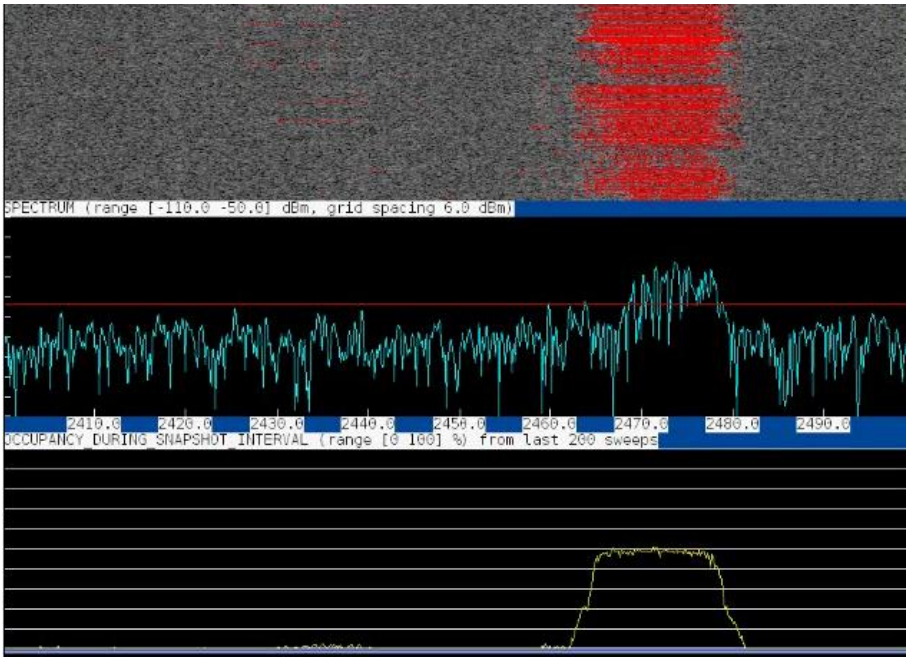

Figure 3-32: WLAN traffic generation with 50% reference occupancy. Spectrum analyzer, one snapshot. On the uppermost picture, red lines denote detected WLAN signal. In the middle, red line is the detection threshold which has been estimated adaptively using some threshold setting method. There is one WLAN signal at 2.47 GHz. On the lowest picture, occupancy from last 200 sweeps is presented. Therein, one horizontal line denotes 10% occupancy (10 lines=100%).

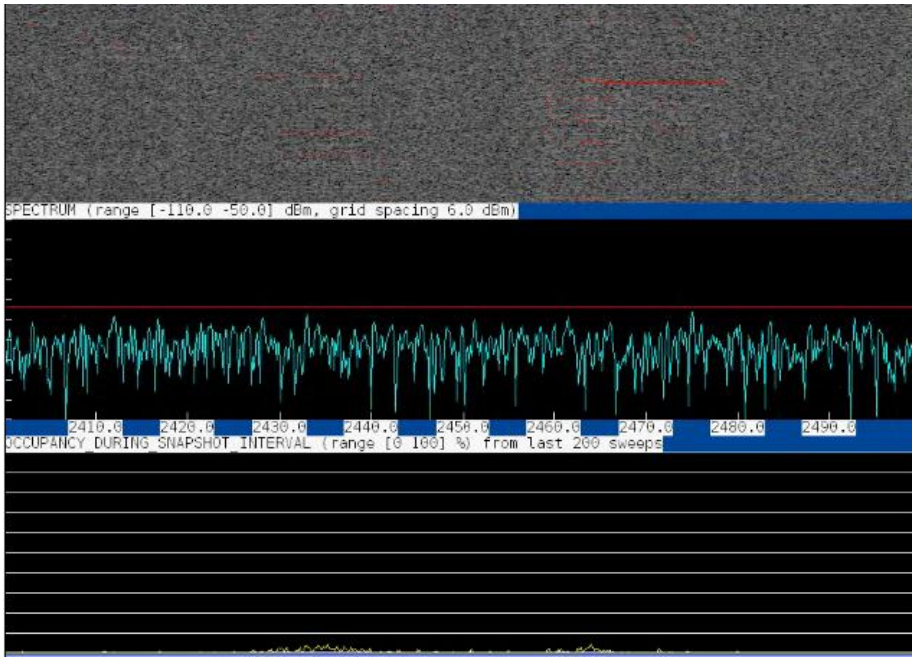

Figure 3-33: Transmitter switched off. Spectrum analyzer, one snapshot. Now, there are no WLAN signals.

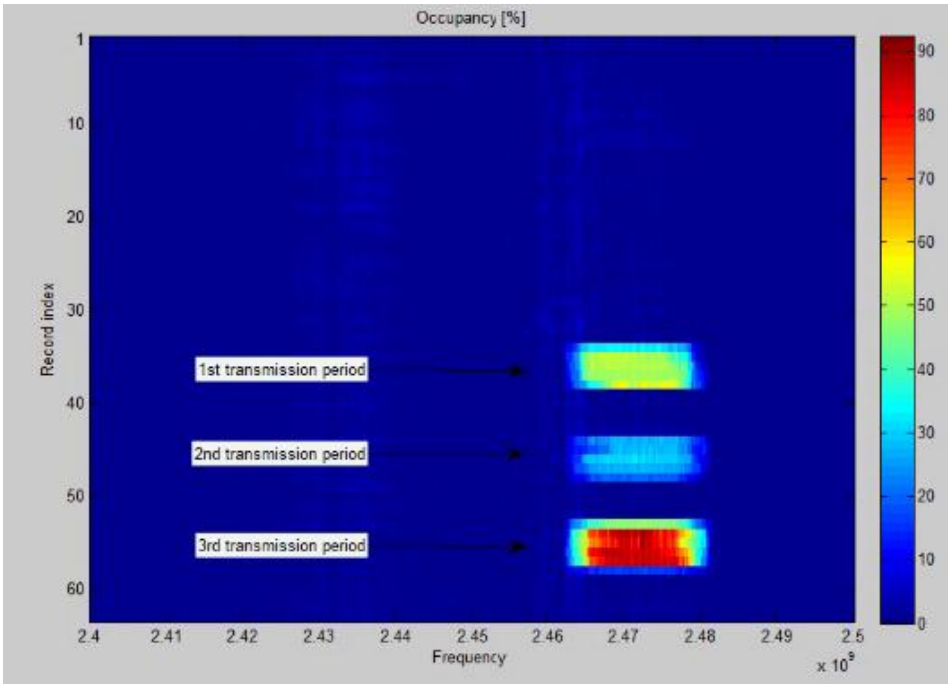

Figure 3-34: Occupancy results in the Matlab, one example. At the 1st transmission period, there were 50% reference occupancy, as in the 2nd transmission period, reference occupancy was 30%. At the 3rd transmission period, peak traffic was considered.

As an example, some results from the Oulu Airport[1] measurements are presented. The measurement duration was one week and the measurement was performed in early November 2011. The studied frequency range was 2400-2500MHz.

Figure 3-35 shows the average spectrum occupancy during the whole measurement. The busiest hour occurred on Wednesday 2nd of November from 17:00 to 18:00 o'clock (results shown in Figure 3-36). Traffic was identified in WLAN channels 1, 6, 9, and 11. Actually, one access point was changing its channel from 11 to 6 and back, even several times per hour. This is likely due to automatic frequency setting in the access point.

The jumping is illustrated in Figure 3-37 and it mainly occurred during idle periods. When there was some traffic, the signal usually stayed on the channel 11. There was also a possible IEEE 802.15.4/Zigbee signal with centre frequency 2465 MHz.

Figure 3-38 shows the average channel occupancy for each WLAN channel during the whole measurement (including the effects due to the overlapping of WLAN channels). The measurements showed rather high spectrum occupancies in Oulu airport. However, results still look promising for sufficiently intelligent cognitive radio systems capable of avoiding other users' signals.

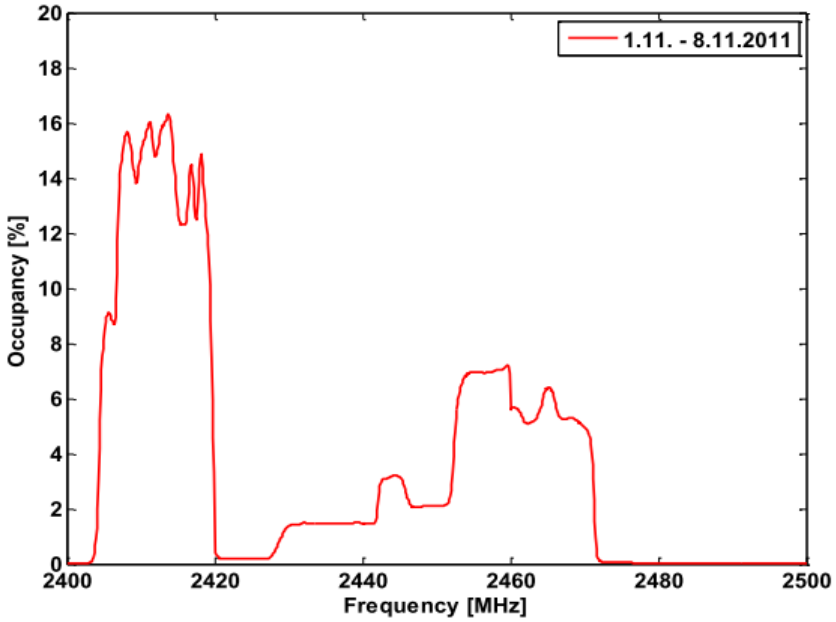

Figure 3-35: Average spectrum occupancy during the whole measurement, resolution bandwidth 242.27 kHz.

[1] The Oulu team wishes to thank Finavia Oyj for their support.

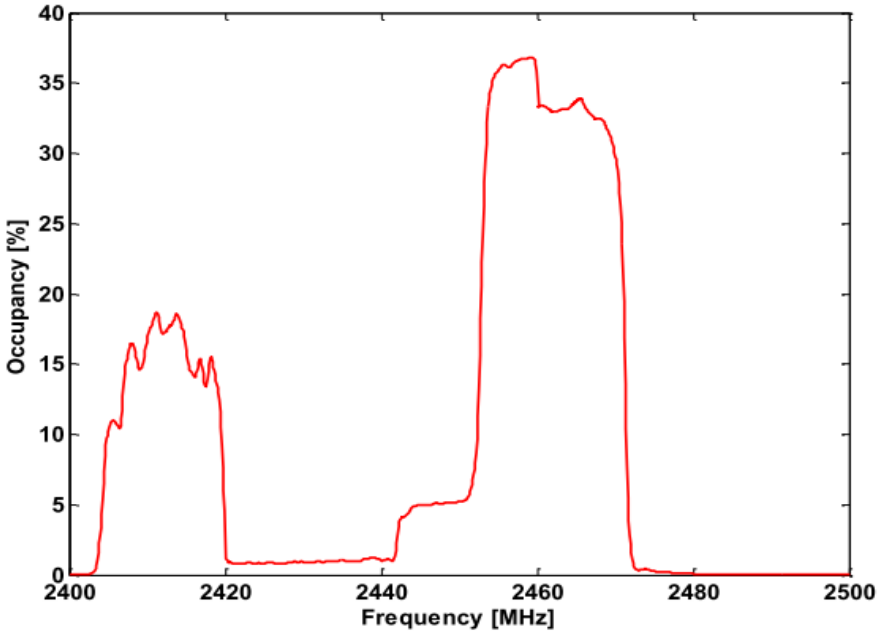

Figure 3-36: Average spectrum occupancy during Wednesday 2nd of November from 17:00 to 18:00 o'clock.

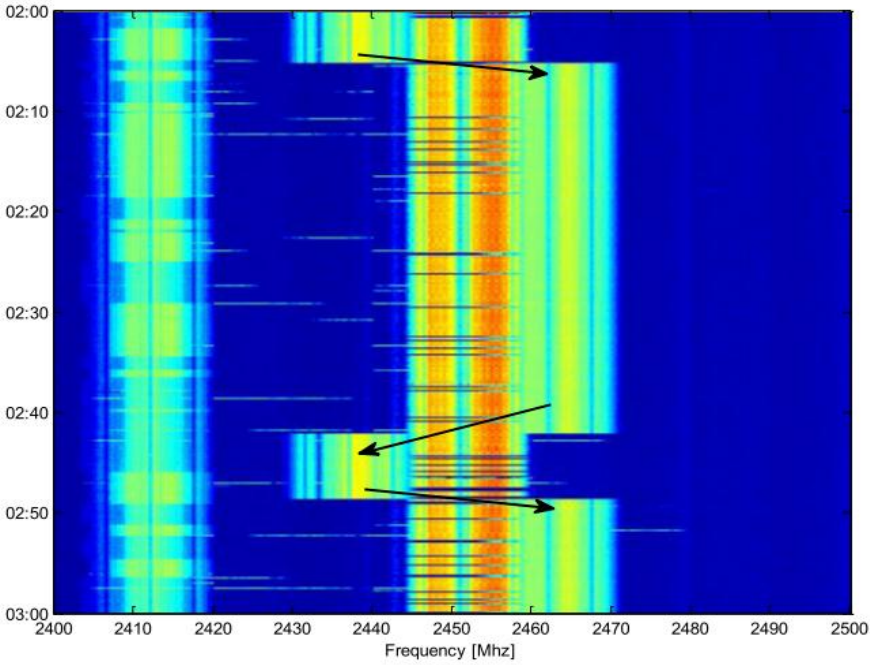

Figure 3-37: Maximum received power, time period 02-Nov-2011 02:00-03:00.

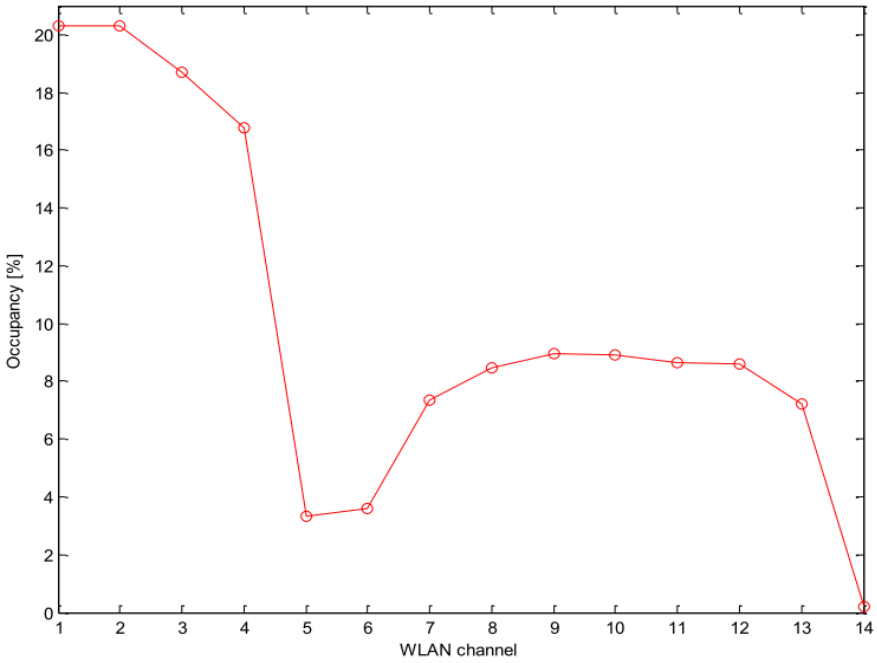

Figure 3-38: The average occupancy of WLAN channels during the whole measurement.

3.6 Exploitation of polarisation in Cognitive Radio devices

Interference management in cognitive radio network is the main challenge for secondary exploitation of spectrum. The research work embarked upon in this section investigates the cognitive exploitation of Television White Spaces (TVWS); in particular the use of polarisation in cognitive radio devices and its effect on quantifying the available TVWS in a particular geographic location. Interference from primary users in particular can be affected by the polarisation of the antenna device concerned. Results are presented in this document from measurements undertaken in three separate areas in Guildford, UK, which show the possible opening of white spaces in a horizontal polarisation when opposite to the polarisation of the television transmitter. Both vertically and horizontally polarised television transmitters are considered in this study.

3.6.1 Introduction

Digital broadcasting uses channels between 465MHz and 860MHz, where different fixed carriers are used in different geographical locations so that at the edge of broadcasting regions, interference is not caused. This therefore creates a highly inefficient usage of the frequencies within this spectrum such that in a given location, there will be television channels which are used in another far away region and thus could not be received with a suitable signal to noise ratio by a television receiver in the given location. Therefore the spectrum of such channels can be considered unused for that location and potentially could be used by other radio devices transmitting over a short range. These sections of frequency spectrum are known as television white spaces.

Cognitive radio devices will therefore be able to intelligently determine which frequency bands are suitably within a TVWS and thus communicate with other cognitive radio devices within that band. There are a variety of ways in which the radio system could do this, one such way is to use a geo-

location database, from which it could determine which channels are unused based on using global positioning system (GPS) data. Another alternative, particularly where GPS data is not available, is to use "frequency sniffing" whereby two radio devices communicating with each other can first detect whether there is a frequency transmitted below a given threshold. However, such techniques do carry a risk with regards to potentially causing interference to television receivers at a frequency they select.

One practical application where cognitive radio devices could be deployed in the future is for long range WLANs in outdoor open areas, which would have a transmission range up to 200m. In some cases these are known as "Super WiFi" systems [11]. This is particularly important to exploit in areas such as railway stations and congress centres where demand for WLAN usage is high and thus the available TVWSs could be readily used to help cater for wireless systems demanding more spectrum availability.

Given that television channels have historically been strictly reserved for the usage of television, there is significant controversy with regards to whether the broadcasting network (primary or incumbent user of the frequency spectrum) will be degraded in its provision due to harmful interference being caused by cognitive devices (secondary users). There are three issues in particular, which have to be noted in this regard when exploiting cognitive radio:

1. The secondary user has to reliably find a white space in the location they are based, whereby it is aware of what received power, if any, the device will receive from the nearest television transmitter using the selected frequency band.

2. The secondary user must not cause harmful interference to the primary user (i.e. television receiver) if it is using an adjacent channel. The primary user is particularly vulnerable in this instance given that the receiver sensitivity is likely to be significantly higher than that of the secondary user. Furthermore, the antenna may have a higher gain if external to the building, while also television receivers using cable connections will also have similar vulnerabilities because the feeder cables are often "leaky" and thus can act as antennas to receive harmful interference from a nearby cognitive device.

3. Two or more CR users may be in proximity to each other, in which case interference between the devices must also be minimised by means of suitable resource allocation and radio access schemes.

The first two of the above points are particularly important and it is necessary to implement all possible measures to avoid risk of harmful interference to the primary user while also maximising opportunity for the secondary users. This research therefore considers how polarisation can be exploited first of all to widen the choice of white spaces by which the secondary user is not interfered by the primary user, while also in turn will consider how the interference to the primary user could be minimised. The measurement details taken in three outdoor locations in Guildford, UK, are herein presented with a further analysis to demonstrate the benefit of exploiting polarization for cognitive radio devices.

3.6.2 Outdoor Measurement Setup

A measurement campaign was set up to measure the TVWS data across the whole UK band for digital broadcasting from 465MHz through to 860MHz using a handheld spectrum analyser and a set of suitable antennas in order to analyse the differences in polarisation. The measurements were undertaken during the summer period in three outdoor locations in Guildford, which is south west of London and within range of several television transmitters.

The three locations in Guildford are named and described as follows:

- Cathedral – Guildford's main cathedral is on the outskirts of the town and based upon one of the highest hills in the area, thus it is well positioned to pick up transmitted television signals from a wide area. Furthermore, there is also a line of sight between the position outside the cathedral and the nearest television transmitter (though it is obstructed by vegetation). This is illustrated in Figure 3-39 (a) where the picture is taken outside the front entrance to the cathedral.

- Stoke Park – An open parkland area situated near to the centre of the town, approximately 1.5km away from the nearest transmitter shown in Figure 3-39 (b). The location is again on a high point, where several television signals could be received over a wide area.

- North Street – This is one of the main shopping streets based in the centre of Guildford, shown in Figure 3-39 (c). There is not a direct line of sight to the transmitter in this instance, thus the blockages from buildings are likely to create more open white spaces compared to the other two locations.

An indoor location was not chosen in this measurement campaign. The reason for this was because the likelihood of high de-polarisation as well as high penetration loss, the majority of television transmissions other than the local ones do fall below the noise floor in general. Therefore only outdoor locations were chosen, where such WLAN systems are likely to be exploited.

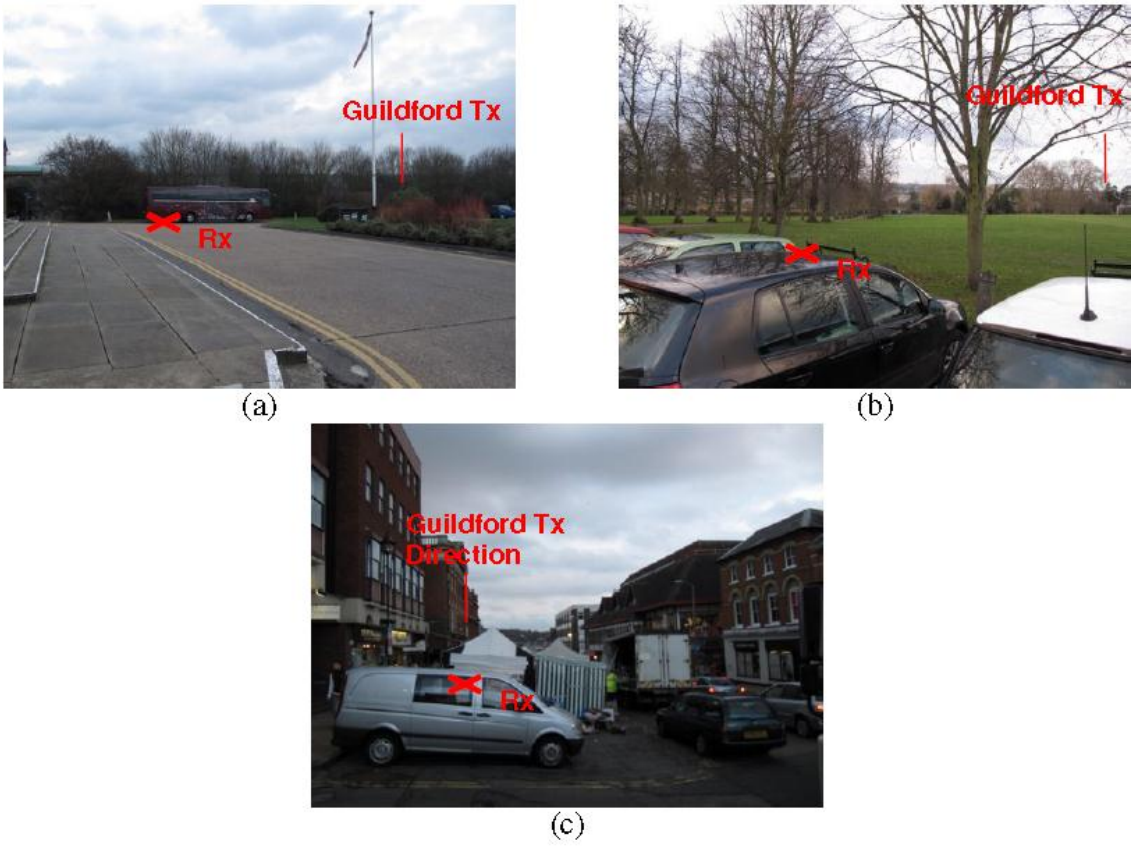

Figure 3-39 : Photograph of the three measurement areas chosen: (a) Cathedral, (b) Stoke Park and (c) North street.

Measurements were undertaken using a handheld spectrum analyser sweeping over the whole band with a resolution bandwidth and video bandwidth of 10 kHz. This was chosen so as to ensure there was both high dynamic range, while also fast sweep time to first take measurements with one polarisation and measurements in the other polarisation. On the day chosen, the weather was dry, with no clouds and sunshine, thus the tropospheric effects were not present while also during the middle of the day, effects of ionospheric refraction would be suitably constant such that, where the measurements were repeated in each case, and there was less than 2dB variation. Such low variation was important in order to ensure fair comparison between polarisations.

To measure the two polarisations, it is necessary to have a polarisation pure antenna to measure both vertical and horizontal polarisations over the whole frequency band. Such an antenna is difficult to build, thus a set of six dipole antennas were used to measure sections of the whole television band at centre frequencies of 470MHz, 540MHz, 590MHz, 640MHz, 700MHz and 750MHz. Each of the antennas were tested for suitable impedance matching and constant gain over the bands they were used for. Since each antenna was used for a separate measurement, three different polarisations were measured one after the other, first of all the dipole was oriented vertically as shown in Figure 3-40 (a), after which two horizontal polarisations were measured as shown in Figure 3-40 (b) and (c). The purpose of rotating the antenna 90^{o} in azimuth in this case is to ensure that if a horizontal polarisation was arriving in the same direction as one of the "nulls" in the dipole gain pattern, then the other measurement would pick up such scenarios. This is clearly not allowing a full comparison of the vertical and horizontal polarisation, since it is well known that the most suitable way to measure the horizontal polarisation Omni-directionally is to use a loop antenna [12]. However, the gain of such an antenna is not comparable to that of a dipole and is therefore difficult to calibrate. Thus in the case of cognitive radio systems, it is necessary to consider a "best case scenario" whereby practical antennas could receive either a vertical polarisation or as much horizontal polarisation as possible. This is comparable to polarisation diversity systems where by the polarisation aspect is inherent within the angular system [13]. Thus measurements are being taken with regard to evaluating whether different polarisations could be exploited if a cognitive radio device was capable of switching between vertical and horizontal linear polarisation.

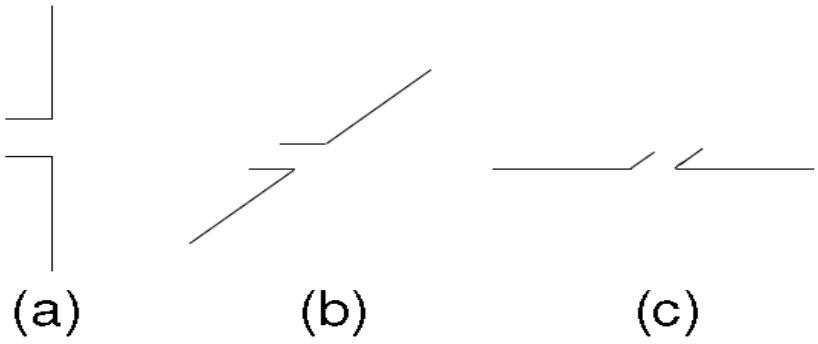

Figure 3-40 : Illustration of Dipole Orientations for the (a) vertical polarisation, (b) horizontal polarisation and (c) horizontal polarisation with 90° re-orientation

For the three locations chosen, it was expected that there is a high likelihood there would be a mix of polarisations over the whole frequency band, which is evidenced from analysing the polarisation of the television transmitters within 25km of Guildford, while also not obstructed by hilly terrain. As can be seen in Table 3-6, only five out of the twenty one transmitters are horizontally polarised, where it is also shown that all channels are widely spread over the television broadcasting spectrum. Though two of the horizontally polarised transmitters have the highest power, they are both more than 10km away from Guildford and thus would not be significantly dominant. Taking the data presented in Table 3-6,

it is therefore expected that the vast majority of measurements taken will be stronger in the vertical (V) polarisation, given only one fifth of the transmitters are horizontal (H).

Table 3-6 : Transmit channels, polarisation and power levels for transmitters within 25km of Guildford not obstructed by hilly terrain. Data obtained from www.bbc.co.uk/reception/transmitters

Location	Channels				Transmit power	Polarisation
Crystal Palace	26	33	23	30	1000kW	H
Dorking H	51	44	41	47	55W	H
Old-Coulsdon	48	64	45	66	6W	H
Sutton	55	62	59	65	9W	H
Midhurst	61	55	58	68	100kW	H
Biggin Hill	45	52	49	67	12W	V
Caterham	55	62	59	65	35W	V
Croydon	49	56	52	67	33W	V
Dorking V	51	44	41	47	14W	V
East Grinstead	40	56	46	59	117W	V
Greenwich	56	50	52	48	15W	V
Guildford	40	46	43	50	10kW	V
Hammersmith	48	62	59	65	10W	V
Micklefield	54	64	57	67	8W	V
Mickleham	61	55	58	68	100W	V
Orpington	55	62	59	66	15W	V
Reigate	57	63	60	53	10kW	V
Sutton	55	62	59	65	9W	V
Wonersh	48	65	52	67	25W	V
Woolwich	57	63	60	67	630W	V
Haslemere	22	28	25	32	15W	V

3.6.3 Measurement Results and Inferences

To give an overview of the measurements taken, the dBm power measurements for the whole television band taken at the cathedral as an example are compared for all three polarisations in Figure 3-41. Clearly it can be shown for a number of cases that there are considerably different power levels as high as 10dB ratios or more when comparing vertical and horizontal polarisations. In some cases

there are higher signals in the horizontal polarisation, while also it is observed that the signals are generally higher between 610MHz and 720MHz, within which the channels for Guildford are contained and demonstrate a stronger vertical polarisation.

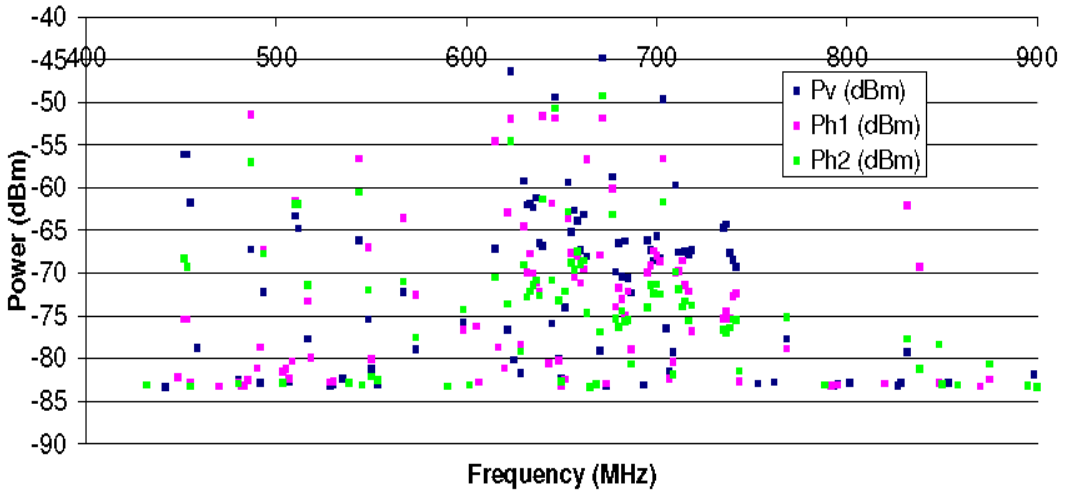

Figure 3-41 : Example measurements taken for the vertical and two horizontal polarisations

A further useful comparison to make is to take each frequency and compare the vertical and horizontal polarised power levels on a scatter plot like that in Figure 3-42 for the Cathedral location. Two separate scatter plots are taken in this case, one where the vertical power is compared with the power of the first horizontal polarisation while in the second case; the vertical power is compared with the second horizontal polarisation. In both cases, there are instances where the vertical is stronger than the horizontal (i.e. below the line) while also in fewer cases the horizontal is stronger than the vertical (i.e. above the line). In cases where either the horizontal or vertical are at a value of -100dBm, this is where the signal of one of the polarisations fell below the noise floor of the spectrum analyser and thus no real comparison can be made.

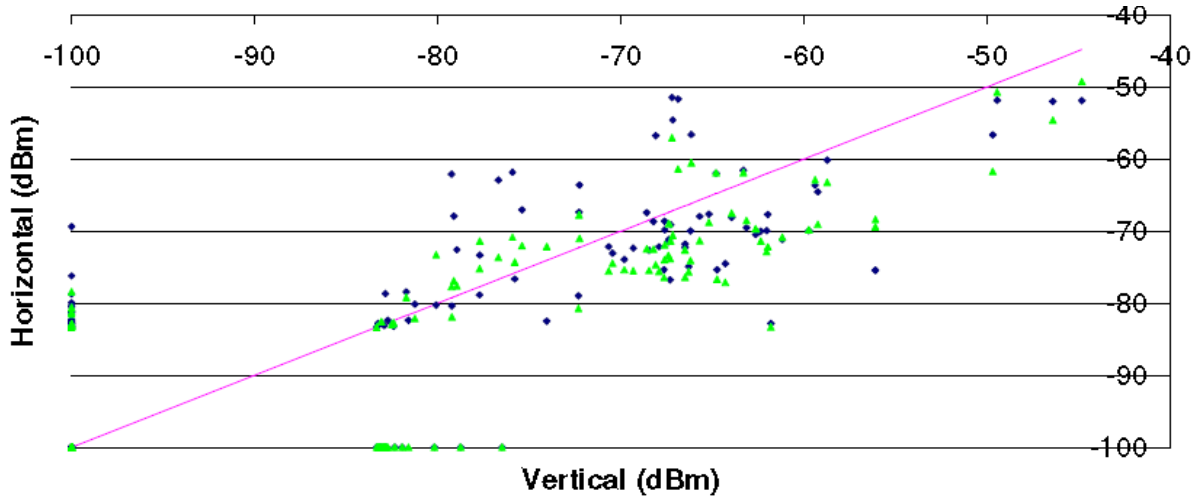

Figure 3-42 : Scatter plot showing direct comparisons of vertical and horizontal power at fixed frequencies in the Cathedral location

It is also interesting to compare the signals from the Guildford transmitter for the three locations shown in Figure 3-43, Figure 3-44, and Figure 3-45. In each case, the three areas are compared with the same polarisation. From observing each figure separately, it is evident that when comparing the Cathedral and Stoke Park cases with the North Street case, the higher built up environment in the North Street case has a number of frequencies where the television signal is attenuated significantly down to the noise floor. At the same time, some of these frequencies can be compared between polarisations in all three figures, whereby even in the urban area of the North Street scenario, there are comparable differences between the vertical and horizontal polarisation, which are worthy of investigation collectively over the whole frequency band.

To gain a general overview of the power ratio from vertical to horizontal polarisations received from television transmitters, a Cumulative Distribution Function (CDF) curve has been derived where the vertical polarisation is compared with both of the horizontal polarisations in each location, thus there are six separate curves for the vertical to horizontal power ratios plotted in Figure 3-46.

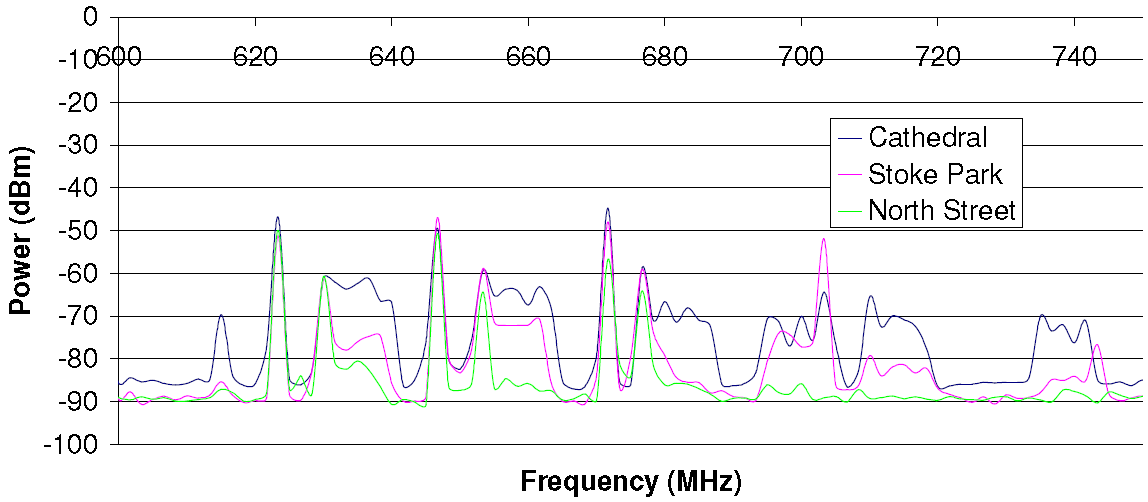

Figure 3-43 : Comparison measurement for vertical polarisation of the three areas

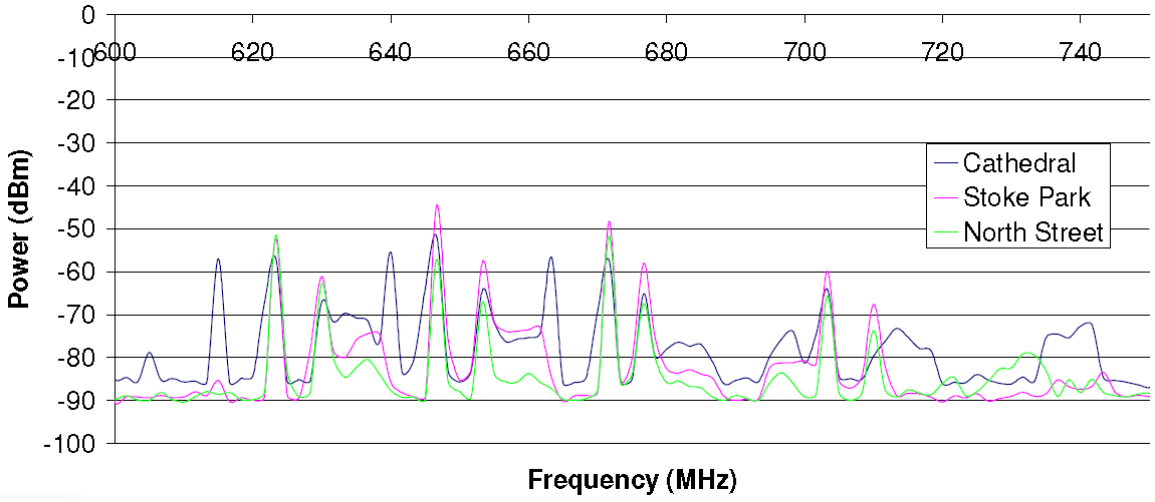

Figure 3-44 : Comparison measurement for the first horizontal polarisation of the three areas

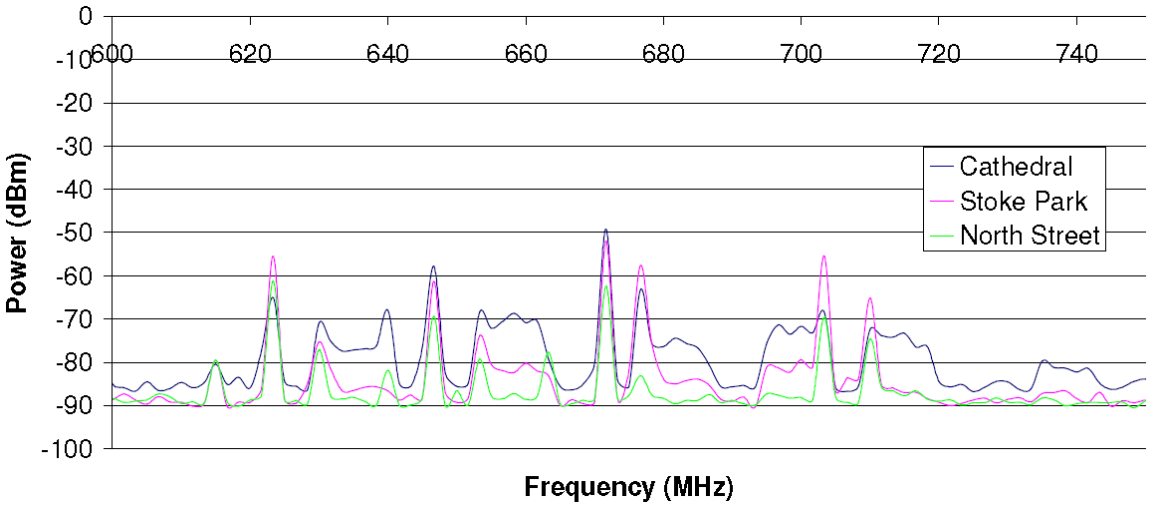

Figure 3-45 : Comparison measurement for the second horizontal polarisation of the three areas

Before analysing the results it is important to note two important factors regarding the data analysis. In all cases, the channels from the Guildford transmitter were included. Though these would not by any means be used by a cognitive radio device, they are still valid to apply for this analysis because the ratio of the two polarisations are being compared, the actual power level of the two polarisations would only be different if the same transmitter was further away and thus the effects of the local scatterers would still be the same, which is what is of particular interest, thus they have been included. A second point to note is that for channels where the weaker polarisation fell below the noise floor, such cases were not included in generating the CDF curve as no true comparison could be made.

Therefore by analysing the curves in Figure 3-46, the following observations can be made:

- All curves crosses 0dB ratio point with a cumulative probability value of 30-35%. This therefore means that for approximately one third of all channels, the vertical polarisation is weaker than the horizontal polarisation and therefore for approximately two thirds of the time (i.e. 67%), the horizontal polarisation is weaker than the vertical.

- Given the above analysis, the horizontal polarisation is vulnerable to less interference from television transmitters in the majority of cases, while it can be further analysed from the curves that in 30% of the channels, the vertical power is 6dB higher than the horizontal.

- Finally in approximately 10% of cases, the vertical is 10dB higher than the horizontal.

For the first case of the Cathedral measurement, the curve is clearly different from the other curves for cases below 0dB. This is due to the high height of the hill enabling reception of horizontal channels with the dipole antenna at the given orientation.

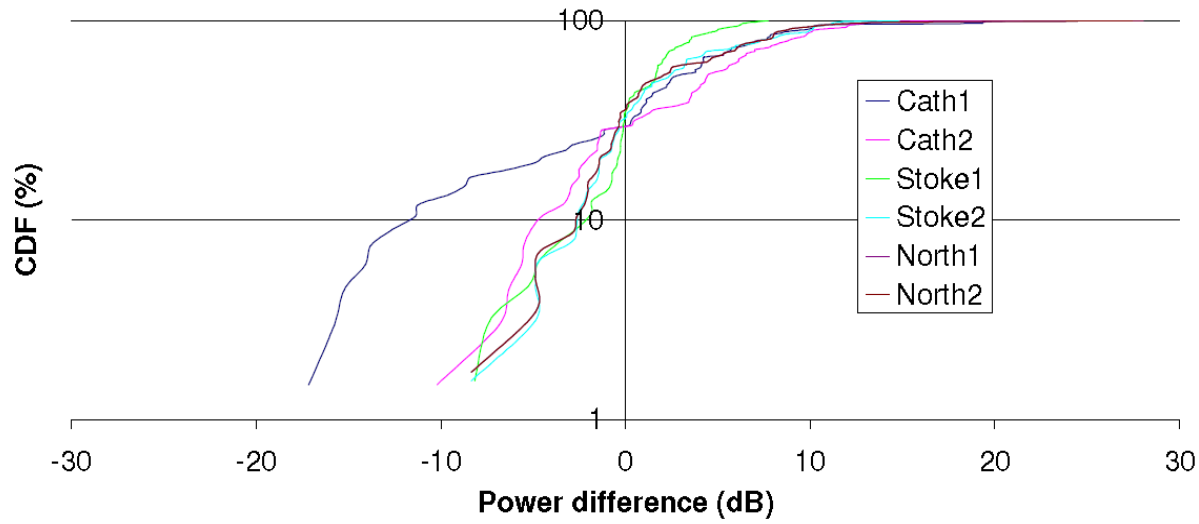

Figure 3-46 : Cumulative distribution plot of the vertical power to horizontal power aggregated over all frequencies

3.6.4 Conclusions

In summary, a set of TVWS measurements have been conducted in three outdoor areas in Guildford, UK, which indicate that due to the vastly higher proportion of vertically polarised television transmitters, the scope for available white spaces for outdoor WLAN systems would have higher opportunity by use of horizontally polarised antennas in two thirds of all cases. In situations where cognitive radio systems were used in urban environments, they would also most likely benefit from using the opposite polarisation to the television transmitters in the local area, since there is chance that interference to primary users would be minimised.

3.7 Statistical models of spectrum opportunities for Cognitive Radio

The research work presented in this section deals with the development of models to characterise the number of spectrum opportunities available using the probability and approximation theory. The Probability Mass Function (PMF) is derived for the total number of spectrum opportunities available depending on the probability of each channel being free. Further analysed is the complexity involved in calculating the PMF of the total number of available channels at any time and location and develop approximate models. Numerical results are provided showing that the proposed approximation models of spectrum opportunities achieve good accuracy at significantly lower computational cost.

3.7.1 Introduction

A number of spectrum measurement campaigns have been carried out in past, unfortunately most of them covered only a few hours and specific locations, thus they could not provide true estimates of spectrum opportunities in a concrete spatial and temporal domain e.g. see [14], [15]. To develop cognitive radio systems that are not restricted to certain locations, further measurements are required. Similar arguments and gaps were also identified by other researchers [15]. Further, the equipment, man power and infrastructure needed to perform such measurements can be excessively expensive and cannot be performed by many members of the research community. An alternative is to develop statistical spectrum opportunity models for a general case, using statistical prediction to estimate the

behaviour of the incumbent users. Moreover, by properly exploiting spectrum opportunity models, performance of spectrum sensing can be significantly improved. The incumbent user occupancy in the entire spectrum is very difficult to calculate based on spectrum sensing only due to its time complexity, as the larger the bandwidth to be scanned, the higher will be the time needed for sensing. Further, sensing a very large bandwidth is energy consuming. It has been shown in the literature that instead of sensing the entire radio spectrum, one can exploit knowledge of historical data to select the most appropriate portions of spectrum and limit the scope for further sensing [16], [17]. According to [16] adaptive sensing based on historical data can improve the probability of choosing the free channel by up to 70%.

Spectrum occupancy analysis using Markov and Semi-Markov chain representation was done in [17] with Poisson and Poisson-normal process implementation of spectrum utilisation considered in [18]. In [19], the authors used conventional URN models for channel occupancy and proposed novel search algorithms. However, the authors used fixed and same probability of each channel being free which is not realistic.

Herefore presented are statistical models of spectrum opportunities in terms of the probability of each channel (or sub-band) being free. The probability of each channel being free is referred to as 'Free probability'. Free probability is a function of time, space and frequency band and it is assumed that this information is made available. In particular, derived is the PMF of the total number of free channels available at any time instant and location which are not being used by the incumbent users.
An accurate and reliable estimate of the total number of free channels is an extremely important parameter because:

1) It indicates the number of cognitive radios that can access the network

2) Gives an estimate of total spectrum utilisation at that particular location and time by the incumbent users

3) It allows careful selection of the portions of spectrum for further sensing and hence significantly reduces sensing time.

Furthermore this work analyses the complexity in calculating the exact PMF of the total number of free channels in terms of number of multiplications and additions. Cognitive radio processing capacity is wasted in running computationally extensive calculations to estimate the number of available free channels. However, this processing capacity can be diverted to a better use so that we further developed approximate models of the PMF of the number of free channels using Normal, Camp-Paulson (CP) and Poisson approximation. Also investigated is the accuracy of approximate models and suggest the applicability of the models depending on location and time of opportunistic access. Accuracy of each approximate model is evaluated in terms of absolute error and efficiency is measured in terms of the time it takes to calculate PMF on a personal computer.

3.7.2 Spectrum occupancy model

Consider a system with incumbent users operating over a wide bandwidth that is divided into N number of non overlapping narrow sub-bands (e.g. OFDM (Orthogonal Frequency Division Multiplexing) based system), set of sub-bands or channels is denoted by $\mathcal{C} = \{1, 2, \cdots, N\}$. The term sub-band and channel are used interchangeably. The value of N depends on the geographic location and in turn the policies of the responsible regulatory agency. At a particular location s and time t, a certain number of channels are available for opportunistic spectrum access and defined as $\tilde{\mathcal{C}}(t, s) \subseteq \mathcal{C}$. Hence, the total number of free channels is given by $\mathbb{N} = \left|\tilde{\mathcal{C}}(t, s)\right|$, where $|\cdot|$ denotes the cardinality of

a set. Let $\mathbf{p} = [p_1, p_2, \cdots, p_N]^{\mathrm{T}}$ represents the free probability of each channel and also dependent on (t, s) and $|\cdot|^{\mathrm{T}}$ denotes the transpose operation. We further define $\mathbf{x} = [x_1, x_2, \cdots, x_N]^{\mathrm{T}}$ being the set of N Bernoulli random numbers and each element of $\mathbf{x}$ represents the state of the corresponding channel, i.e. free or occupied by the incumbent user [18]. Suppose, if the i^{th} channel is free than $x_i = 1$ otherwise $x_i = 0$ so free probability of i^{th} channel is given by $p_i = \text{Prob}\,[x_i = 1]$.
Without loss of generality, we can assume that all Bernoulli random variables defined in $\mathbf{x}$ are independent of each other. Hence, the cardinality of set $\tilde{\mathcal{C}}$ can also be represented as,

$$\mathbb{N} = \left|\tilde{\mathcal{C}}(t, s)\right| \triangleq \sum_{i=1}^{N} x_i \qquad \text{Eq. 3-1}$$

where $\mathbb{N}$ is the sum of N independent Bernoulli random variables and $\mathbb{N} \in \mathcal{C}_f$ where $\mathcal{C}_f = \{0, 1, \cdots, N\}$.

3.7.2.1 Probability Mass Function (PMF) of $\mathbb{N}$:

In this sub-section, we develop the exact PMF of $\mathbb{N}$. It is important to evaluate the Probability distribution of $\mathbb{N}$ as it determines how many cognitive users can access licensed spectrum as well as what are the potential bands for spectrum sensing.

Scenario 1*:* $p_i = p$:

Consider a simple scenario in which free probability of each channel is simply p and hence $p_i = \text{Prob}\,[x_i = 1], \forall i \in \mathcal{C}$. With this assumption, $\mathbb{N}$ can be considered as a binomial random variable i.e. $\mathbb{N}\sim\text{Binomial}\,(N, p)$ for $p \in [0, 1]$. In this scenario, probability distribution of $\mathbb{N}$ is given by:

$$f_{\mathbb{N}}(k; N, p) = \text{Prob}\,[\mathbb{N} = k] = \binom{N}{k} p^k (1-p)^{N-k} \qquad \text{Eq. 3-2}$$

where $k \in \mathcal{C}_f$ and $1 - p$ represents the probability of each channel being occupied by incumbent users and is given as $1 - p = \text{Prob}\,[x_i = 0], \ \forall\, i \in \mathcal{C}$. The mean and variance of $\mathbb{N}$ in this scenario is given by Np and $Np(1 - p)$ respectively.

Scenario 2*:* $\mathbb{E}[x_i] = p_i$ where $i \in \mathcal{C}$*:*

In a realistic environment, free probability of each channel is not necessarily the same and hence each channel has its own free probability p_i. Under such circumstances, we can not approximate distribution of $\mathbb{N}$ as binomial distribution and calculation of the exact distribution is much more complex.
If we assume each addition operation as multiplication, then the complexity in calculating $f_{\mathbb{N}}(k; N, p)$ is given by following lemma.

Lemma 1: Complexity, κ in calculating the distribution of $\mathbb{N}$ such that free probability of i^{th} channel is $p_i = \text{Prob}\,[x_i = 1]$ and total number of available channels N is given by:

$$\kappa = N \times \binom{N}{k} + 1 \qquad \text{Eq. 3-3}$$

Hence, for the more general scenario i.e. scenario 2, calculation of the probability density function of $\mathbb{N}$ is a very tedious task and in general computational complexity is very high. For example, if the number of available spectrum bands is 45 and the computational complexity for calculating the probability of having 20 channels available for opportunistic access is as high as 316 Billion multiplications.

3.7.3 Approximate models of $\mathbb{N}$

Approximate distributions of $\mathbb{N}$ are developed in this section and their accuracy and complexity are compared in the subsequent section of this article. In order to study the accuracy of approximations, we define the following measure of closeness:

Definition 1: For a given approximation, let $\hat{f}_{\mathbb{N}}(k; N, \mathbf{p})$ be the approximate probability that k number of free channels are available, where $k \in \mathcal{C}_f$. The absolute error $\xi(k)$ is defined as:

$$\xi(k) = \left| f_{\mathbb{N}}(k; N, \mathbf{p}) - \hat{f}_{\mathbb{N}}(k; N, \mathbf{p}) \right| \quad \text{Eq. 3-4}$$

The absolute error defined in Eq. 3-4 is different for different values of k and we can define the *Maximum Absolute Error* (MAE) ξ, as:

$$\xi(k) = \max_{k \in \mathcal{C}} \xi(k) \quad \text{Eq. 3-5}$$

Definition 2: For any approximate CDF of $\mathbb{N}$, defined as:

$$\hat{F}_{\mathbb{N}}(N, \mathbf{p}) = \sum_{k \in \mathcal{C}_f} \hat{f}_{\mathbb{N}}(k; N, \mathbf{p}) \quad \text{Eq. 3-6}$$

and for a given value of θ such that $\theta \to 0$, we can define a set $\mathfrak{E} = \left\{ k \middle| \hat{f}_{\mathbb{N}}(k; N, \mathbf{p}) \geq \theta \right\}$, hence, the MAE defined in Eq. 3-5 can be restated as:

$$\xi(k) = \max_{k \in \mathfrak{E}} \xi(k) \quad \text{Eq. 3-7}$$

3.7.3.1 Normal Approximation of the Probability Distribution of $\mathbb{N}$

It is well known from the central limit theorem that for sufficiently large values of N, the exact distribution of $\mathbb{N}$ tends to become Normal. Let us define the mean and variance of $\mathbb{N}$ as follows:

$$\mathbb{E}[\mathbb{N}] = \sum_{i=1}^{N} p_i \quad \text{Eq. 3-8}$$

$$\text{Var}[\mathbb{N}] = \sum_{i=1}^{N} p_i \, (1 - p_i) \quad \text{Eq. 3-9}$$

where $\mathrm{Var}(\cdot)$ denotes the variance operator. The approximate normal distribution of $\mathbb{N}$ denoted by $\hat{f}_{\mathbb{N}}(k;N,\mathbf{p})|_{\mathrm{Normal}}$ is a normal distribution having mean and variance defined in Eq. 3-8 and Eq. 3-9 respectively. Hence, the CDF of $\hat{f}_{\mathbb{N}}(k;N,\mathbf{p})|_{\mathrm{Normal}}$ can be written as:

$$\hat{F}_{\mathbb{N}}(k;N,\mathbf{p})|_{\mathrm{Normal}} \approx \Phi\left(\frac{k+\frac{1}{2}+\mathbb{E}[\mathbb{N}]}{\sqrt{\mathrm{Var}[\mathbb{N}]}}\right) \quad \text{Eq. 3-10}$$

where $\Phi(\cdot)$ denotes the cumulative distribution function of a standard normal random variable. As we are using a continuous function to approximate a discrete distribution we have to use a continuity correction factor, that's the reason why a factor of $\frac{1}{2}$ appears in the argument of $\Phi(\cdot)$ in Eq. 3-10.

3.7.3.2 Camp-Paulson Approximation of the probability distribution of $\mathbb{N}$

Camp-Paulson (CP) approximation is based on the results of Camp and Paulson and it improves normal approximation by one or two orders of magnitude [20]. We consider CP approximation in this paper to approximate exact probability distribution of $\mathbb{N}$. CP approximation uses the following CDF:

$$\hat{F}_{\mathbb{N}}(k;N,\mathbf{p})|_{\mathrm{CP}} \approx \Phi\left(\frac{\Omega-\mu}{\sigma}\right) \quad \text{Eq. 3-11}$$

Whwre, $\Omega=(1-\beta)\rho^{1/3}$, $\mu=1-\alpha$, $\sigma=\sqrt{\beta\rho^{\frac{2}{3}}+\alpha}$, $\alpha=\frac{1}{9N-9k}$, $\beta=\frac{1}{9N+9k}$, $\rho=\frac{r\,N(k+1)\left(1-\frac{\mathbb{E}[\mathbb{N}]}{N}\right)}{(N-k)\mathbb{E}[\mathbb{N}]}$.

3.7.3.3 Poisson Approximation of the probability distribution of $\mathbb{N}$

The distribution of $\mathbb{N}$ can also be approximated by using Poisson distribution and in this case, PMF of $\mathbb{N}$ is written as:

$$\hat{F}_{\mathbb{N}}(k;N,\mathbf{p})|_{\mathrm{Pois}} \approx \frac{\Gamma(\lfloor k+1\rfloor,\mathbb{E}[\mathbb{N}])}{\lfloor k\rfloor!} \quad \text{Eq. 3-12}$$

where $\Gamma(\cdot,\cdot)$ is the incomplete Gamma function and $\lfloor\cdot\rfloor$ is the floor function. Using Cam's inequality, it can be easily proven that the approximation error is dependent on the magnitude of summation of p_i^2[21], hence Poisson approximation gives accurate results when free probability of each channel is significantly low, as explained by numerical examples in the sequel.

3.7.4 Simulation and numerical results

Numerical results are presented in this section. Spectrum occupancy models are tested by comparing approximate models with the exact probability distributions of $\mathbb{N}$. It is shown that the computational complexity of approximate models is much less than the exact probability distribution of $\mathbb{N}$. Computational complexity is evaluated in terms of the processing time on an Intel machine. All experiments were run on a Intel Core(TM)2 Duo CPU with a processor speed of 2.53GHz having 2 Giga Byte of RAM.

We consider three different cases depicting different scenarios and situations in the real life:

Case 1: refers to the situation when all spectrum channels have very low probability of being free with very low variance among the probability values.

Case 2: refers to the situation when all channels have high probability of being free with very low variance.

Case 3: refers to a situation in which all the channels have arbitrarily values of free probabilities with some arbitrarily variance.

In order to generate different values of free probabilities for different cases, a Beta distribution is normally used [16]. The use of beta distribution in modeling channel occupancy of license users has been validated in [22]. The probability function of a beta distribution is given by:

$$f_{\text{Beta}}(u;\alpha,\beta)|_{\text{Pois}} \approx \frac{\Gamma(\alpha+\beta)}{\Gamma(\alpha)\Gamma(\beta)} u^{\alpha-1}(1-u)^{\beta-1} \quad \text{Eq. 3-13}$$

α and β are the shape parameters and determine the shape of distribution, so by varying values of α and β free probability can be generated for each channel in all 3 cases. In all computations, we assumed the total number of available channels as 20. We compute the exact and approximate distributions of $\mathbb{N}$ by assuming a lower value of $\theta = 10^{-5}$ and neglects any value of probability which is less than θ. We test exact probability distribution of $\mathbb{N}$ with its approximations in terms of Absolute Error and MAE as earlier defined. The exact distribution of $\mathbb{N}$ is calculated by considering all possible combinations and subsequent number of multiplications in each possible combination while approximate probability distributions are calculated using equations Eq. 3-10, Eq. 3-11 and Eq. 3-12.
Figure 3-47 shows the exact probability distribution function and approximated probability distribution functions for *case1* when free probability of each channel is small and all the channels are most likely occupied by incumbent users. Figure 3-47 indicates that probability that only one (or few) channels (out of *N*) is available for opportunistic access is high. For a given threshold on probability of $\mathbb{N}$, it can be easily determined that how many channels might be available and then the CR base stations can instruct participating cognitive radios for spectrum sensing in those particular channels, hence reducing sensing time considerably. Figure 3-48 plots the absolute errors for all the approximations and indicates that for case 1 Camp-Paulson approximation provides accurate approximation in terms of the absolute error.

Similarly, for case 2 when all channels have high free probability with small variance, Camp-Paulson approximation provides more accurate results as shown in Figure 3-49 and Figure 3-50. However, when variance among probability values is high then Camp-Paulson approximation is not sufficiently accurate in terms of absolute error. In that case, Normal approximation provides better accuracy, as indicated in Figure 3-51 and Figure 3-52. Hence, a CR system first analyses free probability of all *N* channels and then determine the best approximation model to use.

Table I shows the computational efficiency in terms of time taken to compute CDF of all approximate models as well as the exact distribution of $\mathbb{N}$. We performed all calculations on the machine described earlier in this section. It is clear from Table 3-7 that all Camp-Paulson based approximate model is highly efficient and also provides accuracy in case 2 and 3.
It should be noted here that computational efficiency is not dependent on any particular case (or value of free probability) hence, it is same for all the three cases.

Table 3-7 : Computational Efficiency (Time in Seconds) Comparison Among Exact Distribution of $\mathbb{N}$ And Its Approximate Models, N = 20.

PMF of N		Exact	Normal	Camp-Paulson	Poisson
Time (seconds)		162.5	16.5 × 10−3	4.7 × 10−3	5.4 × 10−3

MAE, as defined in Eq. 3-7, is summarised in Table 3-8 for all 3 cases. MAE is lowest for Poisson approximation for case 1, Camp-Paulson approximation for case 2 and normal approximation for case 3. In general, Poisson approximation gives accurate estimation of the distribution of $\mathbb{N}$ when the number of channels is high i.e. the value of N is very high and free probability of each channel is very low. Otherwise, when the variance among free probability of each channel is low the Camp-Paulson approximation gives better results. However, when the variance of free probability is high, the normal approximation generally provides reasonably accurate results at significantly low computational cost.

Table 3-8 : Maximum Absolute Error in all 3 Cases with N = 20.

		Normal	**Camp Paulson**	**Poisson**
Case 1		0.09752	0.1406	0.0014
Case 2		0.00462	0.0025	0.1915
Case 3		0.0042	0.0919	0.1573

In summary, we have analysed the computational complexity of the model and computationally efficient approximation models have been proposed. It is inferred that accuracy of approximate models is highly dependent on the free probability of channels or in turn dependent on location and time. Camp-Paulson based spectrum opportunity models provide accurate approximation in terms of MAE and with less computational complexity for most of the scenarios. A cognitive radio base station needs to analyse free probability data first and then use appropriate model to calculate how much spectrum is most suitable candidate for opportunistic spectrum access.

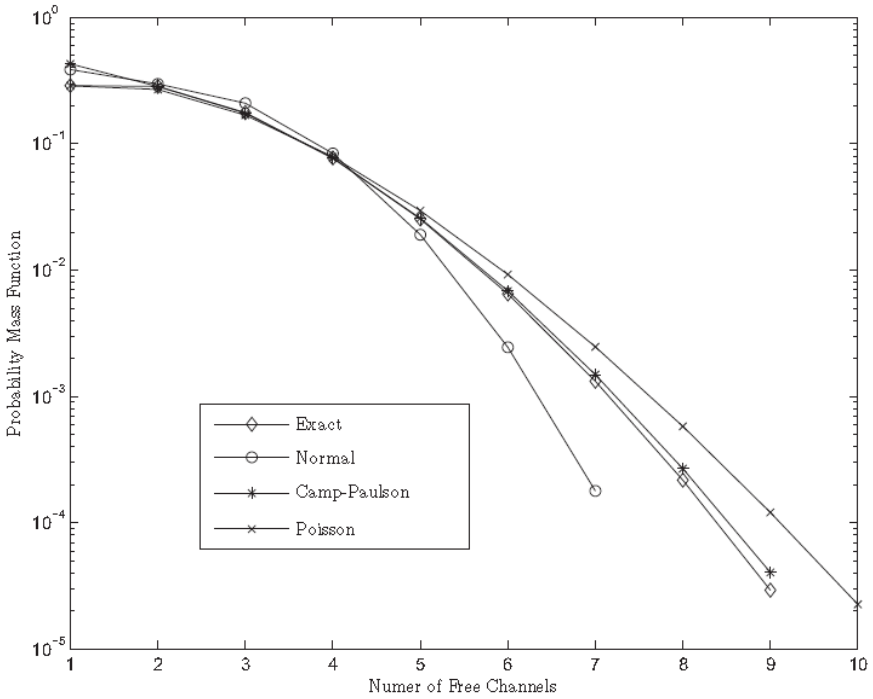

Figure 3-47 : PMF of $\mathbb{N}$ when total number of channels is 20 and free probability of each channel is low with very low variance (Case 1).

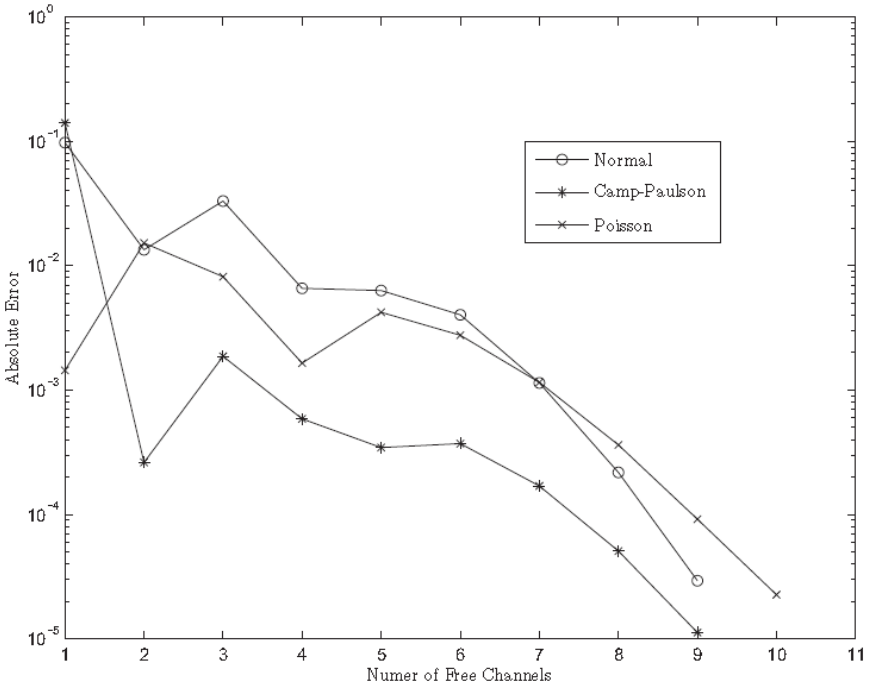

Figure 3-48 : Absolute error plots when total number of channels is 20 and free probability of each channel is low with very low variance (Case 1).

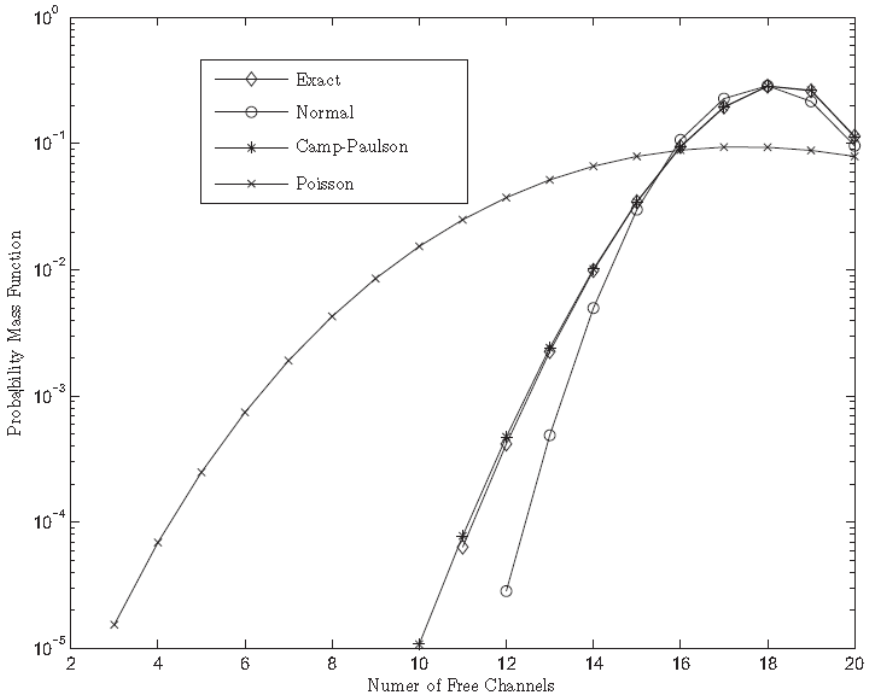

Figure 3-49 : PMF of $\mathbb{N}$ when total number of channels is 20 and free probability of each channel is high with very low variance (Case 2).

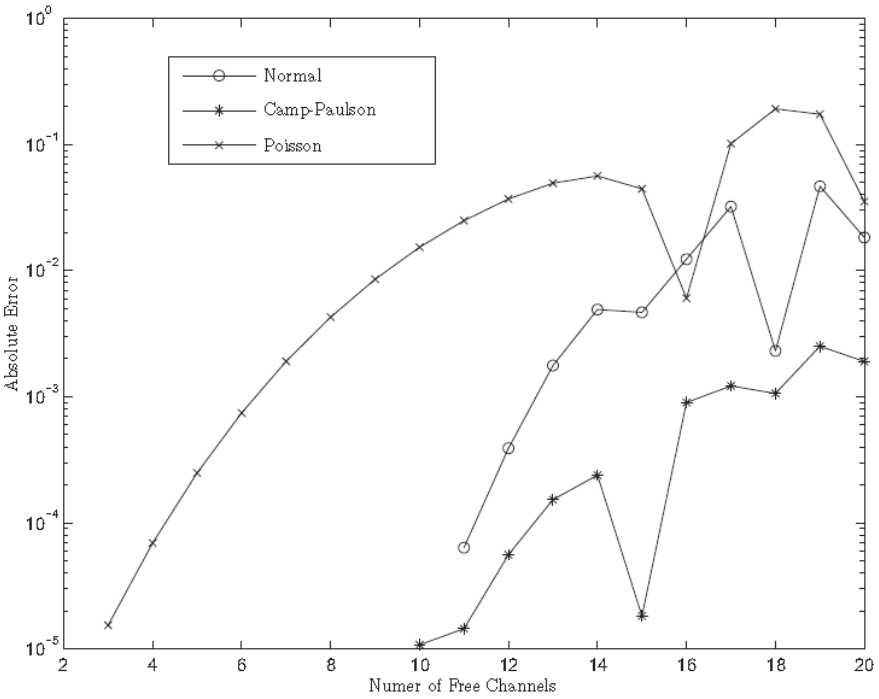

Figure 3-50 : Absolute error plots when total number of channels is 20 and free probability of each channel is high with very low variance (Case 2).

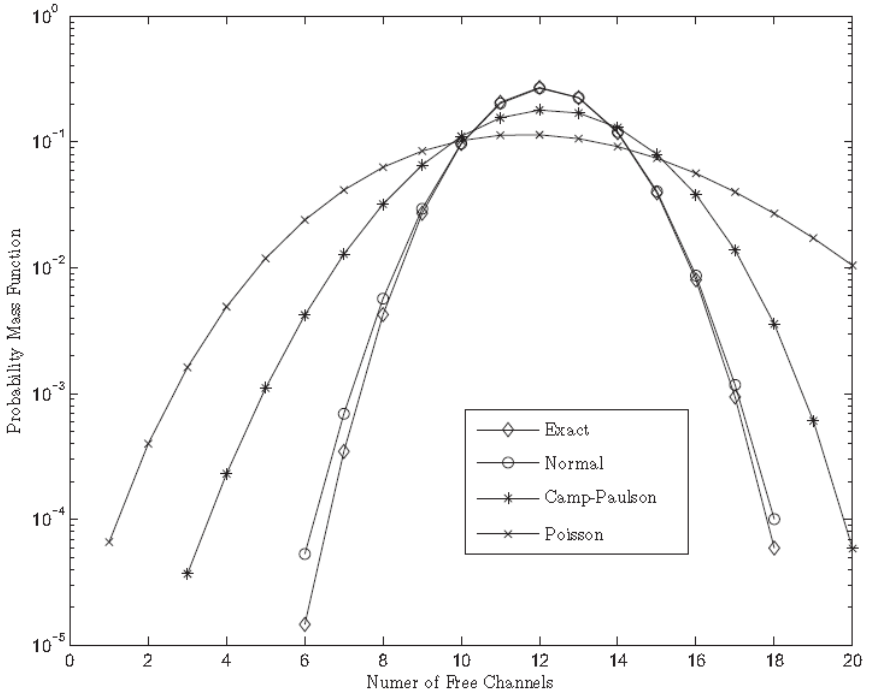

Figure 3-51 : PMF of $\mathbb{N}$ when total number of channels is 20 and free probability of each channel is arbitrarily chosen with arbitrarily variance (Case 3).

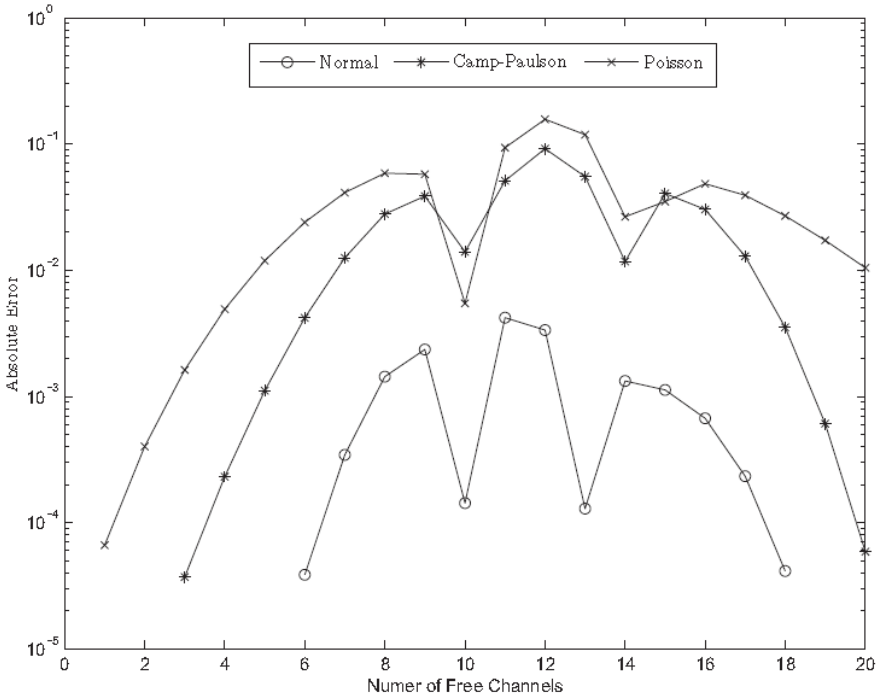

Figure 3-52 : Absolute error plots when total number of channels is 20 and free probability of each channel is arbitrarily chosen with arbitrarily variance (Case 3).

3.8 Propagation modelling for TV White space

This section illustrates the 'flow2' case of the MME approach where modelling is first done from scratch and then confronted with measurements. We address TVWS.

3.8.1 Introduction

The ability to use TV whitespace depends crucially on good management of spectral resources. This in turn needs at least good propagation modeling (as an input to database computations), possibly augmented with sensing. Propagation modeling, an area of classical physics and radio engineering, thus takes on a new importance and it is not clear that traditional models are adequate for this new task. Also, for the pre-computation of database tables, computational speed must be considered. There is always a trade-off between speed and accuracy. The latest ITU (International Telecommunication Union) recommendations relevant to this work are ITU-R P.1812-1 (10/2009) *A path-specific propagation prediction method for point-to-point terrestrial services in the VHF and UHF bands*; and ITU-R P.526-11 (10/2009) *Propagation by diffraction*. However, because of their computational complexity, we have not used these in QoSMOS work. Rather, we have chosen Huffman's Irregular Terrain propagation Model (ITM), which is simpler, but available evidence is that its predictions do not differ greatly from the ITU recommendations.

One of the key functions to enable opportunistic spectrum access is efficient automated spectrum management, via a geo-location database approach, which has been adopted in the recent rules of Federal Communications Commission (FCC) in the US to allow opportunistic spectrum access to use TV whitespace. In the FCC scenarios, the devices of the opportunistic systems identify their locations by using a geo-location capability and then query the database to determine which TV channels they can use at their locations. To verify that the reuse of the TV channel does not cause harmful interference to the incumbent receiver, the database checks whether the signal-to-interference ratio of the incumbent receiver can be kept at a required level. A transmit power which just satisfies the signal-to-interference ratio requirement corresponds to an allowable transmit power of the opportunistic system. Thus, the opportunistic system (or the database) has to estimate the signal-to-interference ratio of the incumbent receiver to determine the allowable transmit power. Pathloss prediction using propagation models is one signal-to-interference ratio estimation method. However, the propagation model inevitably includes prediction error in actual radio environments, resulting in signal-to-interference ratio estimation error. To absorb this error, a margin of the allowable transmit power has to be considered to keep the required signal-to-interference ratio. Consequently, the allowable transmit power has to be limited, and thus white space utilization efficiency might be reduced. Therefore, it is important to improve the signal-to-interference ratio estimation accuracy for expanding the white space opportunities.

QoSMOS has implemented a prototype TV whitespace database (TVWSDB) for demonstration purposes. At present it is populated with United Kingdom TV station data only, but it is designed to make it easy to add new countries. The primary client communication method is XML-RPC (http://xml-rpc.org), a remote procedure call standard which makes writing clients in almost any computer language easy. A demonstration web-browser interface is available at http://www.ict-qosmos.eu/project/demos.html. This uses PHP to translate the user requests into XML-RPC. The C++ spectrum management code of Fraunhofer, developed as part of QoSMOS and described in QoSMOS D6.6 and D6.7, also communicates with this TVWSDB.

3.8.2 White space estimator

There are two fundamental methods for assessing availability of spectrum: sensing, and the use of a pre-computed database. It is likely that many white space secondary devices will have to combine information from both for optimal performance. We here show how the database is generated and used. There are two aspects: a pre-computed database must be generated, and a server and associated protocol must be created and defined. Though there is no novelty in the individual components of this construction, the new field of cognitive radio has created a new need for a good integration of these components, and the QoSMOS project is thus contributing to this integration process.

We thus first describe methods for spectrum availability estimation, with examples for the United Kingdom. The assessment uses Huffman's irregular terrain propagation model (ITM: http://www.its.bldrdoc.gov/resources/radio-propagation-software/itm/irregular-terrain-model-%28itm%29-%28longley-rice%29.aspx), which is a variant of the Longley-Rice model. This model incorporates empirical fitting to measured signal data, especially regarding diffraction effects over hills. As mentioned above, future systems will most likely use more standardized propagation models, such as ITU-R P.546-11 and P.1812-1, though these typically slow the computation considerably.

The database construction starts by pixellating the country to be covered, typically in 1km squares. The modelling assumes that if there is no line of sight to the transmitter from a given pixel (taking account of terrain), the pixel can be taken to be in a whitespace area. This simplifies the calculation, and is found to be true in practice. Otherwise, we compute the field strength at the pixel, using terrain

data and list of TV transmitter information provided by the national regulator. This field strength is recorded in the database. Figure 3-53 gives a rough general impression of spectrum occupancy in Great Britain (blue=low, red=high) computed in this way.

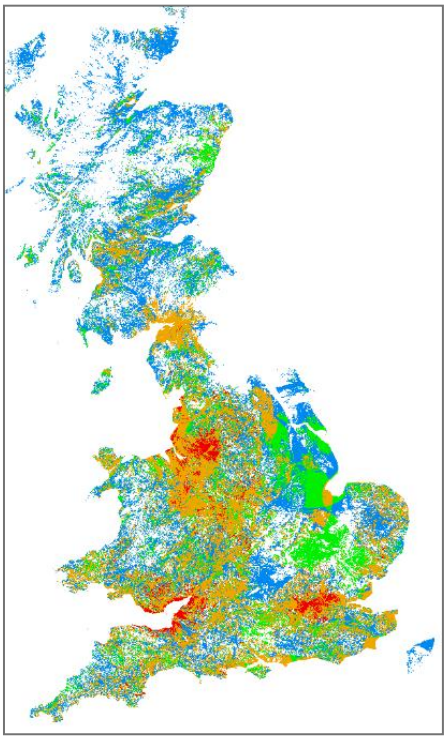

Figure 3-53: General TV spectrum occupancy in Great Britain (blue=low, red=high).

Another requirement for practical application of TVWS is to know the pathloss from a proposed base-station site. For this purpose, we use again the ITS (US Institute for Telecommunications Science) propagation model and plot contours of equal signal strength. Figure 3-54 shows typical results, which are based on the BT research facility in Martlesham Heath, UK.

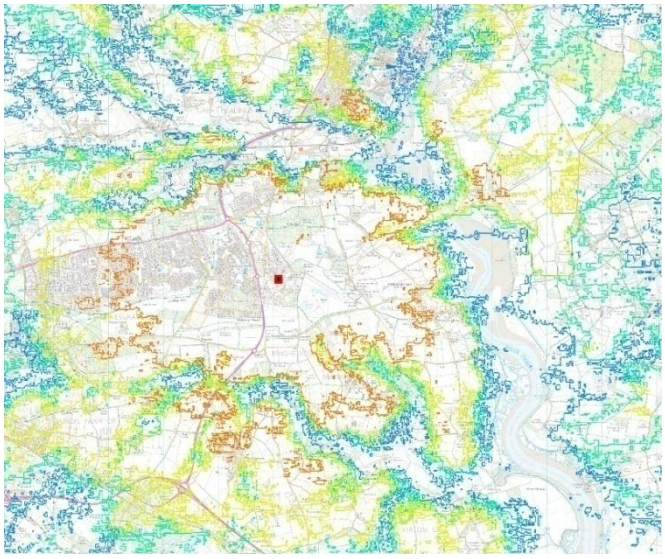

Figure 3-54: Estimated field-strength contours from a base-station at Martlesham Heath (UK).

The pathloss along a specific point-to-point path is even more important for a deployment. Figure 3-55 shows clearly how the terrain (green) affects the pathloss (red). Note that diffraction effects cause a sharp increase in pathloss just behind the lip of a valley, but the signal strength can recover being still in the valley. In practice a pathloss of 140dB is about the maximum that a working deployment can tolerate.

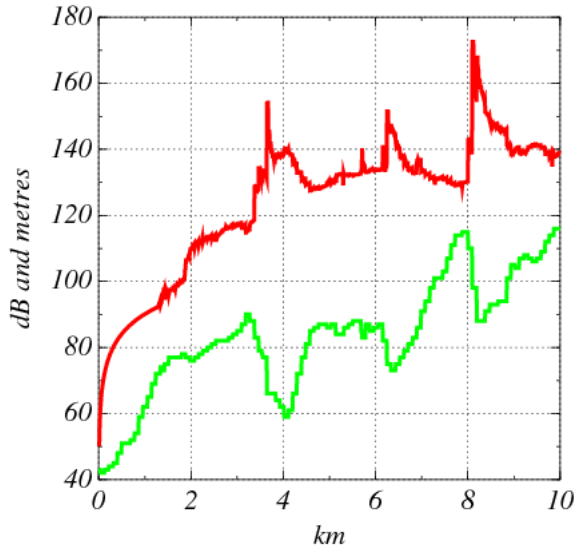

Figure 3-55: Typical pathloss dependence (dB, red) on terrain (green, metres).

The results are most useful if they are weighted with respect to population density, rather than per unit area. This is a neglected issue, and it is difficult to get data on population density. For this purpose the study uses the output of another project, which analyzed maps at the scale of 1 pixel = 1 square metre to locate houses in Britain. In Figure 3-56, the y-axis shows the fraction of population which is located in an area having *x* free channels (each channel is 8MHz). It can be seen, for example, that 80% of the population have 17MHz or free spectrum available. There is a need for such calculations to be extended to other countries, both with higher and lower population density than Great Britain.

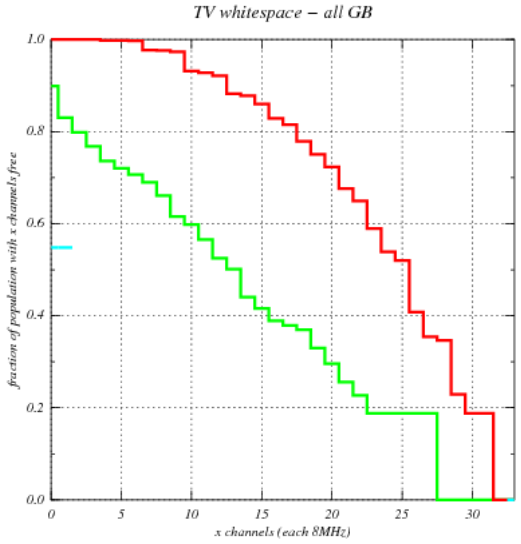

Figure 3-56: Cumulative population-weighted spectrum availability (red) in UK. Green=adjacent channels also required to be free.

3.8.3 TV signal-strength measurement campaign

At BT's research facility in Martlesham, UK, a TV signal-strength measurement campaign has been running from September to December 2012. The aim of this is mainly to gather statistics on the variability of TV signals; such variability is known to occur because of changing atmospheric conditions, changing interference levels, power changes by the operator, and potentially other sources. In addition, these measurements can in principle be used to verify the propagation models discussed above, though getting an absolute verification is very difficult due to challenging calibration requirements. For the moment we focus on the distribution of signal values and their autocorrelation and covariance.

BT's measurement set-up consists of a roof-mounted antenna pointing due west at the Sudbury transmitter about 30km away, a low-noise preamplifier with 15dB gain, and an Ettus USRP software-defined radio. All measurement is controlled by a Linux laptop with python software (controlled by a crontab) which takes a signal-strength reading every 5 minutes for each TV channel.

In Figure 3-57 and Figure 3-58 can be seen raw time-series data. Of interest is a block of interference (in some channels), from about 256 days to 275 days. This most likely comes from a TVWS trail base-station. Apart from this, fluctuations generally consist of short-period bursts of interference. The empirical distributions (estimated probability density functions) of this same data are shown in Figure 3-59 and Figure 3-60. Some of these are multi-modal due to the effect just mentioned. Work is in progress to determine whether the individual unimodal components are log-normal, as is usually assumed in radio modelling work. Figure 3-61 and Figure 3-62 show autocorrelation of four of the time series, and the cross-correlation matrix of the six in-use Sudbury channels. Autocorrelation shows a long tail, with correlation still high at a lag of about two days. There is no clear evidence of a daily cycle.

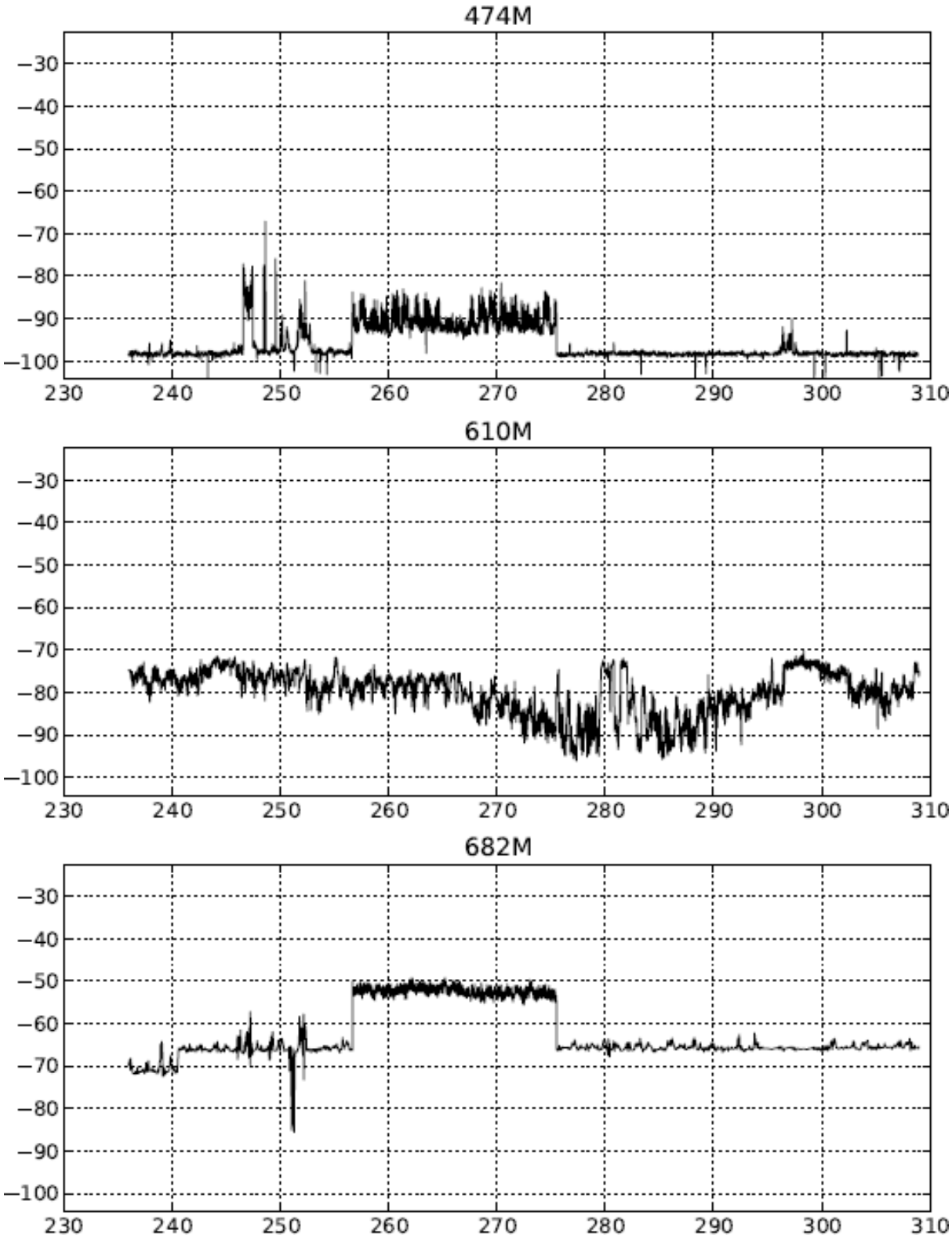

Figure 3-57: Time series of TV measurement data (x axis in days, y axis in dBm).

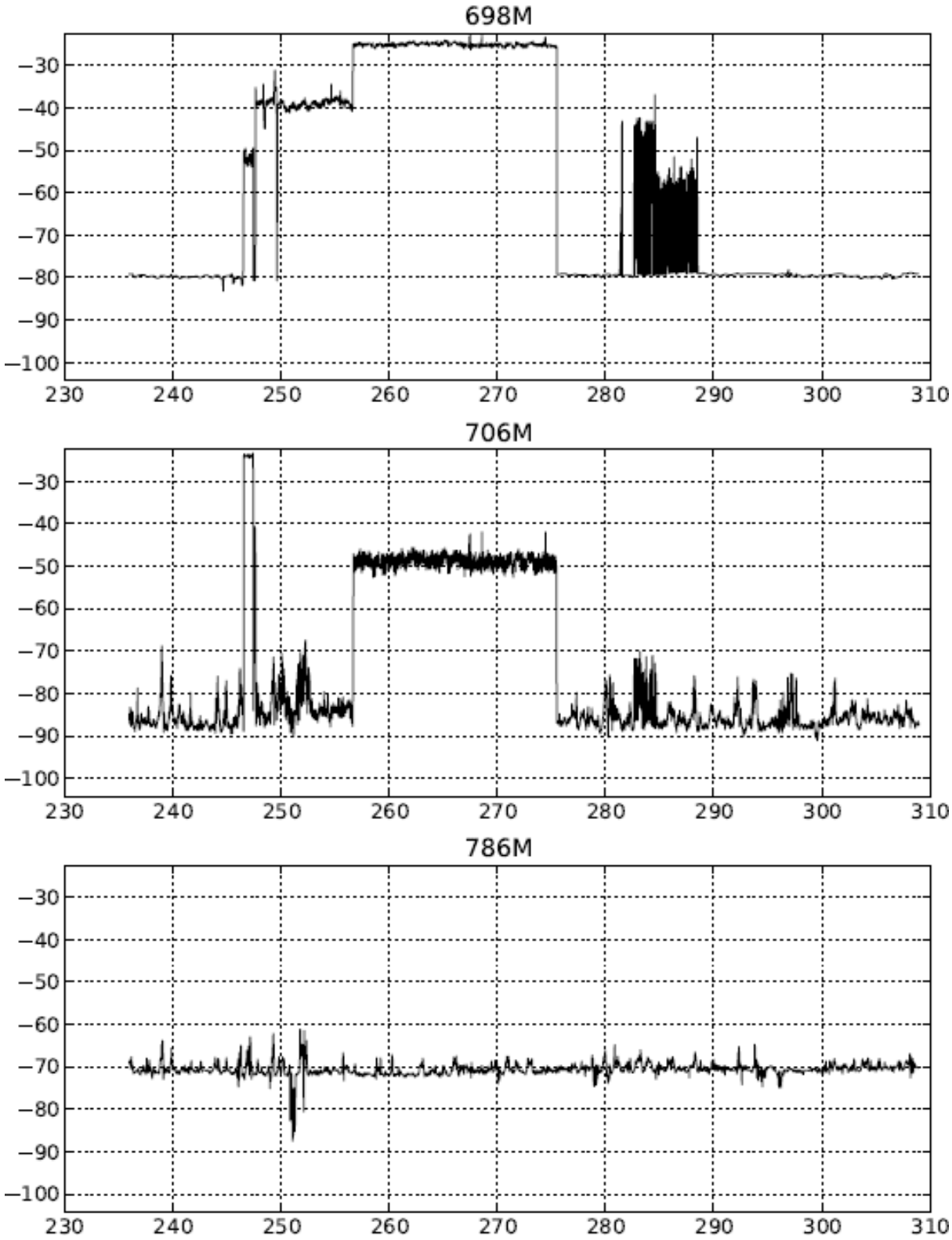

Figure 3-58: Time series of TV measurement data (x axis in days, y axis in dBm).

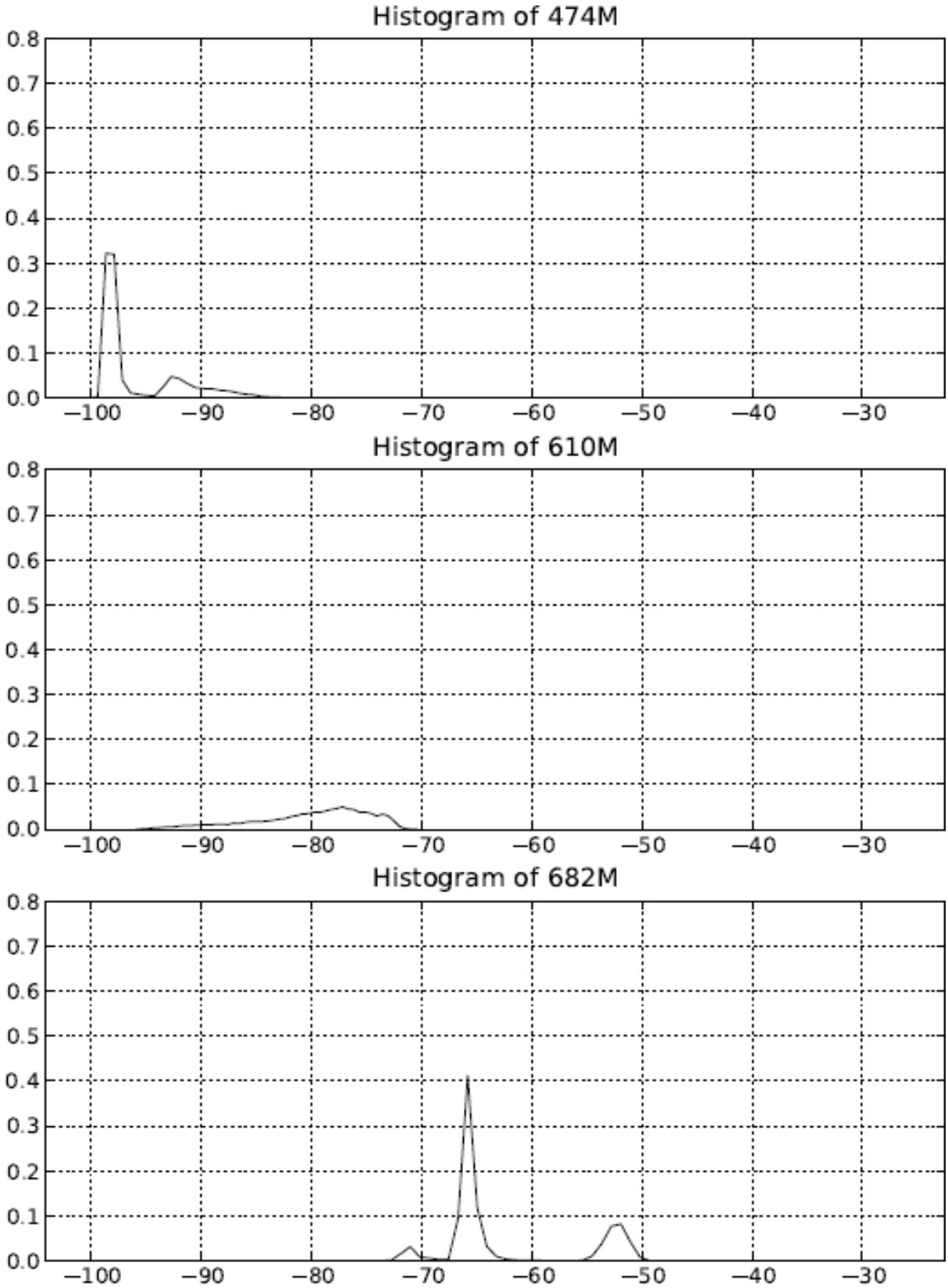

Figure 3-59: Distribution (pdf) of TV measurement data (x axis in dBm).

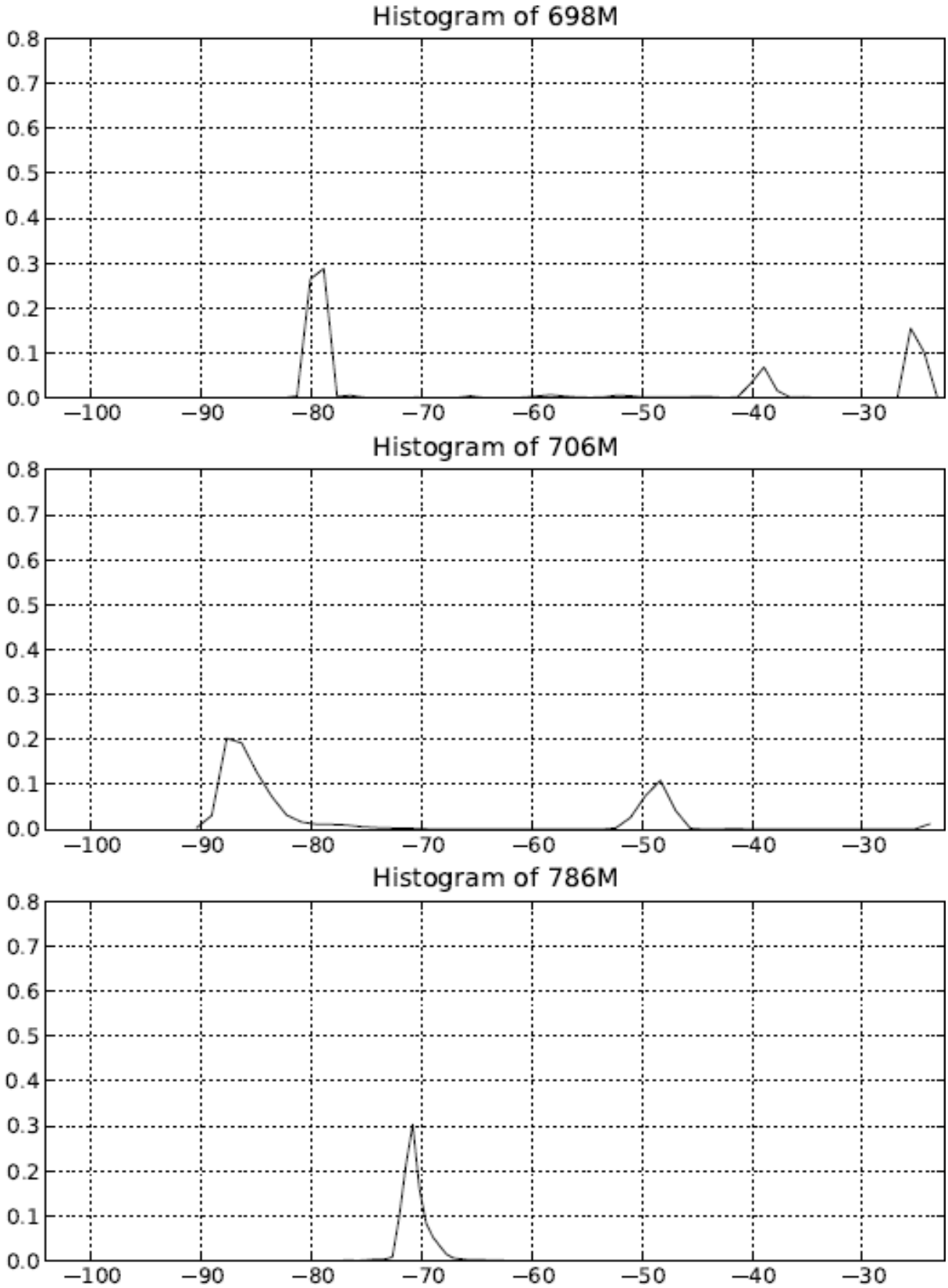

Figure 3-60: Distribution (pdf) of TV measurement data (x axis in dBm).

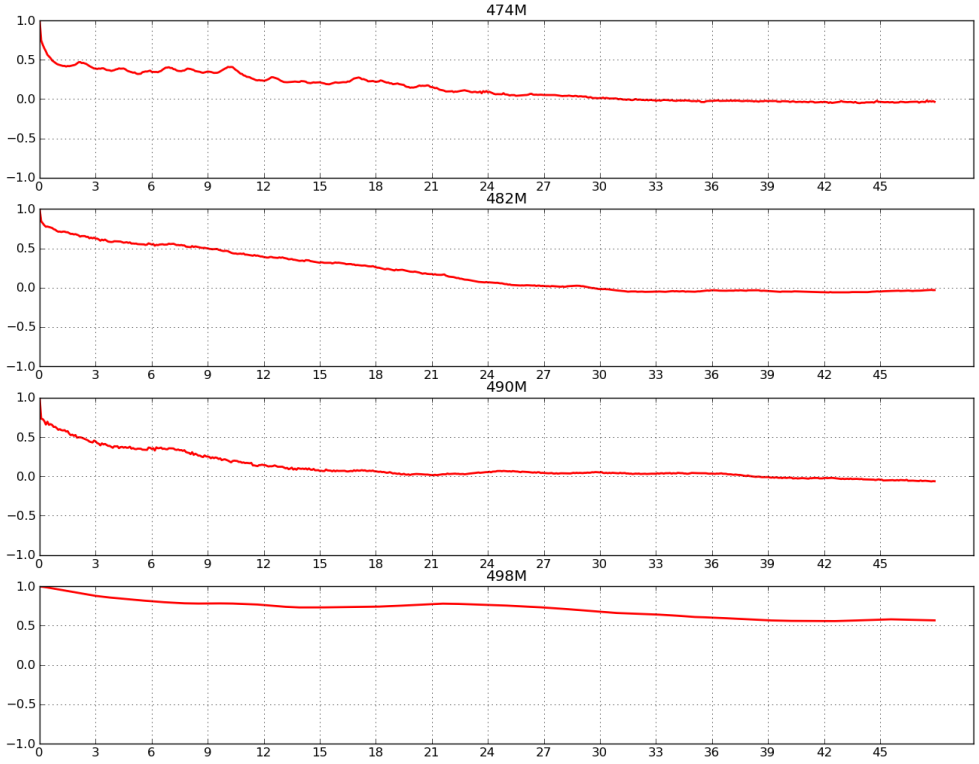

Figure 3-61: Autocorrelation of four TV signal-strength time series (x axis in hours).

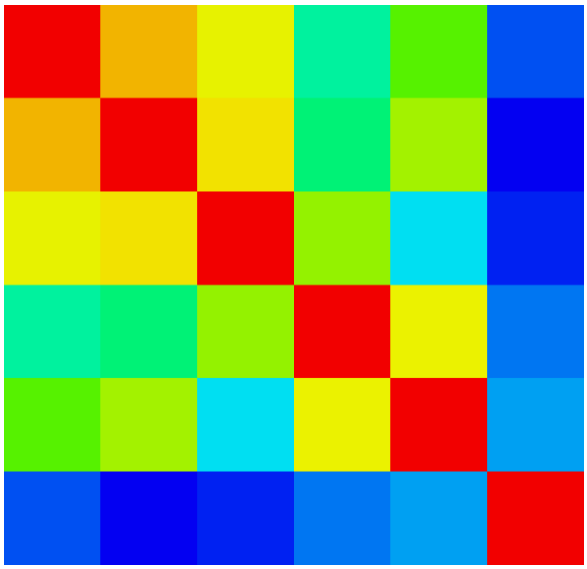

Figure 3-62: Correlation matrix for 634, 658, 682, 754, 770, and 785MHz (red=1, dark blue=0, intermediate values by spectral colour).

3.8.4 Conclusions

The assumption of log-normality of the signal strengths is not disproven, but more data is needed and further careful measurement work would be beneficial. The assumption by Ofcom of a 5.5dB standard deviation is also not too far wrong. All this information can be used to feed into an algorithm for TVWS device power-level determination, and this is why we consider this work fundamental to all TVWS and cognitive-radio applications. The better the input data and the better the power-level algorithms, the better the final system performance, and the better the elimination of interference to TV reception. The correlation matrix work is intended to be used to help predict how well sensing data in one channel helps in forecasting the strength in another channel. Furthermore, we have here looked at time variability of signals, something ignored in much TVWS work.

4 From measurements and models to emulation

4.1 Motivation

Emulation is the third pillar of the proposed MME approach introduced in section 2. The objective is from the models or the measurements to generate signals that would stimulate the sensing engines. In that context, we have developed a *radio scene emulator* for which a US patent application was filed. Both hardware and software versions are considered. The idea is to give full freedom to the user along the time/frequency/power/waveform axis or domains. This will be detailed in the next section.

The developed tool offers the following 'musts' for a test system:

- ✓ **Controllability**: The user should be able to precisely control the emulation scenario;
- ✓ **Repeatability**: The user should be able to repeat any desired sequence of events in the emulation scenario.
- ✓ **Representability**: The emulated RF scene should represent as well as possible the real environment that the CR system will experience. This is guaranteed through the MME vertical approach.

4.2 Radio Scene emulator

4.2.1 Functionalities

A typical signal generator used in the Test and Measurement is used to generate a single always ON waveform. We innovate here in two dimensions as illustrated by Figure 4-1:

- ✓ Frequency axis: the tool offers to generate any number of waveforms along the frequency domain over a wide bandwidth;
- ✓ Time axis: instead of the sole always ON mode, we offer to have ON and OFF sequences. These sequences can be extensively determined by the user or generated following some MME models or other Markov chains.

Figure 4-2 shows a 2D representation in the form of a time/frequency grid and where the different colours represent the different waveforms (LTE, GSM, UMTS, etc.). The user is given full freedom to 'colour' the grid. She/He can define whatever waveform (by drag and dropping from a library) on whatever part of the grid with no constraints. The power of each waveform can of course also be specifically defined.

Once the scene defined, the software (in this case, System Vue), will make the necessary signal processing work to produce a compound file which will be downloaded to a regular signal generator for hardware play.

In addition, channel effects can be incorporated into the scene. We make it so by producing a file compatible with Agilent's PXB channel emulator. Potentially (the only limit comes from the HW resources), all waveforms can be faded independently with virtually any channel model. This reflects the fact that the different sources have potentially different locations (e.g. TV transmitter and GSM tower).

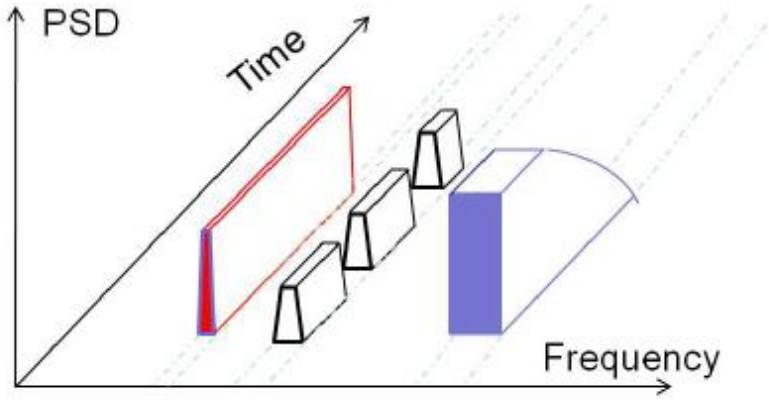

Figure 4-1: Scene emulator: degrees of freedom.

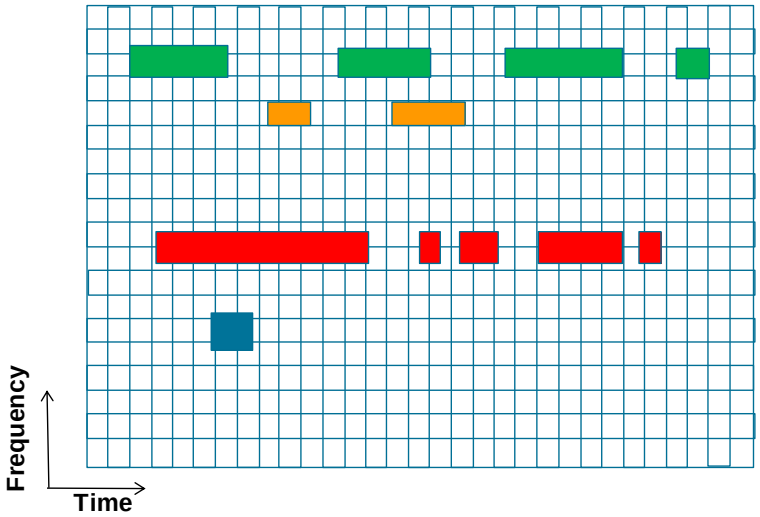

Figure 4-2: Scene emulator: 2D helicopter view.

A very simple scenario is illustrated by Figure 4-3: two periods are considered, the first one includes a unique DVB signal while the second adds a 5MHz LTE signal.

Moreover, note that besides cognitive radio, the potential applications are multiple and are currently being investigated by the company. Let's cite two: interference testing and carrier aggregation signal generation.

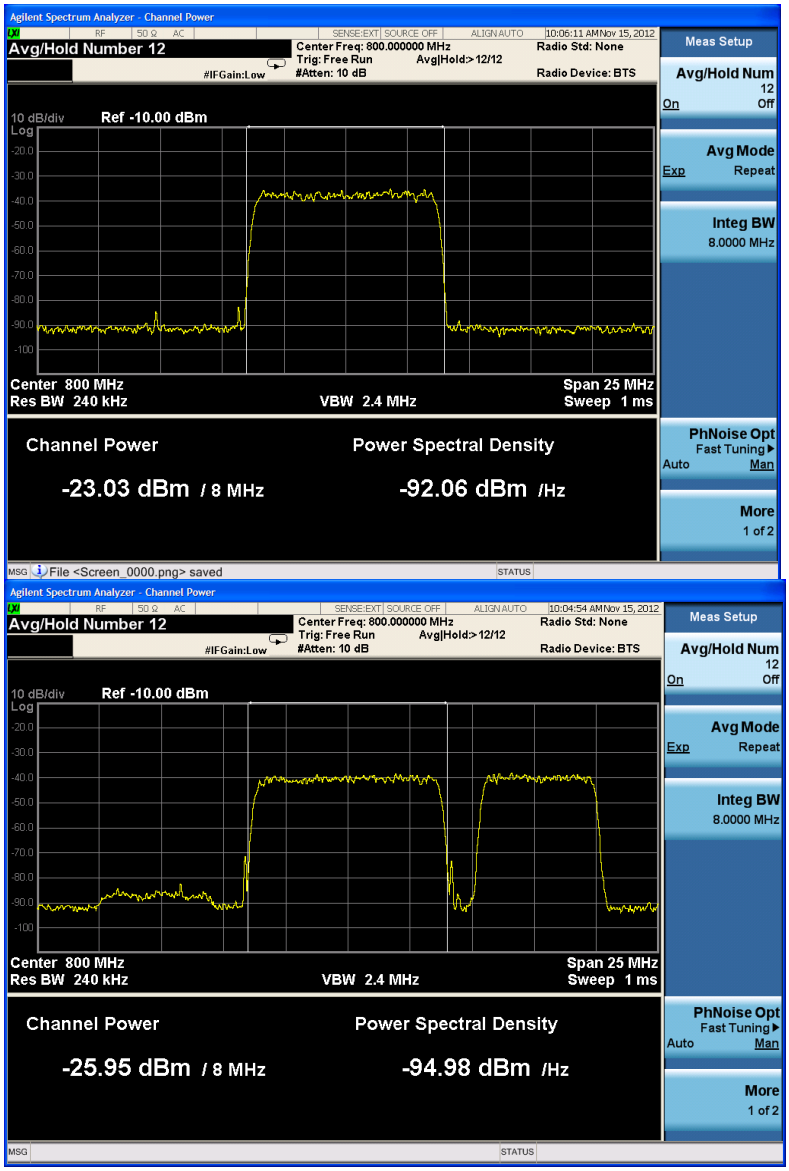

Figure 4-3: Spectral analyzer based view of the output the scene emulator for a basic scenario & with no channel included: at time instant 1 (top), a single DVB signal (8MHz) ; at time instant 2 (bottom), a 5MHz LTE signal is added.

4.2.2 Principles

Because of space constraints and confidentiality issues, the general principles behind the scene emulator will be presented hereafter, not the full details.

4.2.2.1 Waveform library

The starting point is to have access to a library of waveforms. For this, we are using Agilent's Signal Studio library which includes for each standard a fundamental so called 'ARB' file which stores, e.g. in the LTE case, 10 frames, corresponding to 10ms.

For greater durations, which is often the case, the ARB's are simply appended after each other, that is cycled.

4.2.2.2 Resampling

As the radio scene can be composed of various waveforms not sharing the same fundamental sampling period (e.g. GSM and LTE), the different ARBs need to be resampled to a common sampling rate. This problem was essentially worked out in the EU SAMURAI project. In there, we propose a methodology to define the common sampling rate based on the various fundamental sampling periods with the minimization of the complexity as objective. Moreover, the proposed actual resampling job is done thanks to a cascaded polyphase approach, guaranteeing a high performance / complexity operating point.

4.2.2.3 Offset

A single carrier being used, the different waveforms are simply aggregated on the frequency axis along each other with a simple proper offset in baseband.

4.2.2.4 Segmentation and truncation

--Note that this step is only necessary for the HW version of the scene emulator --

To save memory, the different ARB files (segments) are in principle only stored ones and not concatenated after each other into a bigger file. A simple case is given by Figure 4-4. There, it is easy to see that the scene can be represented by four different segments (S1,...,S4) which saves consequent amount of memory. A first step consists then in slicing appropriately the radio scene grid.

Figure 4-4 also emphasizes some potential spectral regrowth effects. Indeed, the different fundamental ARBs typically neither share the same sampling frequency neither the same duration. A slicing aligned with a given waveform (in terms of ARB length) will then typically not be aligned with the others. This will lead to some phase mismatch while cycling. To minimize the effects by choosing an appropriate cutting strategy, we have developed a small Matlab tool whose GUI is given in Figure 4-5 for a simple sinusoid case.

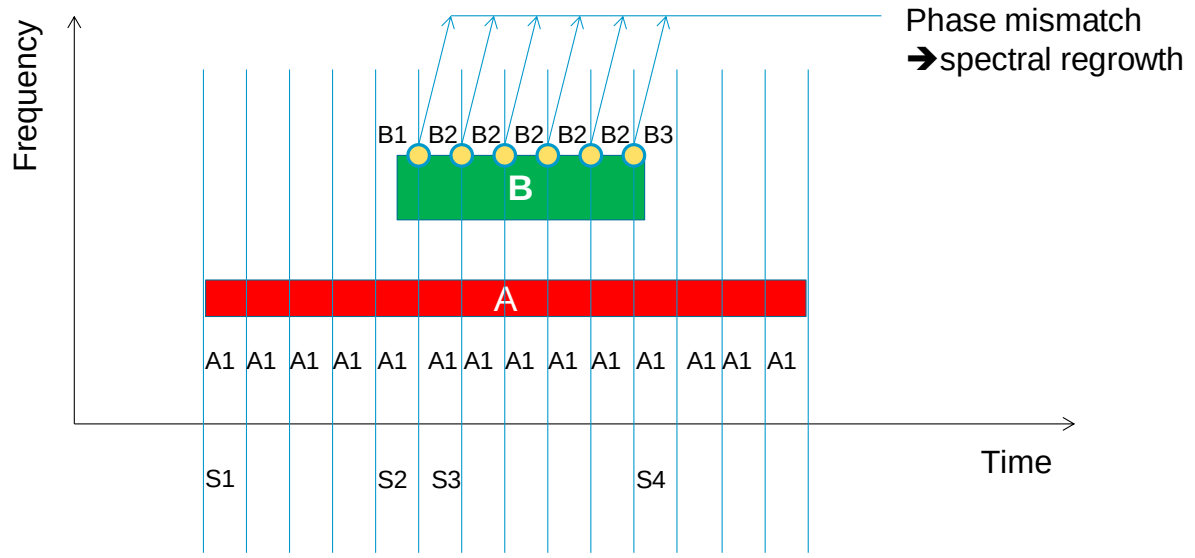

Figure 4-4: Scene emulator: segmentation and truncation leading to spectral regrowth.

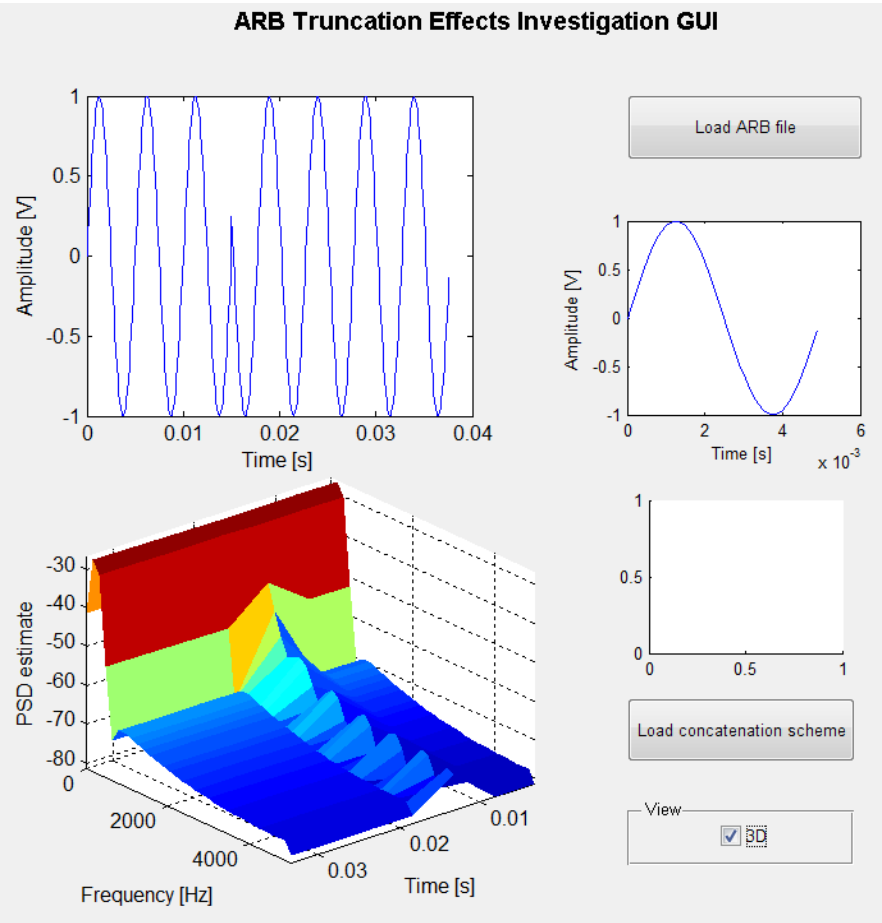

Figure 4-5: GUI of the tool developed to help choosing appropriate slicing pattern.

4.3 MME generic cognitive radio testbed

Figure 4-6 illustrates a generic MME based cognitive radio testbed. It can be a hardware or software version depending on the test objectives (prototypes or algorithms).

In the first deterministic case, the modeling block is skipped and the recorded sequences obtained from the measurement campaign are directly replayed on the emulator without any changes. The incumbent usage pattern (on/off) is emulated without the need for any channel emulation. This emulation scenario serves the link-level performance evaluation and, in particular, the sensing engine performance study.

In the second model-based case, both statistical and database approaches are considered. Here, the incumbent usage pattern emulation is combined with the channel emulation to accurately reproduce the actual RF scene. This emulation scenario serves the system-level performance evaluation.

Figure 4-6 shows that, in the test bed, the sensing estimates of the CR device can be compared with the source to evaluate the performance of the sensing engine. Metrics such as probabilities of detection, false alarm, or the detection speed can be evaluated in this manner. On the other hand, the CR device can also make decisions about the available opportunities based on the sensing engine outputs. In this case, the transmitter of the CR device (secondary) can start transmitting on the available spectrum holes. The output of the secondary transmitter is then added to the stimulus signal and later fed to CR device receiver as well as the incumbent systems receiver. Through bit error rate (BER) measurements (as an example), both the quality of the secondary transmission and its impact on the incumbent systems can be evaluated.

As depicted in the figure, a CR test bed can also include channel emulation blocks. Adding these blocks between the receivers and the modeled (or emulated) transmit sources will enable the inclusion of fading and Doppler effects in the radio scene. A true radio scene experienced by the mobile device is then emulated; hence, both the static and the vehicular cases are appropriately tested.

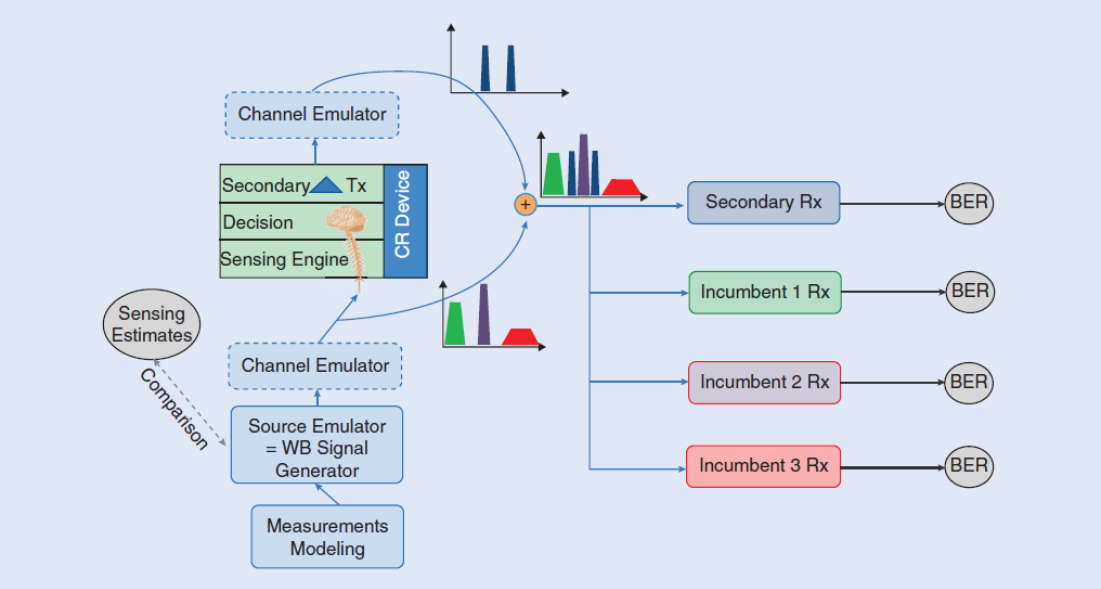

Figure 4-6: Cognitive Radio Testbed.

4.4 Exemplary QoSMOS testbed

Figure 4-7 illustrates a hardware version of the QoSMOS MME testbed. This setup corresponds to the third Proof-of-Concept (PoC) developed in QOSMOS' WP7. The aim is to test a collaborative sensing engine (multi-node sensing). In this case, 4 Ettus energy-based sensors are considered. As for the HW of the scene emulator, Agilent's PXB platform is used. It includes both the required signal generation functionality and the channel fading functionality. In this very case, a single DVB (Digital Video Broadcasting) source is considered and faded via 4 independent fading processes (LTE channel model). Hence, the sensors are stimulated alike the way they would in the field. Testing such system in the field (without the scene emulator) would be hardly possible. With the develop tool, all possible scenarios can be covered and repeated in the lab: *real world in the lab.*

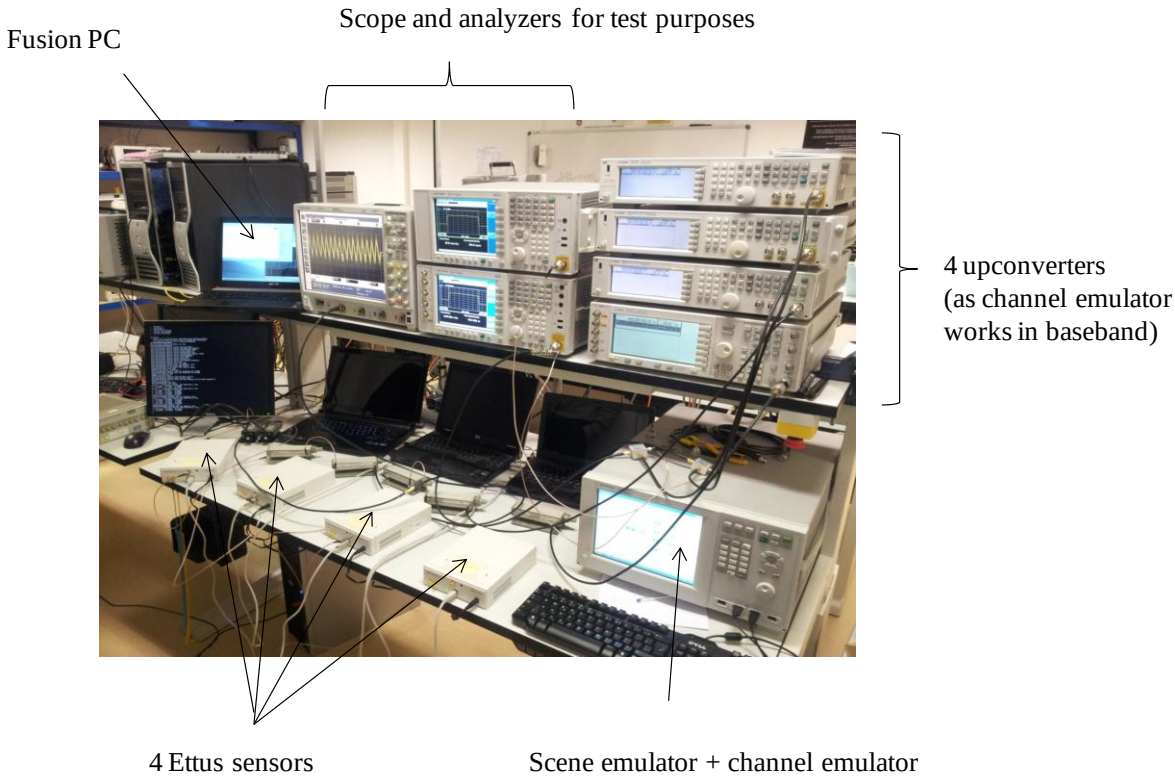

Figure 4-7: QoSMOS WP7 PoC4 testbed.

5 Conclusions

In this deliverable, we have presented the results from several radio activity measurement campaigns performed at various locations, timings and covering various frequency bands. This includes GSM, UMTS, ISM and TV bands. The results clearly show unexploited spectrum resources that could be leveraged thanks to the cognitive radio technology developed in the QoSMOS project. Opportunities exist in the various bands studied, including the 'always ON' UMTS case. Among others, we have also shown that the typical spectrum occupancy metric can be significantly different from the actual traffic occupancy.

Behind these results, the QoSMOS team has developed some novel measurement techniques for these campaigns. They were reported in various publications listed. QoSMOS has also proposed a new two-node measurement setup to investigate spatial correlation.

The team has also developed some activity / occupancy / opportunity models that could be used for sensing or evaluation purposes. Furthermore, the importance of the polarization was emphasized.

All this work fits nicely in the MME (Measurement – Modeling – Emulation) framework we proposed for the assessment of cognitive radio systems as detailed in [1]. The third pillar of the framework consists in the emulation of the radio scene, for which we have developed an innovative 'radio scene emulator' which gives full freedom to the user along the time/frequency/waveform/power axis or domains.

6 References

[1] D. Tandur, J. Duplicy, K. Arshad, K. Moessner, D. Depierre, J. Lehtomäki, K. Briggs, L. Goncalves, A. Gameiro, ``Cognitive Radio Systems Evaluation: Measurement, Modeling, and Emulation Approach,'' *IEEE Vehicular Technology* Magazine, June 2012.

[2] C. Chevallier, C. Brunner, A. Garavaglia, K. P. Murray and K. R. Baker, ``WCDMA (UMTS) deployment handbook, planning and optimization aspects''. John Wiley & Sons Ltd, 2006.

[3] D. Cabric, ``Spectrum Sensing Measurements of Pilot, Energy, and Collaborative Detection,'' *Military Communications Conference*, MILCOM'06, Washington DC, USA, Oct. 2006

[4] M. Wellens et al., ``Evaluation of Cooperative Spectrum Sensing based on Large Scale Measurements,'' *3rd IEEE Symposium on New Frontiers in Dynamic Spectrum Access Networks, DySPAN'08*, Chicago, USA, October 2008.

[5] *R.* Sharma and J. Wallace, ``Experimental Characterization of Indoor Multiuser Shadowing for Collaborative Cognitive Radio,'' *3rd European Conference on Antennas and Propagation, EURACAP'09*, Berlin, Germany, March 2009.

[6] M. Hanif, P. Smith and S. Mansoor, ``Performance of Cognitive Radio Systems with Imperfect Radio Environment Map Information,'' *IEEE Communications Theory Workshop, AusCTW'09,* Australia, 2009.

[7] ``Channel models for HIPERLAN/2 in different indoor scenarios,'' ETSI EP BRAN 3ER1085, Mar. 1998.

[8] J. J. Lehtomäki, R. Vuohtoniemi, K. Umebayashi and J.-P. Mäkelä, ``Energy Detection Based Estimation of Channel Occupancy Rate With Adaptive Noise Estimation,'' *IEICE Transactions on Communications* E95-B: 04. 1076-1084 April 2012.

[9] J. Lehtomäki, R. Vuohtoniemi and K. Umebayashi, ``Duty Cycle and Channel Occupancy Rate Estimation with MED-FCME LAD ACC,'' *Proc. 7th International Conference on Cognitive Radio Oriented Wireless Networks (CROWNCOM)*, Stockholm, Sweden, June 2012.

[10] J. Lehtomäki, R. Vuohtoniemi and K. Umebayashi (2012), ``On the Measurement of Duty Cycle and Channel Occupancy Rate,'' *IEEE Journal on Selected Areas in Communications (under revision).*

[11] D. Noguet, R. Datta, P. H. Lehne, M. Gautier, G. Fettweis, ``TVWS regulation and QoSMOS requirements,'' International Conference on Wireless Communication, Vehicular Technology, Information Theory and Aerospace & Electronic Systems Technology, 2011.

[12] C. A. Balanis, ``Antenna Theory and Design''. Wiley, 2005.

[13] T. W. C. Brown, S. R. Saunders, S. Stavrou and M. Fiacco, ``Characterisation of Polarization Diversity at the Mobile,'' IEEE Transactions on Vehicular Technology, vol. 56, issue 5, part 1, pp2440-2447, September 2007.

[14] F. H. Sanders and V. S. Lawrence, ``Broadband Spectrum Survey at Denver Colorado,'' NTIA Report, Tech. Rep. 95-321, 1995.

[15] M. A. McHenry, P. A. Tenhula, D. McCloskey, D. A. Roberson, and C. S. Hood, ``Chicago Spectrum Occupancy Measurements & Analysis and a long-term Studies Proposal,'' *Proceedings of the first international workshop on Technology and policy for accessing spectrum*, New York, NY, USA, 2006.

[16] M. Wellens and P. Mahonen, ``Lessons Learned from an Extensive Spectrum Occupancy Measurement Campaign and a Stochastic Duty Cycle Model,'' *5th International Conference on Testbeds and Research Infrastructures for the Development of Networks Communities and Workshops*, 6-8 2009, pp. 1 –9.

[17] S. Geirhofer, L. Tong, and B. Sadler, ``Cognitive Radios for Dynamic Spectrum Access - Dynamic Spectrum Access in the Time Domain: Modeling and Exploiting White Space,'' *IEEE Communications Magazine*, vol. 45, no. 5, pp. 66 –72, may 2007.

[18] C. Ghosh, "Innovative Approaches to Spectrum Selection, Sensing, and Sharing in Cognitive Radio Networks," *Ph.D. Thesis*, University of Cincinnati, May 2009.

[19] L. Luo and S. Roy,``Analysis of Search Schemes in Cognitive Radio,'' *4th Annual IEEE Communications Society Conference on Sensor, Mesh and Ad Hoc Communications and Networks*, 18-21 2007, pp. 647 –654, Seattle, USA, June 2007.

[20] B. H. Camp, ``Approximation to the Point Binomial,'' *Annals of Mathematical Statistics*, vol. 22, no. 1, pp. 130–131, 1951.

[21] L. L. Cam, ``An Approximation Theorem for the Poisson Binomial Distribution,'' *Pacific Journal of Mathematics*, vol. 10, pp. 1181–1197, 1960.

[22] C. Ghosh, S. Roy, M. B. Rao, and D. P. Agrawal, ``Spectrum occupancy validation and modeling using real-time measurements,'' *Proceedings of the 2010 ACM workshop on Cognitive radio networks, ser. CoRoNet '10*. New York, NY, USA: ACM, 2010, pp. 25–30.